COLLISION-INDUCED INFRARED ABSORPTION SPECTRA OF THE FUNDAMENTAL BANDS OF HYDROGEN DEUTERIDE AND HYDROGEN

RAM DEO GOPAL PRASAD


CENTRE FOR NFLD. STUDIES
MEMORIAL UNIVERSITY
OF NEWFOUNDLAND

AN ARTICLE NOT MICROFILMED FOR REASONS OF COPYRIGHT:

Infrared absorption spectra of gaseous HD. I. Collision-induced fundamental band of HD in the pure gas and HD-He mixtures at room temperature, The Journal of Chemical Physics, Vol. 62, No. 9, 1 May 1975.

COLLISION-INDUCED INFRARED ABSORPTION SPECTRA OF THE FUNDAMENTAL BANDS OF HYDROGEN DEUTERIDE AND HYDROGEN

by

© Ram Deo Gopal Prasad, M.Sc.

A Thesis submitted in partial fulfillment
of the requirements for the degree of
Doctor of Philsophy

Department of Physics
Memorial University of Newfoundland

January, 1976

St. John's Newfoundland

CONTENTS

ABSTRACT

The infrared absorption spectra of the fundamental band of HD in its binary mixtures with He, Ne, Ar, Kr, and Xe for different base densities of HD and a number of total gas densities up to 190 amagat were recorded at room temperature with a one meter transmission type high-pressure absorption cell. The collision-induced features of the band in these mixtures are similar to those observed for the corresponding spectra of H_2 in its binary mixtures. The binary and ternary absorption coefficients of the band have been derived from the measured integrated intensities. An analysis of the profiles of the enhancement of absorption of the band in all the five mixtures has been performed by assuming appropriate line-shapes, and the three half-width parameters, δ_d and δ_c of the overlap transitions and δ_q of the quadrupolar transitions, are obtained. The half-width δ_c of the intercollisional interference dip of the Q branch increases with density ρ_b of the perturbing gas and satisfies the equation $\delta_c = a_o + a\rho_b$ for all the binary mixtures.

An interesting finding in the enhancement spectra of the fundamental band of HD in HD-Kr and HD-Xe mixtures is the first observation of a narrow line at the $R_1(1)$ position

whose intensity increases with the rare gas density. This line is interpreted as due to a constructive interference between the allowed dipole of HD and the collision-induced dipole of the colliding pair HD-Kr or HD-Xe and the effect is referred to as "intracollisional interference."

The collision-induced absorption spectra of the fundamental band of HD in the pure gas were recorded for gas densities up to 50 amagat at 77 and 196 K on a two meter high pressure absorption cell and at 298 K on the one meter absorption cell. The binary and ternary absorption coefficients of the band have been derived from the experimental profiles. The contribution to the intensity of the band from the short-range overlap induction was obtained from the analysis of the absorption profiles. For the HD-HD molecular pairs, the overlap parameters λ and ρ, which give respectively the magnitude and range of the overlap dipole moment, and $\mu(\sigma)$, the overlap-induced dipole moment at the Lennard-Jones intermolecular diameter σ, were determined by obtaining the best fit of the calculated overlap part from the theory of Van Kranendonk (1958) to the experimental values of the overlap parts. The collision-induced absorption spectra of the fundamental band of H_2 in the pure gas was reinvestigated for densities up to 60 amagat at temperatures 77, 196, and 298 K and the overlap parameters for the H_2-H_2 collision pairs were derived by adopting a procedure similar to the one used for the fundamental band of HD in the pure gas.

ACKNOWLEDGMENTS

The research described in this thesis was carried out under the supervision of Professor S.P. Reddy to whom the author is grateful for suggesting the research project and for his guidance and encouragement through all stages of the work.

The author would like to express his gratitude to the members of the Supervisory Committee, Professor S.W. Breckon (Head of the Department), Drs. R.H. Tipping and M.J. Clouter, for their keen interest in this work. Thanks are also due to Dr. N.H. Rich for helpful conversations and Mr. P. Gillard, a fellow graduate student, for help in several aspects of computer programming. The collaboration of Dr. G. Varghese in the low temperature experiments on hydrogen is gratefully acknowledged. The author also expresses his sincere thanks to Professor J.D. Poll of the University of Guelph, and Dr. R.H. Tipping who contributed a theoretical model for the "intracollisional interference effect" which is outlined in Appendix B.

The cooperation received from the following technical staff of the Physics Department is gratefully acknowledged: Messrs. T.G. White, A.J. Walsh, and M. Ryan in several aspects of the experimental setup; Messrs. R.J. Penny and

A.W. McCloy in problems connected with the electronics; Messrs. R. Guest and R. Tucker for drafting many of the diagrams; Messrs. P. Stone and R. Guest for doing the photographic work. Thanks are due to the Technical Services, Memorial University of Newfoundland, for their help in building the nitrogen flushing system.

The author acknowledges with gratitude the help received from Professors J.F. Ogilvie and D. Barton of the Department of Chemistry, in preparing the HCN calibration standard and performing the mass spectrometric analysis of the HD samples, respectively.

The author wishes to thank Mrs. D. Strange for typing the manuscript.

During his graduate work at Memorial University of Newfoundland, the author has been on study-leave of absence from the Department of Physics, University of Ranchi, Ranchi (Bihar), India. Thanks are due to the University of Ranchi for this, and to Professor M.P. Gupta, Head of the Physics Department there, for his encouragement.

The author appreciates the use of the computer facilities provided by Memorial University of Newfoundland and the Newfoundland and Labrador Computer Services Limited.

The financial support received from Memorial University of Newfoundland and from Dr. Reddy's N.R.C. Operating Grant A-2440, are gratefully acknowledged.

Finally, the author wishes to thank his wife and the members of his family for their understanding and inestimable help during the course of this work.

CHAPTER I

INTRODUCTION

Homonuclear diatomic molecules such as hydrogen, deuterium, nitrogen, oxygen, etc., do not exhibit ordinary electric dipole infrared spectra corresponding to molecular rotation or vibration in the free state because of the symmetry of their charge configuration in their ground electronic states. However, these molecules when compressed in their pure state or in their mixtures with other gases give rise to infrared spectra due to electric dipoles induced in two or more colliding molecules by intermolecular forces mainly because of (i) the overlap of the electron clouds, and (ii) the quadrupolar induction resulting from the polarization of one molecule by the quadrupole field of the other.* Actually, this induced dipole moment is modulated by the internal rotation, vibration, and relative translational motion of the colliding molecules and the resulting absorption spectra are known as collision-

*Weak infrared spectra occur due to the hexadecapole-induced electric dipole moment which arises during collisions from the polarization of one molecule by the hexadecapole field of the other but these are not considered here.

induced infrared absorption spectra. The discovery of collision-induced absorption was first made in compressed oxygen and nitrogen by Crawford, Welsh, and Locke (1949) in the regions of their fundamental vibrational frequencies.

Although the HD molecule, just as the H_2 and D_2 molecules, has no electric dipole moment in the equilibrium position in its ground electronic state, a weak, oscillating dipole moment results in it because, during a molecular vibration, the displacements of the proton are greater than those of the deuteron and the negative charge center of the electrons lags behind the positive charge center of the nuclei. The occurrence of a rotation-vibration spectrum of HD due to this oscillating electric dipole moment was first predicted by Wick (1935). Weak rotation-vibration absorption bands of HD were first observed by Herzberg (1950) near 9650 and 7400 $\mathring{A}$ and were identified as the 3-0 and 4-0 bands, respectively. Later, a detailed experimental investigation of the 1-0, 2-0, 3-0, and 4-0 bands was made by Durie and Herzberg (1960) who obtained precise vibrational and rotational constants of HD in its ground electronic state. Subsequently, the pure rotational spectrum of HD was observed by Trefler and Gush (1968) who determined the dipole moment of HD by measuring the integrated intensities of four R_0 lines.* Recently, McKellar (1973, 1974)

---

*The subscripts in R_0, R_1, Q_0, Q_1, S_0, S_1, etc., denote $\Delta v (= v' - v'')$, the change in the vibrational quantum number.

made a comprehensive study of the 1-0, 2-0, 3-0, and 4-0 bands of HD and measured the intensity of 13 electric dipole transitions and one electric quadrupole transition. Bejar and Gush (1974) also measured independently the intensities of 5 electric dipole transitions of the 1-0 band of HD. The selection rule for the rotational transitions arising from the electric dipole moment is $\Delta J = \pm 1$ and that for the transitions arising from the electric quadrupole moment is $\Delta J = 0, \pm 2$.

Since the first observation of the collision-induced absorption of the fundamental band of H_2 by Welsh et al. (1949), there have been extensive studies of the collision-induced spectra of H_2 and D_2. A comprehensive review of this work has been given by Welsh (1972) (see also Reddy and Chang 1973 and Russell, Reddy, and Cho 1974 and the references therein). The work on the collision-induced absorption in HD has been very limited, however. The pure rotational collision-induced absorption of HD in gaseous and solid phases has been studied by Trefler, Cappel, and Gush (1969). Recently, McKellar (1973) studied the collision-induced fundamental band of HD in the gaseous phase at 77 K. There have also been studies of the fundamental band of HD, in solid HD by Crane and Gush (1966) and in HD dissolved in liquid argon by Holleman and Ewing (1966), and of the pure rotational band of HD dissolved in liquid argon by Holleman and Ewing (1967).

Up to moderate pressures, collision-induced absorption is caused mainly by binary collisions between molecules. Only at high pressures ternary and higher order collisions contribute considerably to the total absorption. According to the theory of the collision-induced absorption of diatomic gases proposed by Van Kranendonk (1957, 1958), the dipole moment induced in a colliding pair of molecules is represented by the so called "exponential-4" model. In this model, the induced dipole moment consists of two additive parts. One part is the isotropic short-range overlap moment which decreases exponentially with increasing intermolecular separation R and the other part is the anisotropic long-range moment, resulting from the polarization of one molecule by the quadrupole field of the other molecule, which varies as R^{-4}. The short-range moment contributes mainly to the intensity of the broad Q (i.e., $Q_{overlap}$) ($\Delta J = 0$) lines. The most interesting feature of the Q branch in the collision-induced fundamental bands is the occurrence of the dips in the $Q_{overlap}$ components. The low- and high-frequency maxima of these dips are known as Q_P and Q_R, the separation of which is strongly density-dependent. This phenomenon was explained by Van Kranendonk (1968) in terms of an "intercollisional interference effect" which will be discussed later in this chapter. The long-range moment contributes to the intensity of the relatively less broad

O ($\Delta J = -2$), Q (i.e., $Q_{quad.}$) ($\Delta J = 0$), and S ($\Delta J = +2$) lines. If the perturbing molecule is monatomic, only single transitions $O_1(J)$, $Q_1(J)$ ($J \neq 0$), and $S_1(J)$ occur in the spectra and if it has a quadrupole moment, these single transitions as well as the double (simultaneous) transitions of the types $Q_1(J) + Q_0(J)$ and $Q_1(J) + S_0(J)$ occur. In a single transition, molecule 1 of the colliding pair makes a vibration or a vibration-rotation transition while the internal energy of molecule 2 does not change. In a double transition both the colliding molecules simultaneously absorb a photon which corresponds to a vibrational transition $Q_1(J)$ in one molecule and a rotational transition $S_0(J)$ or an orientational transition $Q_0(J)$ ($J \neq 0$) in the other molecule.

It was shown that the intensity in the low- and high- wavenumber wings of the Q branch of the fundamental band of H_2 (Chisholm and Welsh 1954) and the intensity of the S lines in the pure rotational spectrum of H_2 (Kiss and Welsh 1959) obey the Boltzmann relation

$$\tilde{\alpha}^-(\nu_m - \Delta\nu) = \tilde{\alpha}^+(\nu_m + \Delta\nu) \exp(-hc\Delta\nu/kT)$$

where $\tilde{\alpha}^-(\nu_m - \Delta\nu)$ is the absorption intensity (with the wavenumber factor removed) at a wavenumber $\Delta\nu$ lower than the molecular wavenumber ν_m (in cm^{-1}) and $\tilde{\alpha}^+(\nu_m + \Delta\nu)$ is the intensity at a wavenumber $\Delta\nu$ higher than ν_m. This relation indicates that in collision-induced absorption a line of

molecular wavenumber ν_m has the summation and difference tones $\nu_m \pm \nu_{tr}$, where ν_{tr} represents a continuum of wavenumbers corresponding to the relative translational energy of the colliding molecules.

The first profile analysis of a collision-induced spectrum was made by Kiss and Welsh (1959) who used a Boltzmann-modified dispersion line shape (see Chapter III) for the individual lines of the pure rotational spectrum of H_2. Similar method was used by Hunt and Welsh (1964) to analyze the profiles of the fundamental band of H_2. Using the dispersion line shape for the high wavenumber component Q_R of the Q branch and a Boltzmann-modified dispersion line shape for the quadrupolar S lines and neglecting the splitting of the Q branch, they were able to make an analysis of the most of the high wavenumber wing of the band. Later, in analyzing the fundamental band of H_2 in the pure gas at low densities and low temperatures, where the dip in the Q branch was not very apparent, Watanabe and Welsh (1967) found that both the overlap and the quadrupolar components could be represented by a Boltzmann-modified dispersion line form. Watanabe (1971) reanalyzed the absorption profiles of the fundamental band of H_2 in the pure gas at 18, 20.4, and 24 K making use of the matrix elements of the quadrupole moment and of the polarizability of H_2, calculated theoretically by Karl and Poll (1967) and Kolos and Wolniewicz (1967), respectively.

Bosomworth and Gush (1965), who investigated the far infrared pure translational spectra of the rare gas mixtures and of H_2 and the pure rotational spectra of H_2 found that the dispersion line form gave too much intensity in the tail. A better fit of the synthetic profile to the experimental profile was obtained by them by attaching an exponential tail to the dispersion line form. Later, Mactaggart and Hunt (1969) used a dispersion line curve with a power-law tail and obtained a much better representation of the experimental data of the high-wavenumber wing of the pure rotational spectrum of H_2.

The line shapes discussed above are empirical in nature and have no theoretical basis. As a matter of fact, in collision-induced absorption the line shape must be derived from the Fourier transform of the intracollisional time correlation function of the induced dipole moment. Levine and Birnbaum (1967) in an attempt to obtain a theoretical line shape for the observed collision-induced pure translational spectra arising on account of the short-range overlap induced dipole moments used a Gaussian-type dipole moment rather than a pure exponential form related to the overlap interaction; this dipole moment tends to zero as the intermolecular separation R tends to zero. Assuming ideal straight-line collision paths for the colliding molecules, Levine and Birnbaum (1967) calculated an intracollisional line shape in the form of a modified

Bessel function of the second kind. Sears (1968) calculated the translational line shape function classically, assuming an isotropic model for the induced dipole moment and a Lennard-Jones potential for the colliding pairs of molecules. Van Kranendonk (1968) showed that the splitting in the overlap Q branch could be interpreted in terms of the negative correlations existing between the short-range dipole moments induced in successive collisions. This "intercollisional interference" effect is density-dependent. When the binary collisions are of finite duration, the total correlation function is the convolution of the intracollisional and intercollisional correlation functions. This means that the overlap Q components must be represented as a product of the intercollisional and intracollisional line shapes. Van Kranendonk (1968) has shown that the intercollisional interference dip of the Q branch can be represented by a dispersion-type intensity distribution; therefore the width of the corresponding dip must increase with increasing density.

Recently, Mactaggart and Welsh (1973) found that in the enhancement profiles of the collision-induced fundamental band of H_2 in pH_2-He mixtures at 77 K, the Levine-Birnbaum line shape gave a better reproduction of the overlap-induced $Q_1(0)$ component than the line form given by Sears. For the quadrupole-induced components, theoretical derivations of the line form are not yet available.

However, the dispersion shape has been found to reproduce the experimental profiles reasonably well. Mactaggart and Welsh (1973) and Mactaggart, De Remigis, and Welsh (1973) have analyzed satisfactorily the enhancement profiles of the fundamental band of H_2 in several H_2- inert gas mixtures using the Levine-Birnbaum line shape and Van Kranendonk's dispersion-type line shape for the intracollisional part and the intercollisional part, respectively, of the overlap-induced Q components and dispersion line shape for the quadrupole-induced Q and S components. Prior to the present work, the new line shapes have not been applied for the absorption profiles of the H_2 fundamental band in the pure H_2 gas where a large number of double transitions make the analysis more complicated.

De Remigis, Mactaggart, and Welsh (1971) discovered a pronounced narrowing of the quadrupole-induced transitions in the fundamental band of H_2 in H_2-Ar mixtures for the argon densities greater than 350 amagat and in H_2-Ar liquid solutions. They found that the half-width of the $S_1(1)$ line remains constant up to $\sim$ 300 amagat and varies inversely as the argon density beyond 350 amagat. These studies have been extended by Mactaggart et al. (1973) to the binary mixtures pH_2-Ar, H_2-Kr, and H_2-Xe. The pressure narrowing of the quadrupole-induced lines has been explained as a diffusional effect by Zaidi and Van Kranendonk (1971). This diffusional narrowing of the quadrupole-induced lines

is not of particular interest in the present thesis.

One of the objects of the present work was to make a systematic study of the collision-induced fundamental band of HD in gaseous phase under a variety of experimental conditions, first by obtaining accurate experimental profiles and then by performing the profile analysis using the most recently derived line shapes. The main experimental difficulty was the strong absorption of the atmospheric water vapor in the region of the fundamental band of HD and this was solved by careful experimentation. The details of the experimental techniques used in the present work are given in Chapter II.

The enhancement absorption profiles of the fundamental band of a diatomic gas in its binary mixtures with inert gases are simpler than the corresponding profiles in the pure gas because the former contain only single transitions. The collision-induced fundamental band of HD was studied in the binary mixtures HD-He, HD-Ne, HD-Ar, HD-Kr, and HD-Xe at room temperature for different base densities of HD and for a large number of total densities of mixtures up to 190 amagat using a one meter high pressure absorption cell. The results of the work on HD-He have recently been published (Prasad and Reddy 1975). The experimental data and the results of the profile analysis in all these five mixtures are presented in Chapter III.

During the course of these experiments, the occurrence of a narrow line at the $R_1(1)$ position in the enhancement spectra of the fundamental band of HD in HD-Kr and HD-Xe mixtures was discovered. The intensity of this line was found to increase with the rare gas density. This line is interpreted as due to a constructive interference between the allowed dipole moment of HD and the collision-induced dipole moment of the colliding pair of molecules. This effect is referred to as "intracollisional interference". Chapter IV presents the experimental results and the theoretical calculations (Poll, Tipping, Prasad, and Reddy 1976) of this work.

The absorption profiles of the HD fundamental band in the pure gas were obtained for densities up to 50 amagat at 77 and 196 K on a two meter high pressure absorption cell and at 298 K on the one meter cell. The overlap contribution to the intensity of the band at the three temperatures was separated by the method of profile analysis making use of the new line shapes. It was then possible to obtain the overlap parameters λ and ρ, which give respectively the magnitude and the range of the overlap dipole moment, and $\mu(\sigma)$, the overlap-induced dipole moment at the Lennard-Jones intermolecular diameter σ, for the HD-HD collision pairs from the theory of Van Kranendonk (1958). Some of the results of the work on the fundamental band of HD in the pure gas at 298 K have been recently

published (Prasad and Reddy 1975). The results of this work are given in Chapter V.

Even though a great deal of experimental work has been done in the past on the collision-induced fundamental band of H_2, the new line shapes have not been applied so far to the profiles in the pure gas mainly because of the complexity of the spectrum due to a large number of double transitions. It is also the object of the present work to perform the profile analysis of the H_2 fundamental band recorded in the pure gas at different temperatures using the new line shapes and to derive the various overlap parameters for the H_2-H_2 collision pairs. The profiles of the fundamental band of H_2 in the pure gas were recorded for densities up to 60 amagat at 77, 196, and 298 K with the same apparatus which was used for the work on HD and their analysis was completed. The results of this phase of the work are presented in Chapter VI.

CHAPTER II

APPARATUS AND EXPERIMENTAL PROCEDURE

The work reported in the present thesis on the collision-induced fundamental bands of hydrogen deuteride and hydrogen at temperatures 77, 196, and 298 K was carried out with different absorption cells, an infrared recording spectrometer, a high-pressure gas handling system and other necessary apparatus. In this chapter a description of the apparatus and experimental procedure will be presented.

1. Absorption Cells

(a) The 1 m Absorption Cell

Several experiments on the collision-induced fundamental band of HD in the pure gas and in its binary mixtures with inert gases He, Ne, Ar, Kr, and Xe, and an experiment on the collision-induced fundamental band of H_2 in the pure gas, at room temperature, were carried out with a transmission type 1 m absorption cell (for the original description, see Bishop 1966, and Chang 1971). The details of construction of this cell are shown in Fig. II-1.

The main body A of the absorption cell is a 303 stainless steel tube 1 m long, 3/4 in. in diameter and 1/8 in. in wall thickness. The inner flange F was

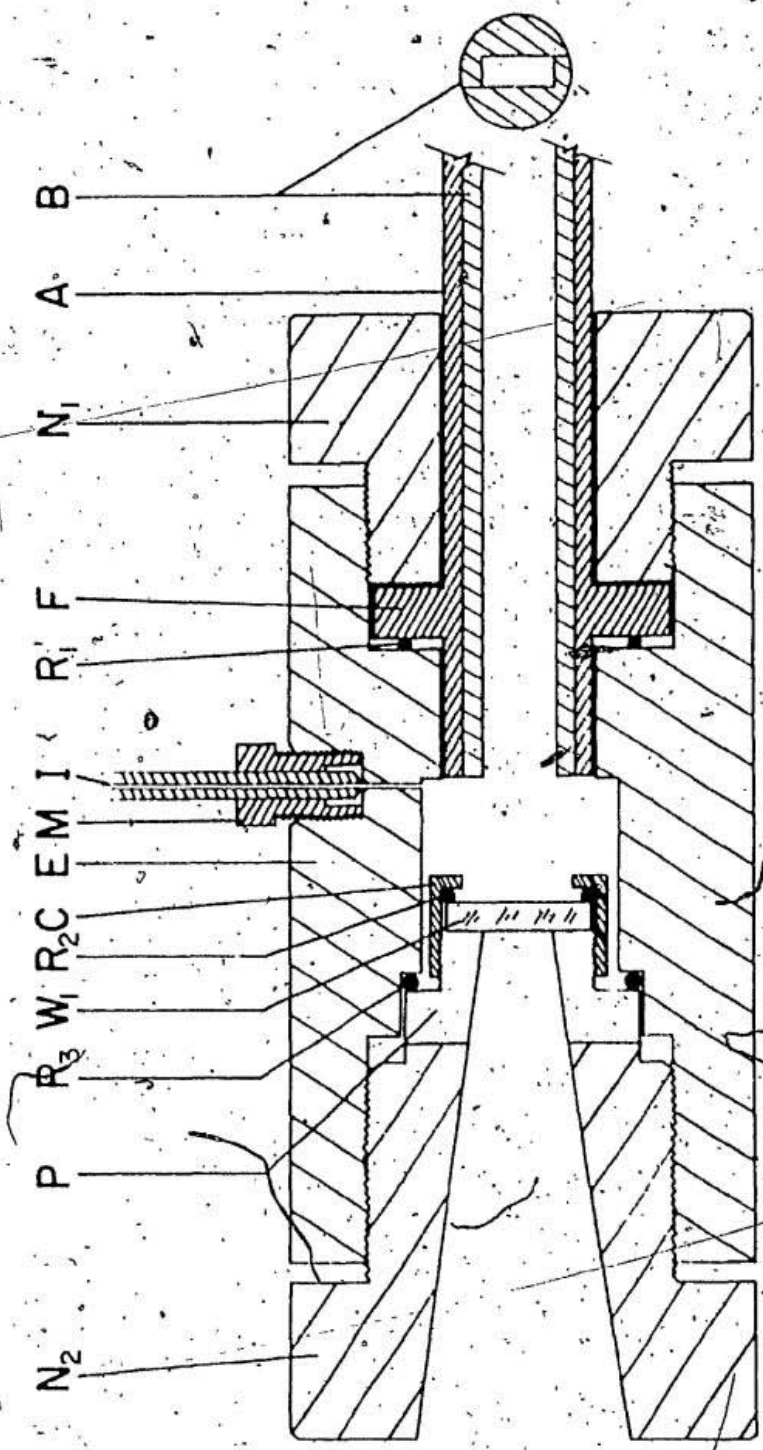

Fig. II-1. A cross-sectional view of one end of the 1 m absorption cell.

hard-soldered to the cell body A. The end piece E was made from a 303 stainless steel cylinder 3 in. in diameter and 5 in. long. Each end piece was attached to the cell body by means of a steel closing nut N_1. A pressure-tight seal between the cell A and end piece E was obtained by means of the stainless steel ring R_1. The light guide B was made in four sections with rectangular aperture 0.4 in. x 0.2 in. and was highly polished inside. Optically flat synthetic sapphire plates 1 in. in diameter and 5 mm thick constituted the entrance or exit window W_1. General Electric RTV-108 silicone rubber cement was used to hold the sapphire window against the optically flat window plate P. The window plate holder is of rectangular aperture 0.5 in. x 0.2 in. Teflon ring R_2 fitted in steel cap C prevented the window from becoming loose during evacuation. With teflon ring R_3 between the window plate P and the end piece E, the stainless steel nut N_2 was tightened until a pressure-tight seal was obtained. The square-shaped portion of the window plate fitted into a matched recess of the end piece E, thus preventing the misalignment of the window plate with the light guide while the nut N_2 was tightened. The gas inlet I consists of a stainless steel capillary tube, 1/4 in. in diameter, which was connected to the cell body by means of an Aminco fitting M. The sample path length of the cell is 105.2 cm.

(b) The 2 m Absorption Cell

A 2 m transmission type absorption cell which was originally constructed for the room temperature work (Reddy and Kuo 1971) and later modified for the low temperature work (Chang 1974) was adopted in the present study of the fundamental band of HD in the pure gas at 77 and 196 K and of the fundamental band of H_2 in the pure gas at 77, 196, and 298 K. Its constructional details are shown in Fig. II-2.

The absorption tube made from a 2 m stainless steel (type 303) bar, has a 3 in. outer diameter and a 1 in. central bore which was drilled with a $\pm$ 0.010 in. tolerance by Industrial Machining Limited, Montreal. The polished stainless steel light guide B which was made in five sections has a rectangular aperture 1 cm x 0.5 cm. Optically flat synthetic sapphire window W_1, 1 in. in diameter and 1 cm thick, was attached to the polished stainless steel window seat P_1 which has a rectangular aperture 0.4 in. x 0.2 in. General Electric RTV-108 silicone rubber cement provided the necessary sealing between the window and the seat. In order to obtain a pressure-tight seal between the window seat and the absorption tube, invar ring R_1 was placed between them and the end piece E was tightened against the cell body by means of eight Allenoy steel Allen head screws S_1.

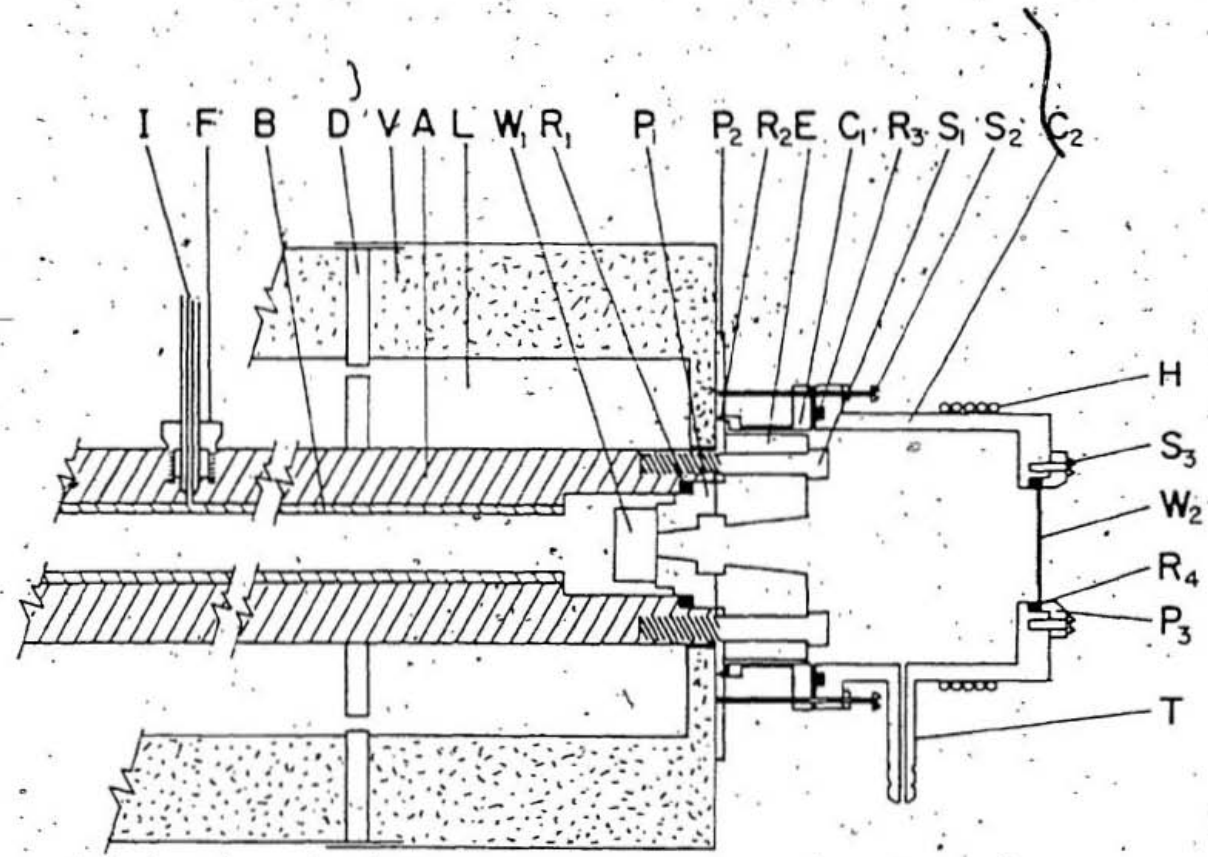

Fig. II-2. A cross-sectional view of one end of the 2 m absorption cell.

Two concentric cylinders made of stainless steel sheet 1/32 in. thick provided the cooling and the insulating jackets for the absorption cell. The weight of the absorption cell was supported by two stainless steel discs D, which in turn were welded to the inner cylinder that had a diameter of 5 7/8 in. These discs have holes which allow the coolant to flow freely in the inner jacket. The outer cylinder, 11 in. in diameter, was made in three pieces and is capable of accommodating the contraction of the inner cylinder when the absorption cell is cooled. The outer and inner cylinders were welded to stainless steel sheets fitting around the absorption cell. Finally, the outer jacket was steel-welded to the body of the cell. The space between the inner and outer jackets was insulated with vermiculite V.

A cylindrical vacuum chamber C was provided at each end of the cell. This consists of two cylindrical adapters, C_1 of stainless steel and C_2 of plexiglas. Adapter C_1 has a thin central portion to prevent flanges connecting C_1 and C_2 from getting too cold. Aluminum foil was wrapped over the end piece E and also inside C_1 and C_2 to reflect back the heat from the outside. A flat synthetic sapphire window W_2, 2 in. in diameter and 3 mm thick, was sealed with a neoprene O-ring R_4 against the plexiglas adapter C_2 by the plexiglas end plate P_3 by means of three screws S_3. Adapter C_1 was sealed to C_2 with a neoprene O-ring R_3 by

tightening six screws S_2 into a 1/4 in. thick stainless steel plate P_2 welded on to the outer jacket. These screws also serve to obtain a seal between P_2 and C_1 with an indium ring R_2. The flanges connecting C_1 and C_2 were later covered with General Electric RTV-108 silicone rubber cement. Heating coils H were wound around the plexiglas chamber, and a small current ($\sim$ 0.2 amp) was maintained to prevent the window W_2 from frosting. The chamber C was under constant evacuation through the side tube T in order to prevent the window W_1 from frosting.

The capillary tube I fitted to the cell by means of a 1/2 in. Aminco fitting F served as the gas inlet. The coolants used for the low temperature experiments were liquid nitrogen (77 K) and acetone-dry ice mixture (196 K). An opening in the central section of the jacket was provided to admit the coolants. The sample path length of the cell at room temperature is 195.3 cm.

2. The Experimental Arrangement

(a) The Optical System

The optical system used for the low temperature experiments is shown schematically in Fig. II-3. The arrangement for the room temperature experiments was the same in principle. The infrared radiation source S is a 600 watt General Electric FFJ quartzline projection lamp mounted in a specially prepared water cooled brass housing (for details see Chang 1974). The power to operate this

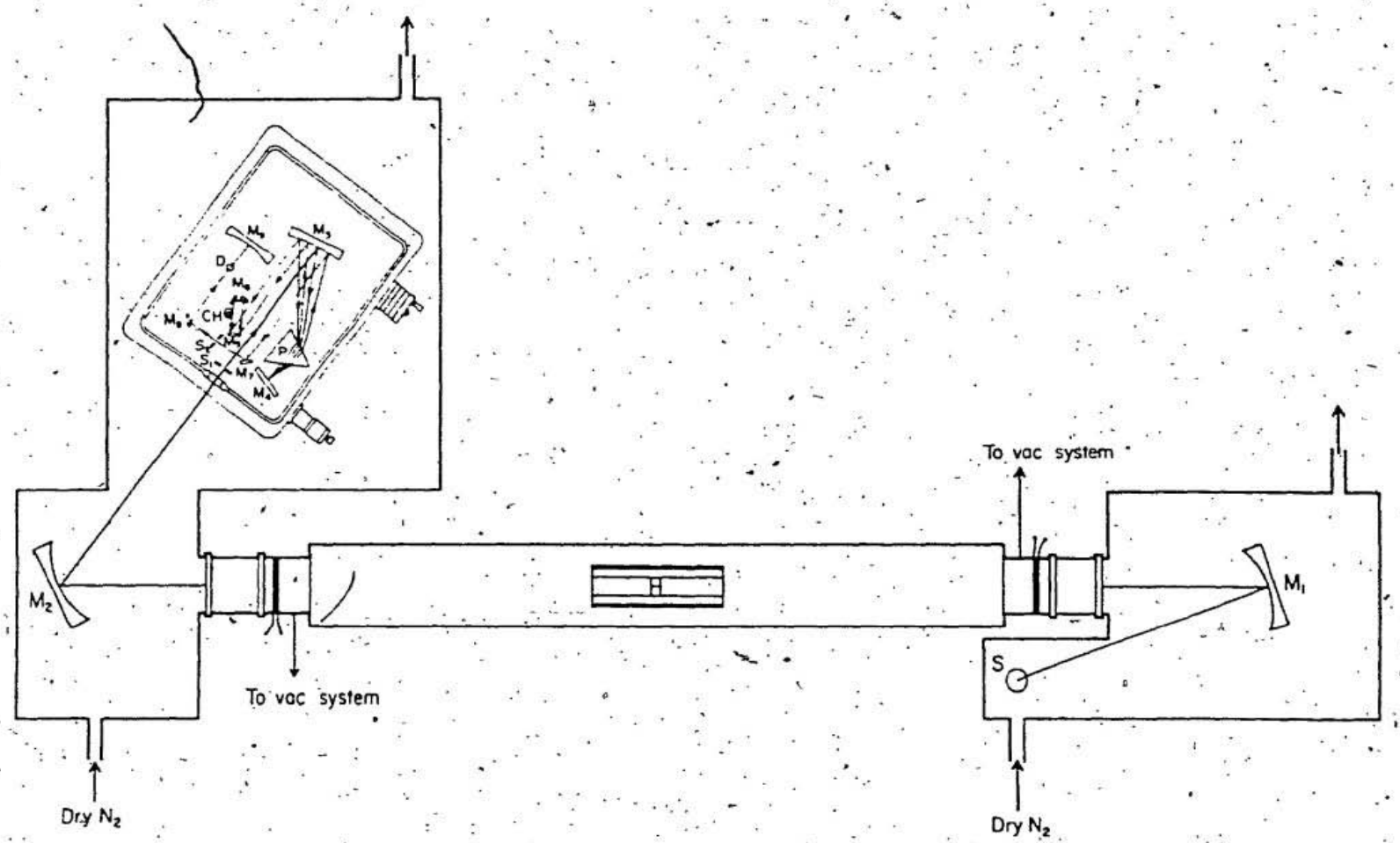

Fig. II-3. The optical arrangement.

lamp was obtained from a Sorenson ACR-2000 a.c. regulator. Concave mirror M_1 focused radiation from the lamp on the entrance window of the absorption cell H. The radiation coming out of the absorption cell was focused on the entrance slit of the spectrometer by means of a similar concave mirror M_2. Each of M_1 and M_2 is a front-coated spherical mirror with a radius of curvature of 60 cm and a diameter of 15 cm.

A Perkin-Elmer Model 112 single-beam double-pass infrared spectrometer equipped with a lithium fluoride prism and an uncooled lead sulfide detector was used to record the spectra. The arrows in Fig. II-3 show the path of the radiation in the monochromator. The chopper is located such that only light which has doubly passed the prism is modulated. The slit of the spectrometer maintained at widths of 50 μm (for the experiments at room temperature) and 35 μm (for the low-temperature experiments) gave spectral resolutions of $\sim$ 3.0 cm^{-1} and $\sim$ 2.0 cm^{-1}, respectively, at the origin (3632 cm^{-1}) of the fundamental band of HD and the accuracy of the wavenumber measurement was $\sim$ 1.0 cm^{-1}. A slit width of 35 μm gave a spectral resolution of $\sim$ 3.0 cm^{-1} at the origin (4161 cm^{-1}) of the fundamental band of H_2. The plexiglas end pieces of the cell were connected to the plexiglas boxes.

(b) The Detection-Amplification System

The electrical and mechanical arrangements of the experimental set up are shown schematically in Fig. II-4. The infrared radiation transmitted by the absorption cell was focused on the lead sulfide detector by the optical system (not shown). The infrared energy received by the detector is converted into an electrical signal which is proportional to the intensity of the energy. The signal is then amplified, rectified, filtered and fed to the recorder.

The experiments on the HD fundamental band at room temperature were initially completed with the spectrometer equipped with a Perkin-Elmer amplifier Model 107 and a Leeds and Northrup strip chart recorder (not shown in Fig. II-4). This amplifier is a lock-in 13 Hz type and the rectifiers are breaker-type synchronous rectifiers activated by the rotations of the 13 Hz chopper shaft. Noise components are removed by electrical filters in the amplifier unit. The signal is supplied to the recorder amplifier and a battery voltage is supplied to the slide wire of the recorder. The recorder permits continuous recording of the spectrum.

The electronics in the detection-amplification system was modified somewhat for the low temperature work on HD and for the work on H_2 on the basis of the following considerations.

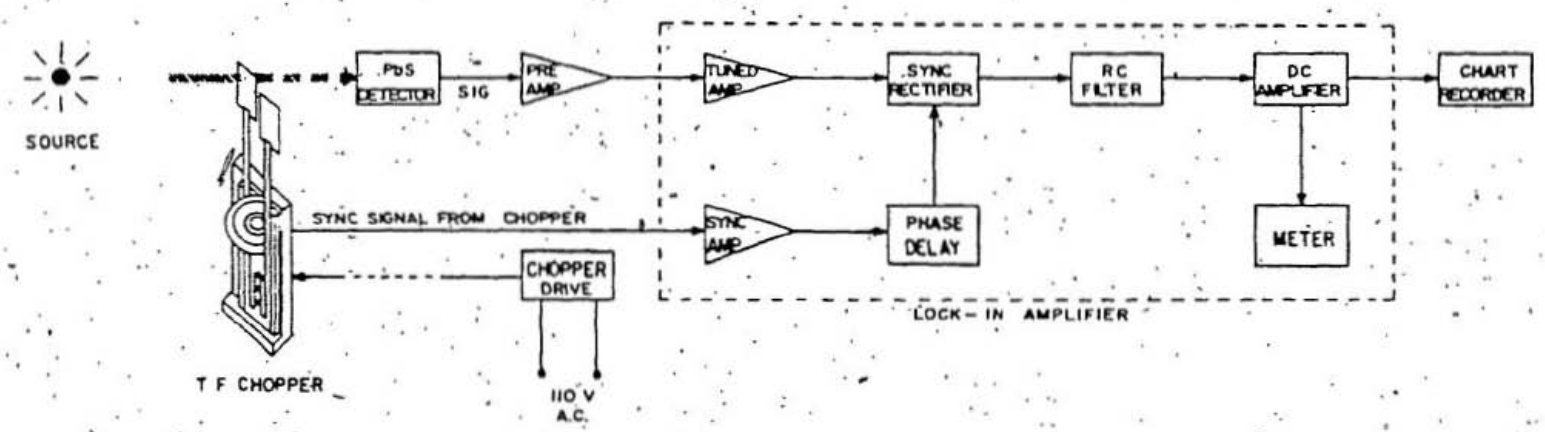

Fig. II-4. A schematic diagram of the signal detection-amplification system with a tuning fork chopper.

(i) With the 13 Hz mechanical chopper, noise in the electronics comes mainly from the dirt picked up by the breaker points.

(ii) A self-checking electronic system would be much preferred.

(iii) A PbS detector is expected to give an optimum signal-to-noise ratio when the radiation signal is modulated with a chopper having much larger frequency than 13 Hz.

The 13 Hz mechanical chopper in the spectrometer was replaced by a 260 Hz tuning fork chopper Model L-40 supplied by American Time Products. The size of this tuning fork is small enough to fit it into the position of the 13 Hz chopper in the monochromator so that it chops only the second pass signal. The previous preamplifier and the 13 Hz amplifier were replaced by a DUNN Model LI-101 preamplifier and a Brower Laboratories Model 101 lock-in voltmeter. The reference signal was supplied by the power supply unit for the tuning fork and the phasing adjustment is a part of the lock-in voltmeter. With these modifications in the experimental set up (Fig. II-4), it was possible to obtain an optimum signal-to-noise ratio for the PbS detector.

3. Calibration of the Spectral Region and Reduction of Recorder Traces of the Spectra

The spectral region 2800 - 6000 cm^{-1} which covers the fundamental bands of HD and H_2 was calibrated with the standard wavenumbers of the Hg emission lines (Humphreys 1953, Plyler et al. 1955), absorption peaks of atmospheric water vapor and absorption lines of the fundamental bands of HCN and HCl (I.U.P.A.C. Tables of Wavenumber 1961). The standard HCN and HCl quartz absorption cells were prepared in our laboratory for the purpose of calibration. A computer program was used to obtain a smooth curve through the points on a graph of wavenumber against position on a recorder trace. The procedure adopted for this purpose is as follows: The distances of the standard emission and absorption peaks were accurately measured from a reference H_2O absorption peak on the recorder charts. These distances $d(\nu)$ were then expressed as a polynomial function of wavenumber $\nu(cm^{-1})$ in the form

$$d(\nu) = A + B\nu + C\nu^2 + D\nu^3 + E\nu^4 + F\nu^5. \quad (2\text{-}1)$$

A least-squares fit was obtained to calculate the constants A to F, and these constants were in turn used to obtain wavenumber against position on a recorder trace at 5, 10, or 20 cm^{-1} intervals. A calibration chart was then drawn on a tracing paper giving the position along the recorder trace at these intervals.

The absorption coefficient $\alpha(\nu)$ at a given wavenumber ν(in cm^{-1}) of an absorbing gas at a density ρ_a in

a cell of sample path length ℓ is given by the quantity $(1/\ell) \ln [I_0(\nu)/I(\nu)]$, where $I_0(\nu)$ and $I(\nu)$ are the intensities of radiation transmitted by the evacuated cell and by the cell filled with the absorbing gas, respectively. The enhancement in the absorption coefficient $\alpha_{en}(\nu)$ due to the addition of a perturbing gas at a density ρ_b into the absorption cell containing the absorbing gas at a fixed base density ρ_a is given by $(1/\ell) \ln [I_1(\nu)/I_2(\nu)]$, where $I_1(\nu)$ and $I_2(\nu)$ are the intensities transmitted by the cell filled with the absorbing gas and with the binary gas mixture, respectively. The wavenumber calibration chart was positioned on the recorder traces and the quantity $\log_{10} [I_0(\nu)/I(\nu)]$ or $\log_{10} [I_1(\nu)/I_2(\nu)]$ was measured at the marked intervals on the chart with the help of a standard logarithmic scale. Absorption profiles were obtained by plotting $\log_{10} [I_0(\nu)/I(\nu)]$ or $\log_{10} [I_1(\nu)/I_2(\nu)]$ against ν. The integrated absorption coefficient of the band $\int \alpha(\nu) d\nu$ and $\int \alpha_{en}(\nu) d\nu$ (in cm^{-2}) were then derived from the areas measured under the experimental profiles.

4. Removal of Water Vapor from the Optical Path

The fundamental band of HD falls in the spectral region where there is a very strong absorption due to the atmospheric water vapor. It was, therefore, imperative to remove all traces of atmospheric water vapor from the path of the infrared radiation from the source to the detector in order to make reliable intensity measurements of the HD

absorption band. In the experimental arrangement with the 1 m absorption cell, the whole optical system, including the radiation source, the absorption cell, and the monochromator, was enclosed in an airtight plexiglas box which was provided with a side window fitted with a neoprene glove to facilitate the necessary adjustments without breaking the airtight seal. The system was flushed continuously with the dry nitrogen gas produced by evaporating liquid nitrogen by an electrical heater constructed from a 220 ohm 5 watt resistor and immersed in the dewar containing liquid nitrogen. The consumption of liquid nitrogen was about 10 litres a day. Initially, it took several days of flushing to obtain background recorder traces almost free from absorption of the atmospheric water vapor.

For the experiments with the low temperature 2 m absorption cell it was not possible to enclose the entire system in an airtight box as the jacket surrounding the absorption cell had to be filled with coolants at regular intervals during the experiments. The isolation of the system from the atmospheric water vapor was achieved by constructing two suitable plexiglas boxes and coupling them at the ends of the cell (see Fig. II-3) to the vacuum chamber with the help of rubber tubes. The radiation source and one of the spherical mirrors were arranged in one box whereas the spectrometer and the second mirror were arranged in the other box. The boxes were flushed

separately with dry nitrogen gas and the consumption of liquid nitrogen for this purpose was about 10 litres a day. As before, several days of flushing was found necessary to reduce the atmospheric water vapor absorption to a minimum. The actual experiments were carried out when the background recorder traces were found very steady. In fact, for the empty cell, the background recorder traces taken prior to an experiment, which took nearly 10 hours at times, matched very well with the ones taken after the experiment.

5. Isothermal Data of Gases and Estimation of Partial Density of a Foreign Gas in a Binary Mixture

In this thesis, the densities of the gases are expressed in units of amagat, which is the ratio of the density of a gas at a given temperature and pressure to its density at the standard temperature and pressure (S.T.P.). If ρ_a (or ρ_b) represents the density of a gas expressed in amagat, $\rho_a n_0$ (or $\rho_b n_0$) gives the number of gas molecules per cm^3, n_0 being the Loschmidt's number (number density of an ideal gas at S.T.P.: $2.687 \times 10^{19}\ cm^{-3}$).

The pressure-density data for HD are not readily available from the literature. In the present work, these data for HD at a given temperature were obtained from the isothermal data for H_2 and D_2 at the same temperature by the method of interpolation. In fact, the isothermal data of H_2 are almost identical with those of D_2 in most of the pressure ranges used in the present experiments and in such

situations the data for HD were directly obtained from those of either H_2 or D_2. Isothermal data for H_2, D_2, He, Ne, Ar, Kr, and Xe are obtained from various references which are summarized in Table II-1.

TABLE II-1

References for the isothermal data of experimental gases*

Gas	Temperature (K)	Reference
H_2	77	Dean (1961)
	196	Michels et al. (1959)
	298	Michels and Goudeket (1941)
		Michels et al. (1959)
D_2	77	Sinha (1967)
	196	Michels et al. (1959)
	298	Michels and Goudeket (1941)
		Michels et al. (1959)
He	298	Mann (1962)
		Michels and Wouters (1941)
Ne	298	Michels et al. (1960)
Ar	298	Michels et al. (1956)
Kr	298	Trappeniers et al. (1966)
Xe	298	Michels et al. (1954)

*The isothermal data for H_2 and D_2 at 196 K (-77°C) were interpolated from their respective data at -75 and -100°C.

The partial density ρ_b of the perturbing gas in a binary mixture was determined from the formula (see, for example, Reddy and Cho 1965)

$$\rho_b = \left(\frac{1}{1+\beta}\right)\left[(\rho_a)_P + \beta(\rho_b)_P\right] - \rho_a \qquad (2\text{-}2)$$

where $(\rho_a)_P$ is the density of the absorbing gas at the

total pressure P of the mixture and $(\rho_b)_P$ is the density of the perturbing gas at the same pressure P, and $\lambda = \rho_b' / \rho_a$, where ρ_b' is the approximate partial density of the perturbing gas corresponding to the partial pressure $P_b = P - P_a$, P_a being the pressure of the absorbing gas. The quantity ρ_a is the base density of the absorbing gas. The final value of ρ_b was determined by the method of successive iterations.

6. Gas Handling and Sample Analysis

The gas handling system used for the experiments at the room temperature is shown schematically in Fig. II-5. The Bourdon tube pressure gauges G_1 and G_2 which were calibrated against an Ashcroft dead-weight pressure balance (accuracy > 1%) have ranges 0-1000 and 0-5000 p.s.i., respectively. The liquid nitrogen trap C was made of a copper coil 1/4 in. in outside diameter. Each of C_1 and C_2 consists of two columns of molecular sieve of type 4A kept in copper tubings, 3/8 in. in outside diameter. Thermal compressors T_1 and T_2 were made from stainless steel and H represents the high pressure absorption cell. All the valves in the system are Aminco high-pressure needle valves. Except for the part containing the copper tubing, the assembled system was tested for pressures up to 5500 p.s.i.

Prior to the actual mixture experiments, each of the perturbing gases He, Ne, Ar, Kr, and Xe was tested for

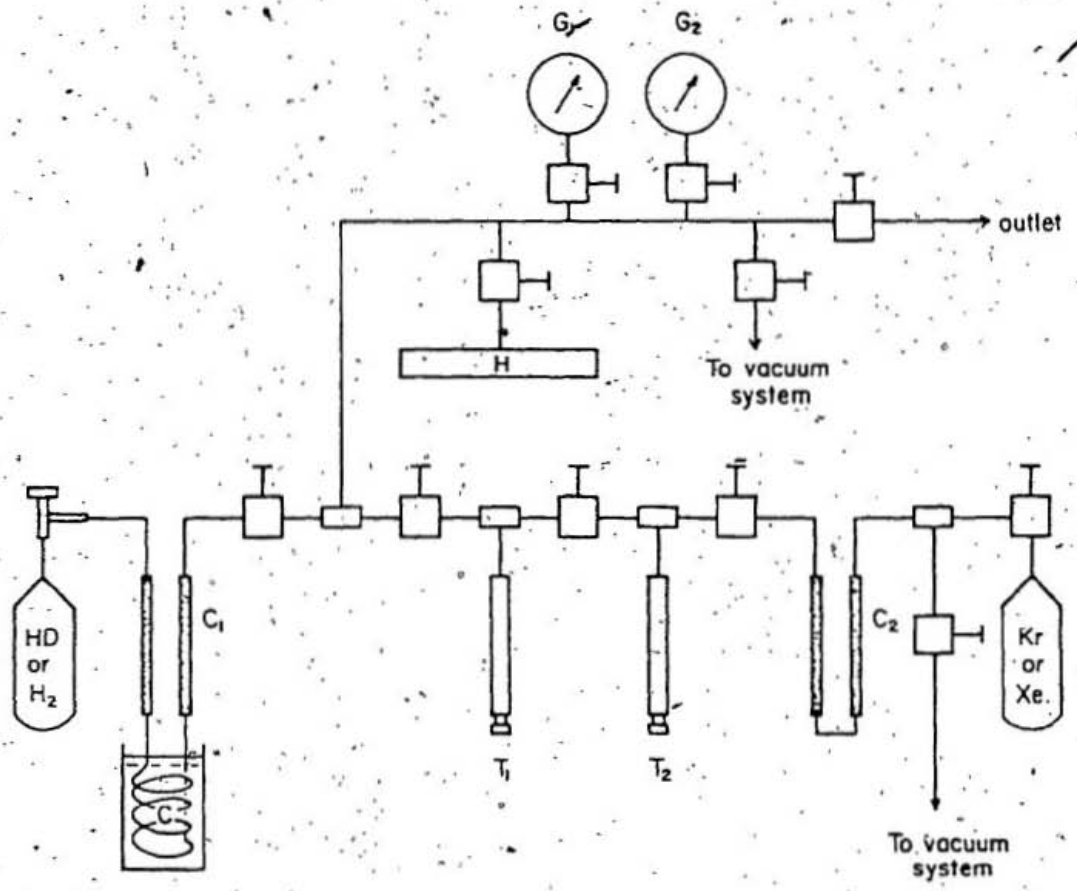

Fig. II-5. The gas handling system.

impurities such as water vapor, carbon dioxide, etc., by obtaining spectrometer traces in and around the region of the HD fundamental band. Helium supplied by Canadian Liquid Air, and Ne and Ar supplied by Matheson of Canada Limited, were found to be free from any detectable water vapor or any other impurity. However, Kr and Xe (both of research grade) supplied by Matheson of Canada Limited were found to contain traces of carbon dioxide, ethane, and water vapor. Therefore, a careful attempt was made to remove these impurities from Kr and Xe. The stainless steel cylinder containing Kr was immersed in an ethanol-liquid nitrogen bath (157 K) and that containing Xe was immersed in a methanol-liquid nitrogen bath (175 K), and thus the impurities CO_2, C_2H_6, and H_2O were frozen. Krypton or xenon was then allowed to solidify in thermal compressors immersed in liquid nitrogen, after allowing it to pass through two columns of molecular sieve, type 4A. Any impurities left in either liquid or gaseous state in the thermal compressors were then pumped out of the system. This process of purification of Kr and Xe was repeated a number of times. Purified Kr and Xe were then tested for impurities and it was found that Kr for pressures up to 1700 p.s.i. and Xe for pressures up to 800 p.s.i. did not show any impurities. However, above these pressure limits, both gases showed collision-induced absorption features of ethane in the region 4000-4500 cm^{-1}. Because of this

limitation, our experiments for HD-Kr and HD-Xe were confined to total gas pressures less than 1700 and 800 p.s.i., respectively.

For the pure gas experiments, hydrogen deuteride gas supplied by Merck, Sharp, and Dohme Canada Limited, and "ultra high pure" hydrogen supplied by Matheson of Canada Limited, were used. Each of the gases was passed through molecular sieve (type 4Å) columns C_1 and the liquid nitrogen trap C, and then admitted at required pressures into the absorption cell which was initially evacuated.

For the HD-inert gas binary mixture experiments, the HD gas was first admitted into the evacuated cell to obtain a particular base pressure. The perturbing gas He, Ne or Ar from a commercial cylinder was admitted into the cell through a liquid nitrogen or liquid oxygen trap in a few quick pulses to obtain the required total pressures of the HD-inert gas mixture. In the case of Kr and Xe, thermal compressors T_1 and T_2 were used to develop required pressures. Actually, in a given mixture experiment, the base density of HD was kept constant and the profiles of the enhancement of absorption of the band were obtained for a series of partial densities of the perturbing gas. In HD-Kr and HD-Xe experiments, after all the recorder traces were taken, both Kr and Xe were recovered from the mixtures by first freezing them into their original storage cylinders immersed in liquid nitrogen and then pumping the residual

HD out slowly through a two-stage stainless steel trap. The solidified Kr or Xe was later allowed to evaporate. The process of solidification, evacuation and evaporation was repeated several times until all traces of HD were removed from these gases. A photograph of the entire experimental set up for the 2 m absorption cell is shown in Fig. II-6.

7. Isotopic Impurities in the HD Gas

The experimental gas HD was supplied to us by Merck, Sharp, and Dohme Canada Limited in two separate batches, 100 and 200 litres, respectively. The first one was used in all the experiments at the room temperature and the second one was used in the experiments at low temperatures. Mass-spectrometric analysis of these two batches of the gas showed the following compositions:

	HD	H_2	D_2
	%		
Batch I	89.8	6.4	3.8
Batch II	94.4	4.4	1.2

On the basis of this analysis, appropriate corrections were made to the density of HD as well as to the absorption profiles. For example, for the experiments with the binary mixture HD-B, where B is the perturbing gas He, Ne, Ar, Kr, or Xe, it was necessary to subtract from the "observed"

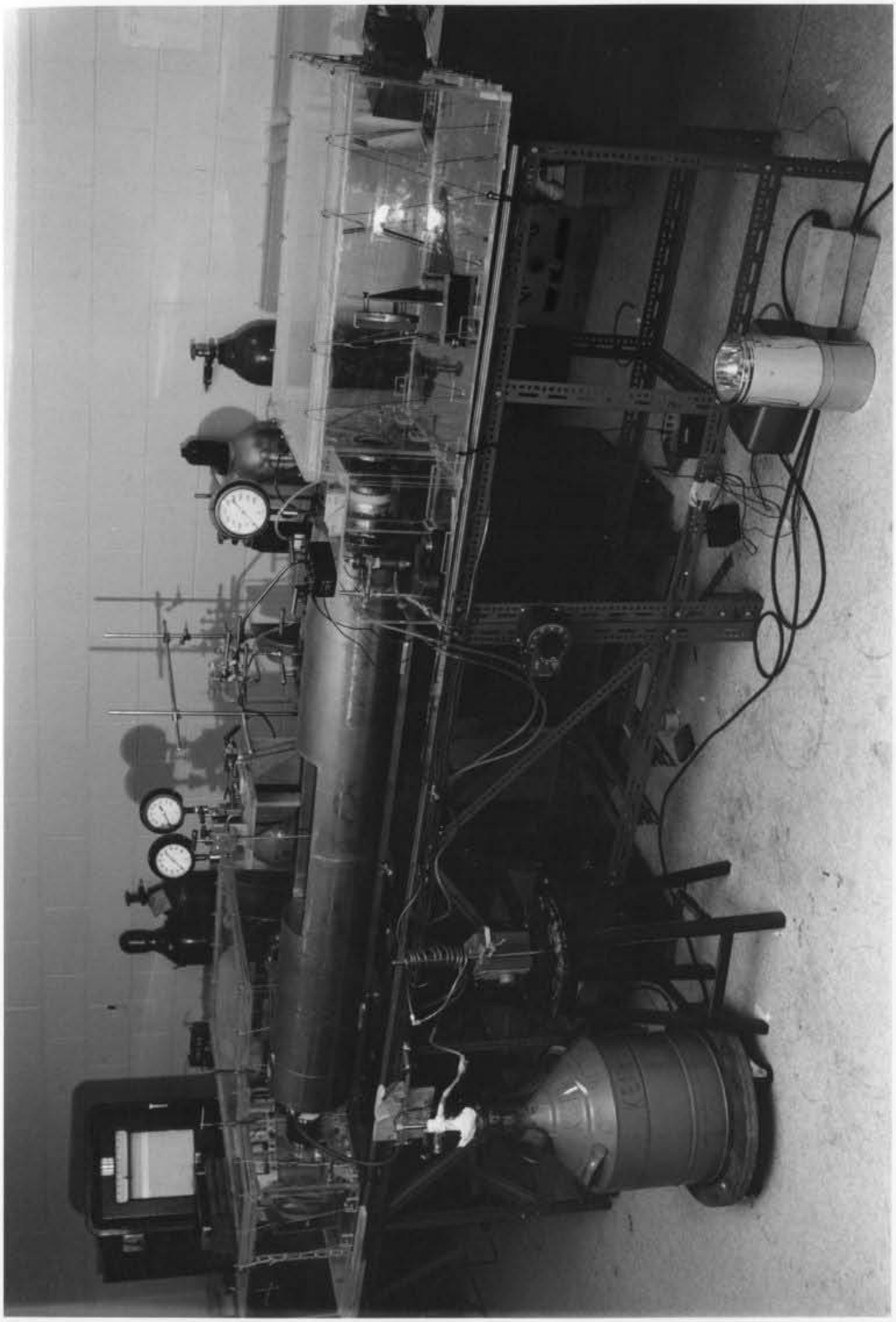

Fig. II-6. A photograph of the experimental arrangement for the 2 m absorption cell.

absorption profiles the absorption arising from the collision-induced fundamental band of H_2 due to the binary collisions H_2-B and H_2-HD. This absorption was estimated from the absorption profiles obtained with the pure H_2 gas and with H_2-B mixtures. The contribution to the integrated intensity of the HD fundamental band from the intensity of the D_2 fundamental band was found to be insignificant.

CHAPTER III

COLLISION-INDUCED ABSORPTION OF THE FUNDAMENTAL BAND OF HD IN HD-INERT GAS MIXTURES AT ROOM TEMPERATURE

The apparatus and experimental method described in the previous chapter were used to make a systematic study of the collision-induced absorption of the fundamental band of HD in its binary mixtures with He, Ne, Ar, Kr, and Xe at 298 K and in the pure HD gas at 77, 196, and 298 K. The enhancement spectra of the fundamental band of a diatomic gas in its binary mixtures with inert gases at not too high densities consist of only single transitions and do not have the complexity of the corresponding spectra of the pure gas, which consist of many double transitions in addition to the single transitions. It is logical to analyze the profiles of the relatively simpler enhancement spectra first by a method of analysis using line shapes which are consistent with the most recent theories and then to extend that method to the more complex spectra of the pure gas. The present chapter is devoted to the study of the enhancement spectra of the fundamental band of HD in HD-inert gas mixtures. The profiles of the enhancement of absorption of the band in HD-He, HD-Ne, HD-Ar, HD-Kr, and HD-Xe are presented in Section 1 and the absorption coefficients are given in

Section 2. Section 3 presents an analysis of the enhancement profiles of the band together with the results and discussion. The results of the work on the pure HD gas will be presented in Chapter V.

1. Profiles of the Enhancement of Absorption

For experiments with each of the perturbing gases He, Ne, Ar, Kr, and Xe, at least two base densities of HD were used. The base densities were in the range 5.9 to 22.6 amagat and the maximum density of the mixtures varied from 80 amagat for HD-Xe to 190 amagat for HD-He. The profiles of the enhancement of absorption were obtained at room temperature (298 K) using the absorption cell having a path length 105.2 cm. Table III-1 gives a summary of the conditions under which profiles of the enhancement of absorption were obtained.

TABLE III-1

Summary of the experiments

Mixture	Base densities of HD (amagat)	Maximum density of the mixture (amagat)	Number of mixture densities
HD-He	21.0, 22.6	190	14
HD-Ne	17.2, 19.6	125	13
HD-Ar	8.6, 10.0, 11.4	175	22
HD-Kr	5.9, 6.7	140	14
HD-Xe	5.9, 6.1	80	12

In general, the profiles of the collision-induced absorption of a gas such as HD or H_2 are dependent on the nature of the perturbing gas and some of their features such as the separation of the two maxima of the Q branch are dependent on the density. Representative profiles of the enhancement of absorption of the HD fundamental band in binary mixtures of HD with He, Ne, Ar, Kr, and Xe at room temperature are presented in Figs. III-1 to III-5. In each figure, three absorption profiles of the band for a fixed base density of HD and three different partial densities of the perturbing gas are reproduced to illustrate all the salient features. In these figures the positions of the collision-induced single transitions $O_1(2)$, $Q_1(J)$, and $S_1(J)$ for $J = 0$ to 4 calculated from the constants of the free HD molecule obtained from the high resolution Raman data of the low pressure gas (Stoicheff 1957) are marked along the wavenumber axis.

The usual collision-induced features of the profiles of the enhancement of absorption in HD-He, HD-Ne, HD-Ar, HD-Kr, and HD-Xe are similar to those observed in the corresponding binary mixtures of H_2 (see for example, Reddy and Chang 1973 for H_2-He and H_2-Ne, Varghese, Ghosh, and Reddy 1972 and Reddy and Lee 1968 for H_2-Ar and H_2-Kr, and Varghese and Reddy 1969 for H_2-Xe). In all the absorption profiles (Figs. III-1 to III-5) the main dip of the Q branch occurs at the position of the $Q_1(1)$ line (3628 cm^{-1}) of the

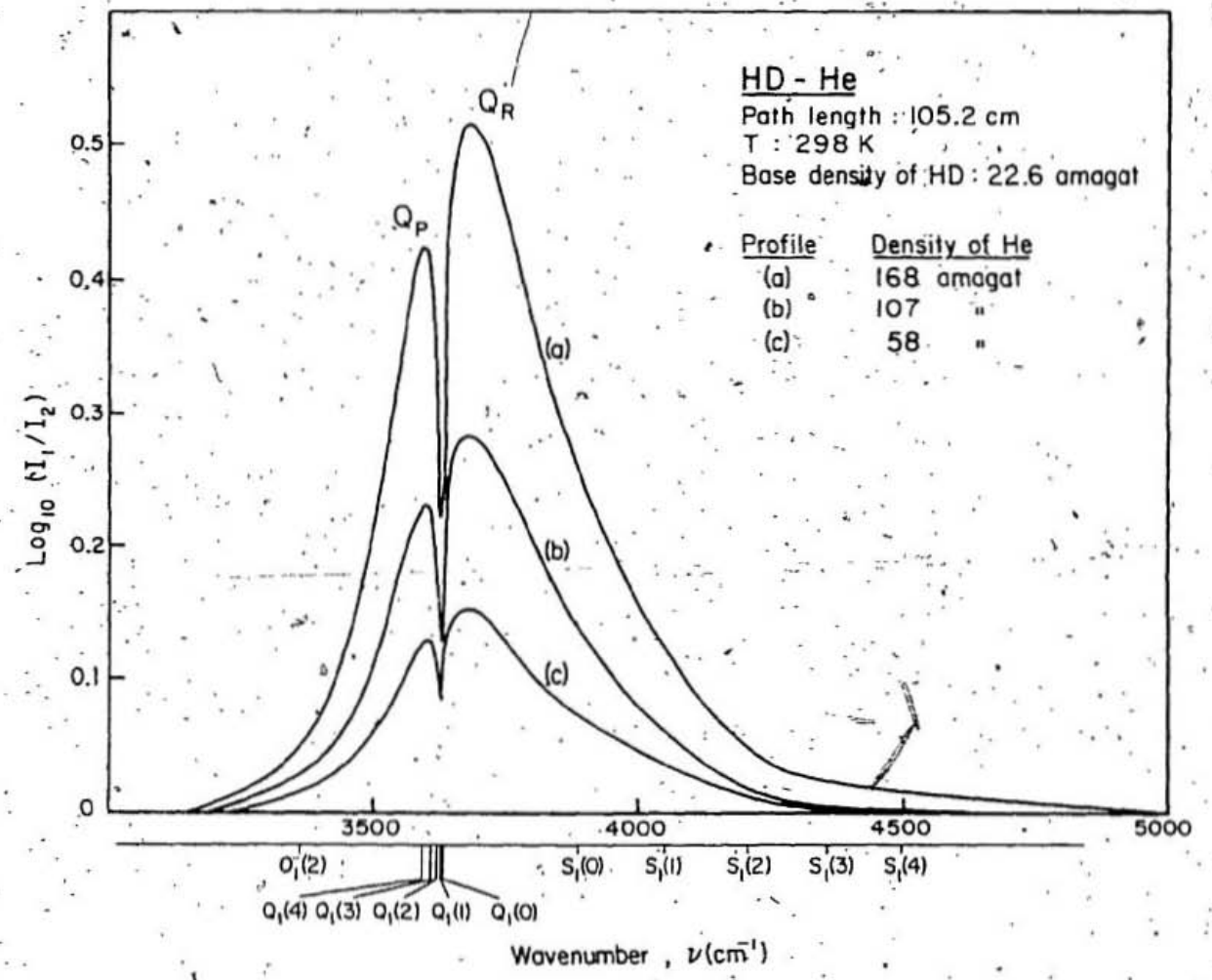

Fig. III-1. Profiles of the enhancement of absorption of the collision-induced fundamental band of HD in HD-He mixtures at 298 K.

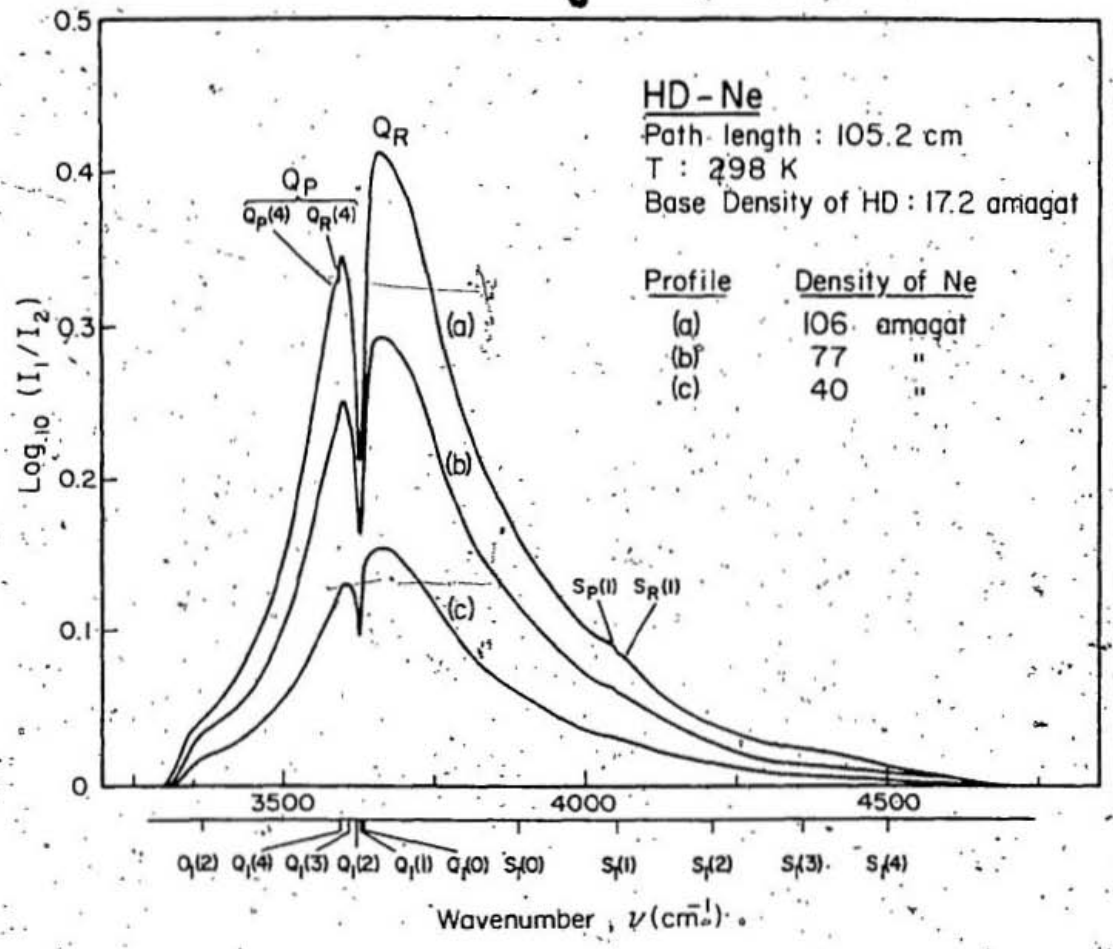

Fig. III-2. Profiles of the enhancement of absorption of the collision-induced fundamental band of HD in HD-Ne mixtures at 298 K.

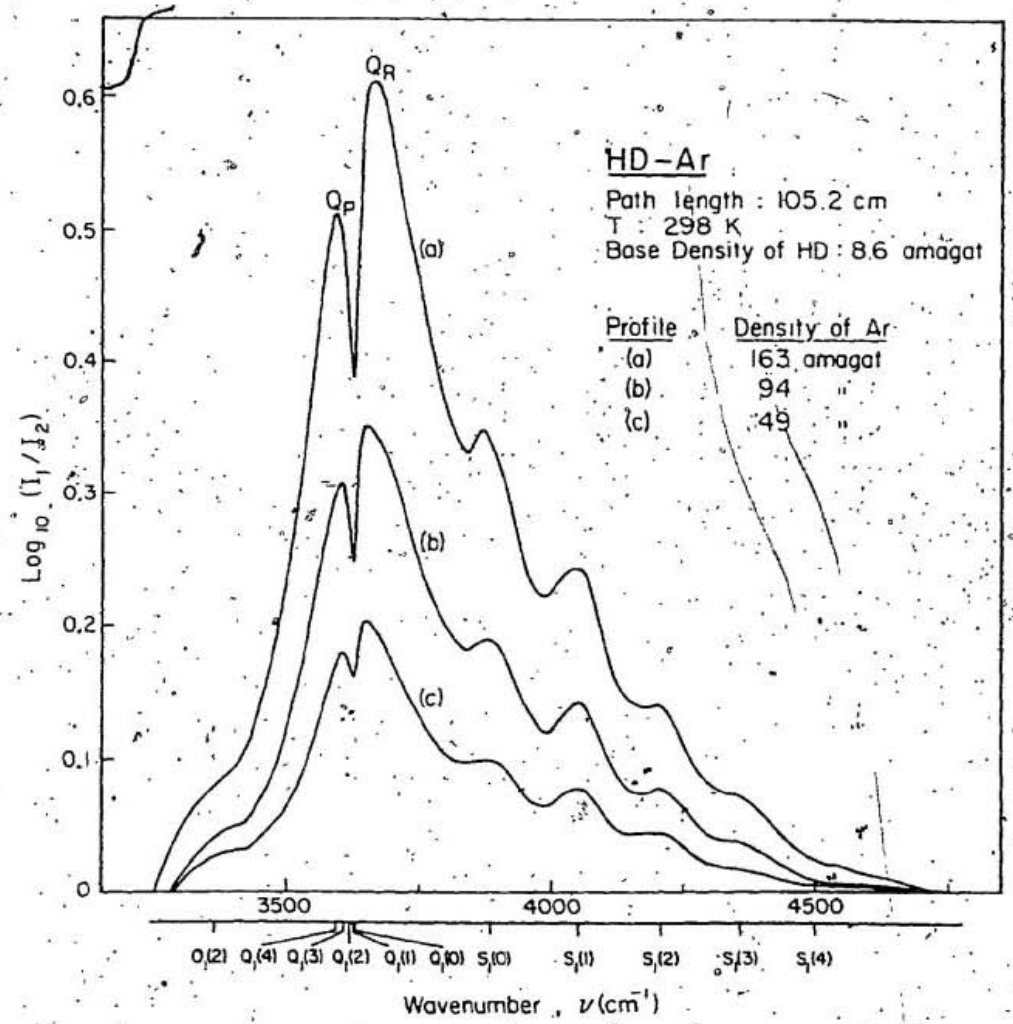

Fig. III-3. Profiles of the enhancement of absorption of the collision-induced fundamental band of HD in HD-Ar mixtures at 298 K.

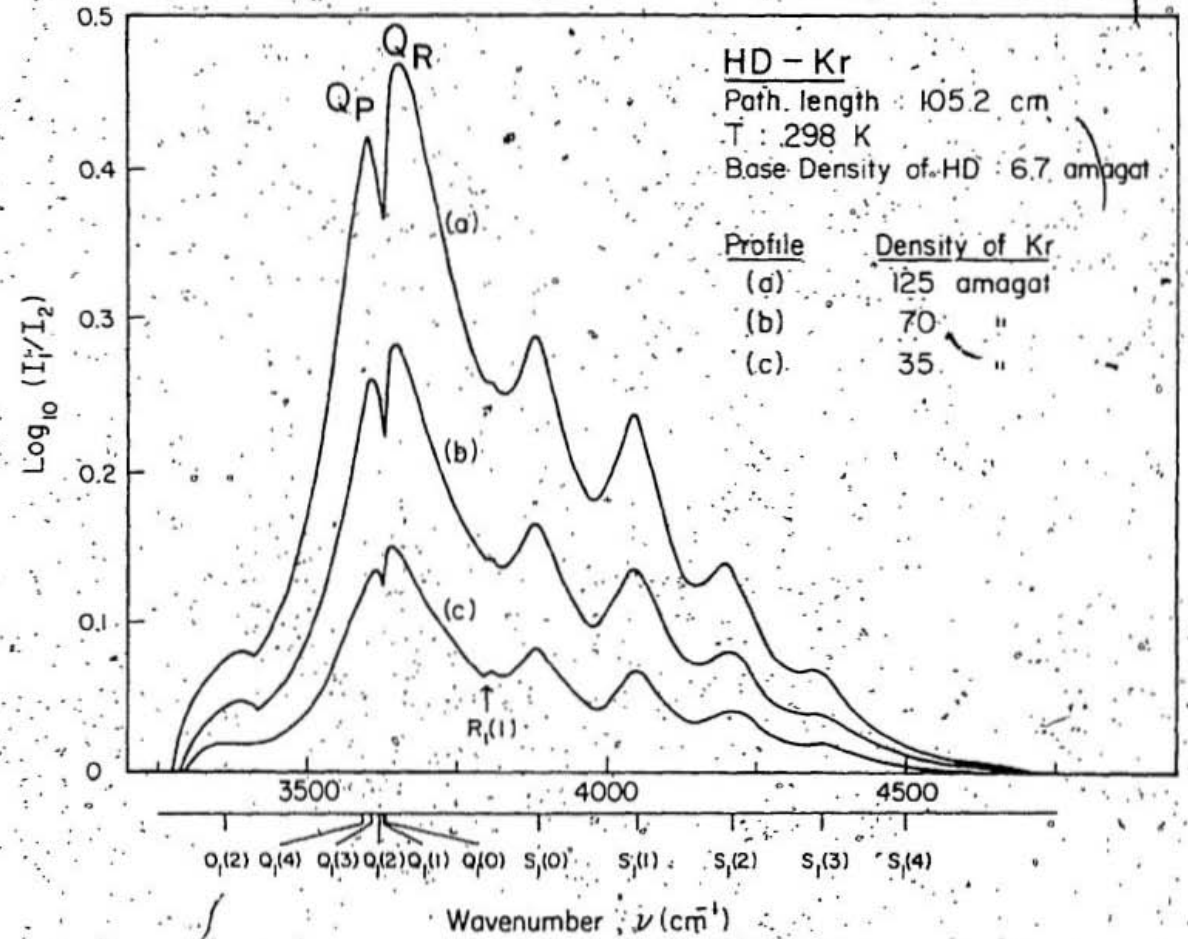

Fig. III-4. Profiles of the enhancement of absorption of the collision-induced fundamental band of HD in HD-Kr mixtures at 298 K.

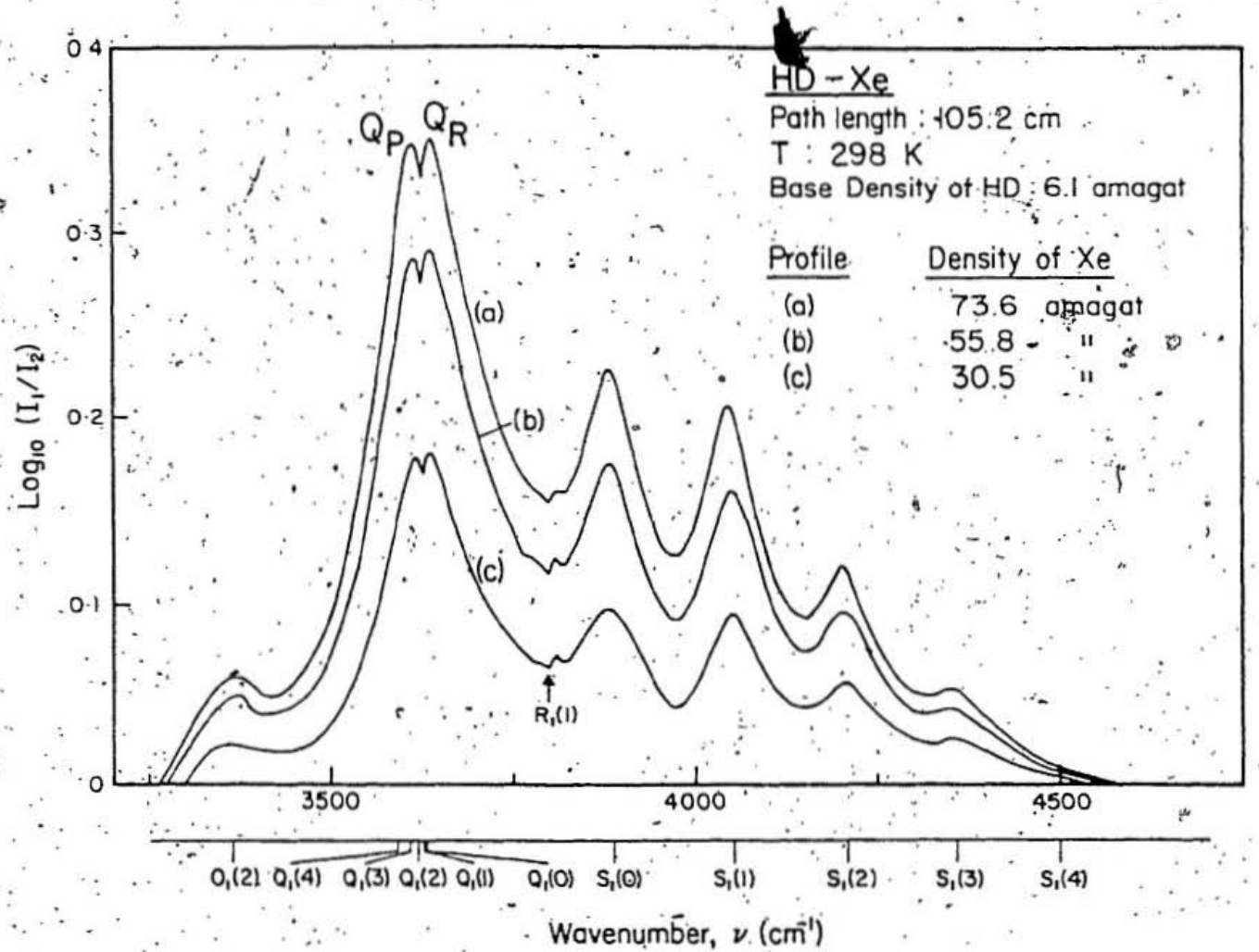

Fig. III-5. Profiles of the enhancement of absorption of the collision-induced fundamental band of HD in HD-Xe mixtures at 298 K.

free HD molecule. As mentioned in Chapter I, the dip in the Q branch of the collision-induced fundamental bands was explained by Van Kranendonk (1968) in terms of an inter-collisional interference effect due to negative correlations existing between the overlap dipole moments in successive collisions. In the experimental profiles of HD-He, HD-Ne, HD-Ar, and HD-Kr (Figs. III-1 to III-4), the separation $\Delta\nu_{PR}^{max}$ between the peaks of the components Q_P and Q_R of the Q branch increases with the density of the perturbing gas. However, for the profiles of HD-Xe (Fig. III-5), $\Delta\nu_{PR}^{max}$ appears to be approximately constant. For example, for the profiles (a), (b), and (c) of HD-He in Fig. III-1, $\Delta\nu_{PR}^{max}$ has the values 85, 83, and 80 cm^{-1}, respectively, whereas it is approximately 25 cm^{-1} for the profiles of HD-Xe (Fig. III-5).

The polarizability of the inert gas atoms increases with their size and the number of electrons; for example, $\alpha_{He} = 1.4\ a_0^3$ and $\alpha_{Xe} = 27.4\ a_0^3$. The intensity of the quadrupolar components $O_1(2)$, $Q_{1\ quad}(J)$, and $S_1(J)$ in the profiles of enhancement is dependent on the square of the polarizability of the perturbing gas. The half-width of these components is dependent on the relative translational motion of the colliding pairs of molecules; for example, the relative velocity of HD-He is greater than that of HD-Xe at the same temperature. For the binary mixtures of HD the quadrupolar components get more pronounced with a heavier

perturbing gas than with a lighter one. The differences in the intensities and half-widths of the quadrupolar lines in Figs. III-1 to III-5 can be understood in terms of the polarizability of the perturbing molecules and the relative translational motion of the colliding pairs of molecules.

In the profiles of the enhancement of absorption of HD-Ne, in addition to the main splitting of the Q branch into Q_P and Q_R components, a secondary splitting of the main Q_p component is observed (Fig. III-2). Here the minimum of the dip occurs at the position of the $Q_1(4)$ line of the free HD molecule (3594 cm^{-1}) and its low- and high-wavenumber components are therefore referred to as $Q_P(4)$ and $Q_R(4)$, respectively. The dips corresponding to the other Q lines do not appear on the traces because of their close proximity to the dips of the most intense $Q_1(1)$ line. Another prominent feature of the HD-Ne profiles is the occurrence of the dip in $S_1(1)$ position (4052 cm^{-1}) of the free HD molecule with its low- and high- wavenumber components S_P and S_R. The dip in the S lines can be attributed to the intercollisional interference in the anisotropic overlap components of the short-range dipole moments in successive collisions (see Poll, Hunt, and Mactaggart 1975 and Reddy and Chang 1973).

A very interesting feature of the HD-Kr and HD-Xe profiles (Figs. III-4 and III-5) is the occurrence of a relatively weak but narrow absorption peak at the position

of the $R_1(1)$ transition corresponding to the rotational selection rule $\Delta J = +1$. A detailed account of this together with a possible mechanism will be presented in Chapter IV.

2. Absorption Coefficients

For the collision-induced band, the integrated absorption coefficients $\int \alpha_{en}(\nu)d\nu$ in mixtures of HD with inert gases were obtained from the areas under the profiles of the enhancement of absorption. These absorption coefficients can be represented by the relation

$$\int \alpha_{en}(\nu)d\nu = \alpha_{1b}\rho_a\rho_b + \alpha_{2b}\rho_a\rho_b^2 + \ldots , \qquad (3\text{-}1)^*$$

where α_{1b} and α_{2b} are the binary and ternary absorption coefficients, and ρ_a and ρ_b are the densities of HD and the perturbing gas, respectively. For all the five HD-inert gas mixtures studied, plots of $(1/\rho_a\rho_b)\int \alpha_{en}(\nu)d\nu$ vs ρ_b are shown in Figs. III-6 to III-8. In each case the plot is found to be a straight line. The intercepts and slopes of the straight lines in these figures, which give the binary absorption coefficient α_{1b} (cm^{-2} $amagat^{-2}$) and ternary absorption coefficient α_{2b} (cm^{-2} $amagat^{-3}$), respectively, are calculated by a linear least-squares fit of the experimental data and their values are listed in Table III-2. In the derivation of the absorption coefficients the contribution of the integrated intensity due to $R_1(1)$ transition in HD-Kr and HD-Xe was considered, but was found to be several orders

---

*In this equation, the contribution to the integrated intensity from the terms arising from the other ternary (i.e., $\alpha_{2ab}\rho_a^2\rho_b$) and higher order collisions is assumed to be negligible.

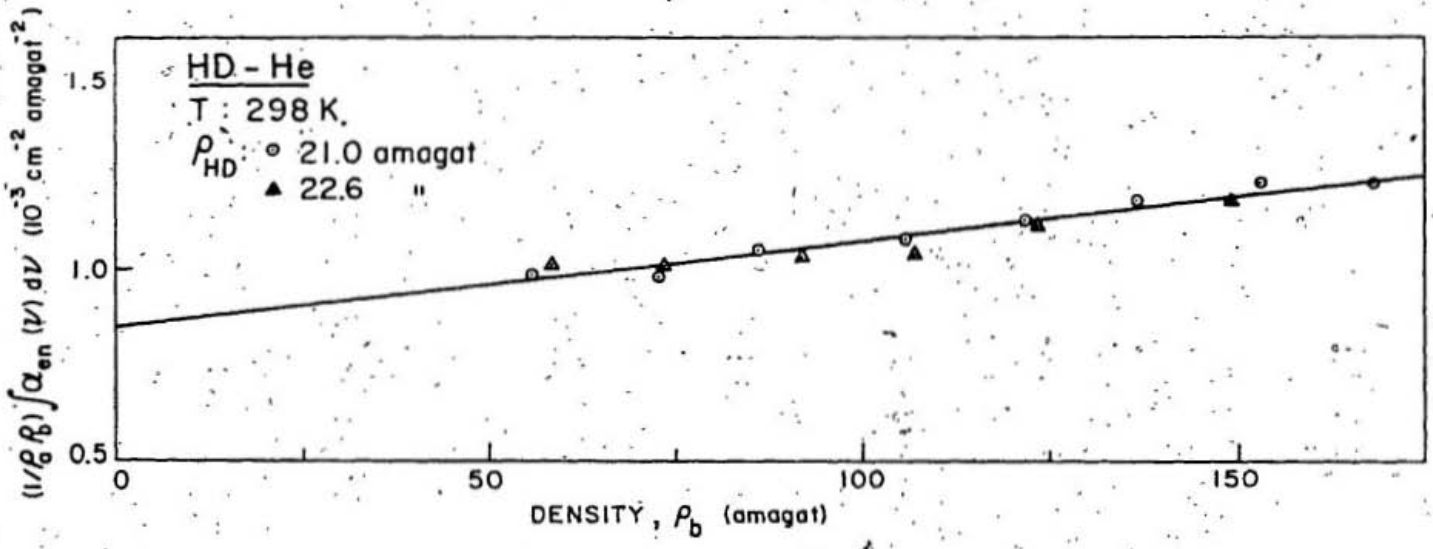

Fig. III-6. A plot of $(1/\rho_a\rho_b)\int\alpha_{en}(\nu)\,d\nu$ against ρ_b for HD-He mixtures at 298 K.

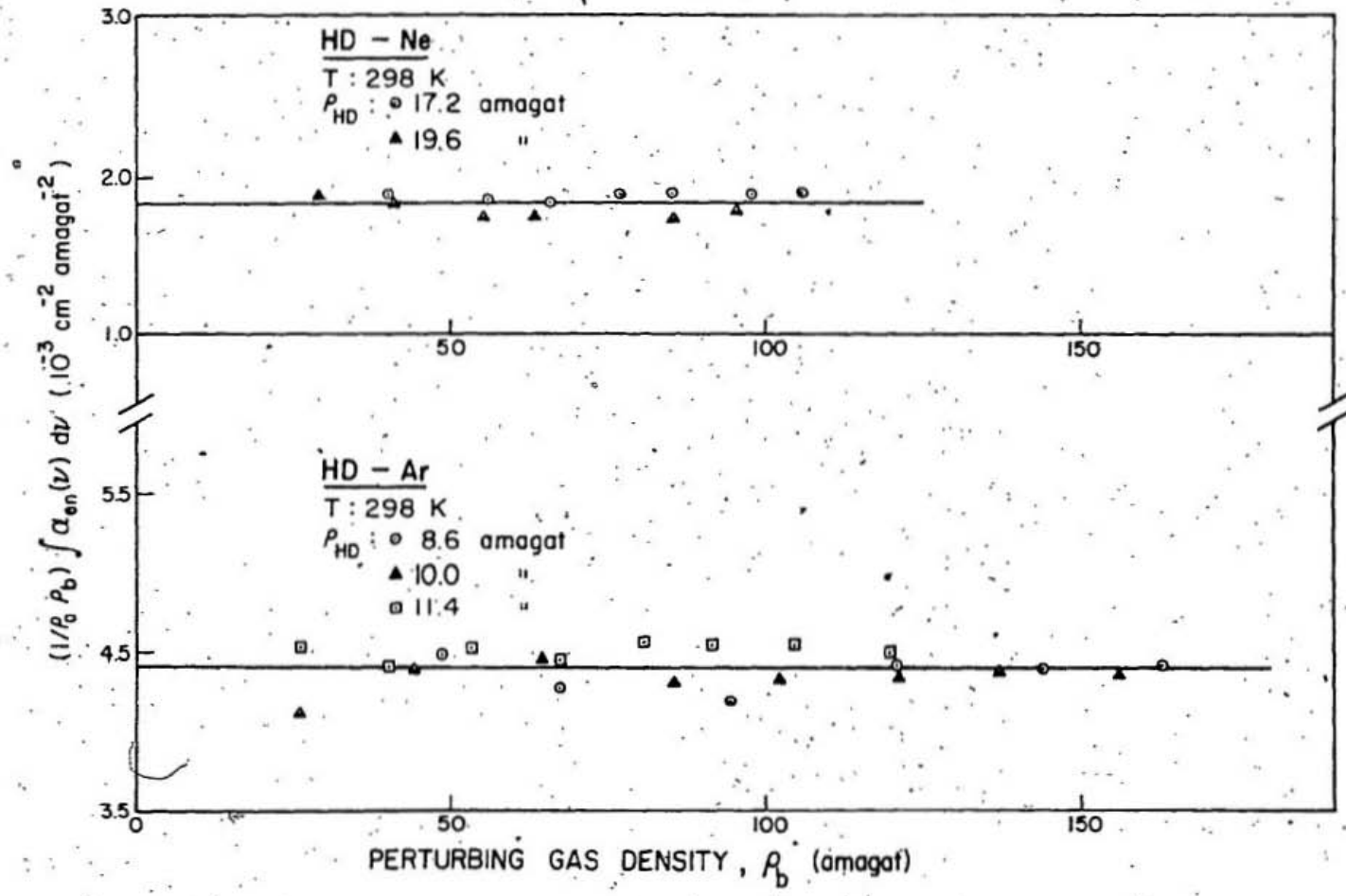

Fig. III-7. Plots of $(1/\rho_a \rho_b) \int \alpha_{en}(\nu)\, d\nu$ against ρ_b for HD-Ne and HD-Ar mixtures at 298 K.

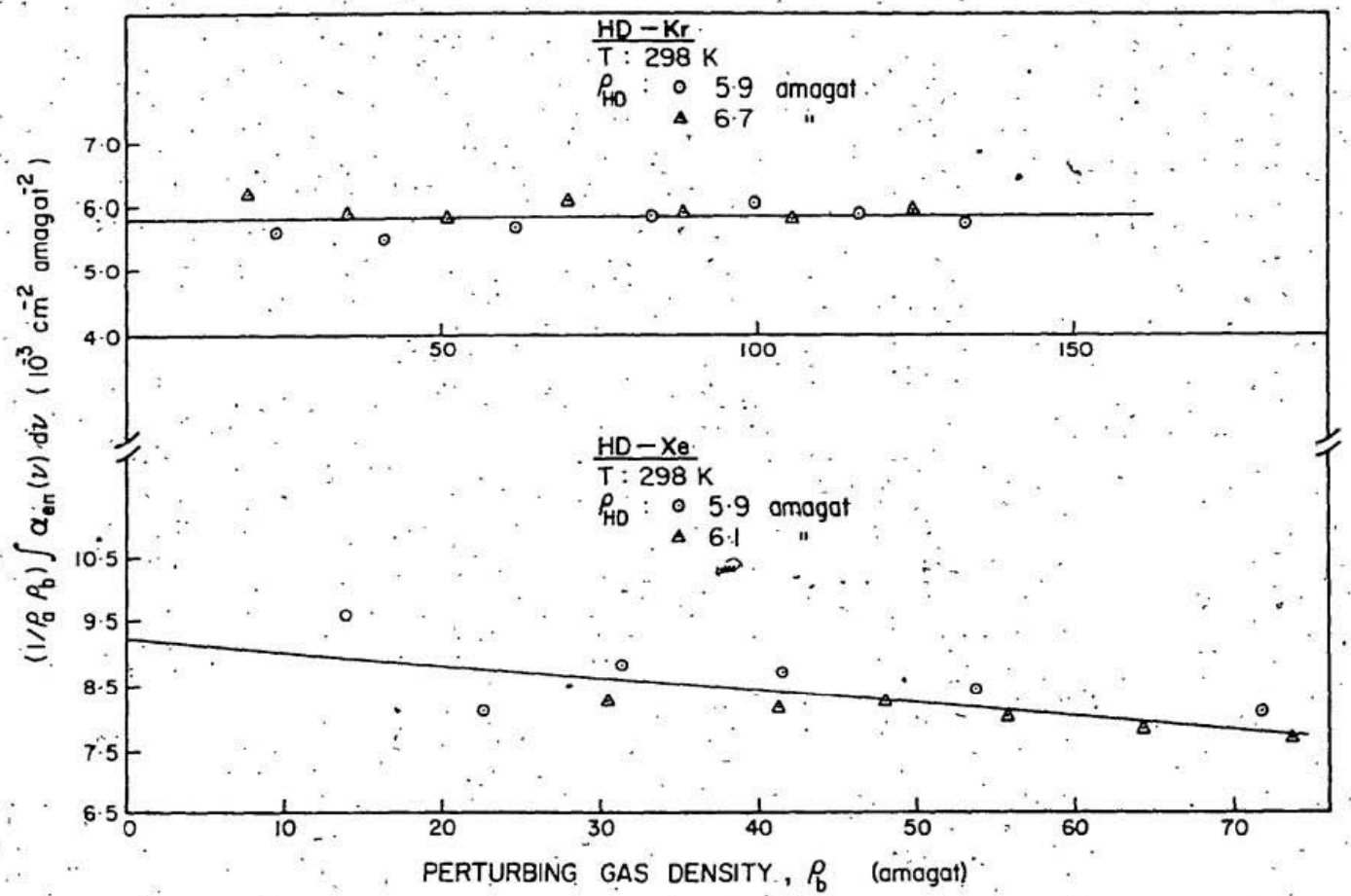

Fig. III-8. Plots of $(1/\rho_a \rho_b) \int \alpha_{en}(\nu)\, d\nu$ against ρ_b for HD-Kr and HD-Xe mixtures at 298 K.

TABLE III - 2

Absorption coefficients* of the fundamental band of HD at 298 K

Mixture	Binary absorption coefficient		Ternary absorption coefficient
	(10^{-3} cm^{-2} amagat^{-2})	(10^{-35} cm^{6} s^{-1})	(10^{-6} cm^{-2} amagat^{-3})
HD-He	α_{1b}: 0.84±0.02	$\tilde{\alpha}_{1b}$: 0.94±0.02	α_{2b}: 2.3±0.2
HD-Ne	: 1.84±0.06	: 2.03±0.06	: 0.0±0.9
HD-Ar	: 4.41±0.06	: 4.84±0.06	: 0.1±0.6
HD-Kr	: 5.81±0.11	: 6.34±0.11	: 0.6±1.3
HD-Xe	: 9.22±0.29	: 10.05±0.29	:-19.7±6.0

*Ranges of error indicated are standard deviations.

of magnitude smaller than the contribution of the usual collision-induced O, Q, and S transitions. The binary absorption coefficient for the HD-He is the smallest [$(0.84\pm0.02)\times10^{-3}$ cm^{-2} $amagat^{-2}$] and that for HD-Xe is the largest [$(9.22\pm0.29)\times10^{-3}$ cm^{-2} $amagat^{-2}$]. Except for HD-Xe, the ternary absorption coefficients are very small compared to the binary absorption coefficients. This means, for HD-He, HD-Ne, HD-Ar, and HD-Kr, under the experimental conditions used in the present work, most of the intensity of the band arises from the binary collisions. One interesting thing for HD-Xe is that the ternary absorption coefficient is large and negative [$(-19.7\pm6.0)\times10^{-6}$ cm^{-2} $amagat^{-3}$]. This shows that there is a negative contribution to the absorption due to triple collisions of the type HD-Xe-Xe, which can be explained on the basis of the so-called "cancellation effect" (see Van Kranendonk 1959). It may be mentioned here that a similar situation exists in the collision-induced fundamental band of H_2 in H_2-Xe (Varghese and Reddy 1969).

The integrated absorption coefficient can also be expressed as

$$c\int\tilde{\alpha}_{en}(\nu)d\nu = \tilde{\alpha}_{1b}\rho_a\rho_b n_0^2 + \tilde{\alpha}_{2b}\rho_a\rho_b^2 n_0^3 + \ldots, \quad (3\text{-}2)$$

where c is the speed of light and n_0 is the Loschmidt's number (2.687×10^{19} cm^{-3}). The new coefficients are related to the earlier ones by the expressions

$$\tilde{\alpha}_{1b} = \frac{(c/n_0^2)\alpha_{1b}}{\bar{\nu}} \quad , \quad \tilde{\alpha}_{2b} = \frac{(c/n_0^3)\alpha_{2b}}{\bar{\nu}} \quad . \tag{3-3}$$

where the effective band center $\bar{\nu}$ is given by

$$\bar{\nu} = \int \alpha_{en}(\nu) d\nu \; / \int \alpha_{en}(\nu) \nu^{-1} d\nu \; , \tag{3-4}$$

The average values of $\bar{\nu}$ of the band for HD-He, HD-Ne, HD-Ar, HD-Kr, and HD-Xe are 3736, 3753, 3785, 3802, and 3809 cm^{-1}, respectively.

For the purpose of comparison the values of the binary and ternary absorption coefficients of the fundamental bands of H_2, HD, and D_2 in their binary mixtures with inert gases at room temperature are listed in Table III-3. Values of the binary absorption coefficients for HD-inert gas mixtures are in general lower than those for H_2-inert gas mixtures. The value of the binary absorption coefficient of the H_2 fundamental band in H_2-He as reported by Reddy and Chang (1973) appears somewhat higher than the value obtained by us, which is $(1.71 \pm 0.02) \times 10^{-3}$ cm^{-2} $amagat^{-2}$. The value for HD-Ar seems close to that for H_2-Ar. Recent experiments performed with H_2-Ar mixtures by us show that the value of the binary absorption coefficient is $(5.99 \pm 0.06) \times 10^{-3}$ cm^{-2} $amagat^{-2}$ which is larger than that reported by Hare and Welsh (1958). The values of α_{1b} for the D_2-inert gas mixtures are lower than those of HD-inert gas mixtures. However, it must noted that the D_2-He mixture experiments by Russell et al. (1974) were performed with a small absorption cell and the binary absorption

TABLE III-3

Binary absorption coefficients of the fundamental bands of H_2, HD, and D_2 at 298 K

Mixture	Binary absorption coefficient $(10^{-3}$ cm^{-2} amagat$^{-2})$	Binary absorption coefficient $(10^{-35}$ cm^6 s$^{-1})$	Reference
H_2-He*	α_{1b}: 2.08±0.6	$\tilde{\alpha}_{1b}$: 1.99±0.06	Reddy and Chang (1973)
H_2-Ne	: 2.51±0.03	: 2.40±0.03	Reddy and Chang (1973)
H_2-Ar*	: 4.1	: 3.86	Hare and Welsh (1958)
H_2-Kr	: 8.02±0.01	: 7.56±0.01	Reddy and Lee (1968)
H_2-Xe	: 11.99±0.05	: 11.34±0.05	Varghese and Reddy (1969)
HD-He	α_{1b}: 0.84±0.02	$\tilde{\alpha}_{1b}$: 0.94±0.02	Present work: Prasad and Reddy (1975)
HD-Ne	: 1.84±0.06	: 2.03±0.06	"
HD-Ar	: 4.41±0.06	: 4.84±0.06	"
HD-Kr	: 5.81±0.11	: 6.34±0.11	"
HD-Xe	: 9.22±0.29	: 10.05±0.29	"

TABLE III-3 (Continued)

Mixture	Binary absorption coefficient $(10^{-3}$ cm^{-2} amagat$^{-2})$	Binary absorption coefficient $(10^{-35}$ cm^{6} s$^{-1})$	Reference
D_2-He	α_{1b}: 0.82±0.01	$\tilde{\alpha}_{1b}$: 1.08±0.01	Russell, Reddy, and Cho (1974)
D_2-Ne	: 1.24±0.02	: 1.66±0.03	"
D_2-Ar	: 2.71±0.04	: 3.57±0.06	Pai, Reddy, and Cho (1966)

*see text.

coefficient was obtained by the extrapolation of the experimental data at high densities. Experiments with larger path lengths and lower mixture densities may give more accurate values.

3. Profile Analysis

The profiles of the enhancement of absorption of HD in the binary mixtures of HD with inert gases consist of only single transitions. The collision-induced fundamental band of HD at room temperature consists of a superposition of the overlap-induced Q lines and the quadrupole-induced O, Q, and S lines.*

(a) The Line Shapes

In the "exponential-4" model of Van Kranendonk (1957, 1958), two types of inductions give rise to the induced dipole moment in the colliding pair of molecules; these are the short-range overlap induction and the long-range quadrupolar induction. It was shown by Poll (1960) that transitions arising from the same induction mechanism have the same line shape. This means that for the collision-induced fundamental bands only two line shapes should be considered: $W_0(\Delta\nu)$ for the overlap-induced transitions and $W_1(\Delta\nu)$ for the quadrupole-induced transitions.

The enhancement absorption coefficient $\tilde{\alpha}_{en}(\nu)$ of an overlap-induced transition may be expressed as (see Van Kranendonk 1968 and Mactaggart and Welsh 1973)

*In the profile analysis it was assumed that the intensities of the O and S lines are completely due to the quadrupolar induction.

$$\alpha_{en}(\nu) = \frac{\alpha^0_{om} W_0(\Delta\nu)}{1 + \exp(-hc\Delta\nu/kT)} \qquad (3\text{-}5)$$

where α^0_{om} is the fictitious relative maximum intensity of the overlap-induced transition at $\nu = \nu_m$; ν_m being the molecular frequency of the HD line, $W_0(\Delta\nu)$ with $\Delta\nu = \nu - \nu_m$ represents the symmetrical line shape, and the factor in the denominator, namely $[1 + \exp(-hc\Delta\nu/kT)]$, converts the symmetrized line form into the observed Boltzmann-modified line form. According to Van Kranendonk (1968), the quantity $W_0(\Delta\nu)$ can be expressed as

$$W_0(\Delta\nu) = D(\Delta\nu) W_0^0(\Delta\nu), \qquad (3\text{-}6)$$

where $W_0^0(\Delta\nu)$ is the intracollisional line form arising from the single binary collisions and $D(\Delta\nu)$ is the intercollisional line form which takes into account the correlation existing between the dipole moments in successive collisions. The quantity $D(\Delta\nu)$ has the form (Van Kranendonk 1968)

$$D(\Delta\nu) = 1 - \gamma[1 + (\Delta\nu/\delta_c)^2]^{-1}, \qquad (3\text{-}7)$$

where γ is a constant (which is assumed to be unity in the present analysis) and δ_c is the intercollisional half-width at half-height. The line shape proposed by Levine and Birnbaum (1967) was found to represent well the quantity $W_0^0(\Delta\nu)$ for the overlap-induced transitions in H_2 (cf. Mactaggart and Welsh 1973) and the same form was used in the present analysis. It may be represented as

$$W_0^0(\Delta\nu) = (2\Delta\nu/\delta_d)^2 K_2(2\Delta\nu/\delta_d), \qquad (3\text{-}8)$$

where K_2 is a modified Bessel function of the second kind and δ_d is the intracollisional half-width (i.e., half-width at half-height of the symmetrized line form). Figure III-9 illustrates the line shape for an overlap component.

For the quadrupole-induced components, the Boltzmann-modified dispersion line form (cf. Kiss and Welsh 1959) was used. Here, the enhancement absorption coefficient is represented by the following equations:

$$\tilde{\alpha}^{+}_{en} = \tilde{\alpha}^{0}_{qm} W_1(\Delta\nu) = \frac{\tilde{\alpha}^{0}_{qm}}{1 + (\Delta\nu/\delta_q)^2}, \quad \Delta\nu \geq 0 \qquad (3\text{-}9)$$

and

$$\tilde{\alpha}^{-}_{en} = \tilde{\alpha}^{+}_{en} \exp(-hc\Delta\nu/kT), \quad \Delta\nu < 0 \qquad (3\text{-}10)$$

Here, $\tilde{\alpha}^{+}_{en}$ and $\tilde{\alpha}^{-}_{en}$ (where $\tilde{\alpha}_{en} = \alpha_{en}/\nu$) are the absorption coefficients at wavenumbers $\nu_m + \Delta\nu$ and $\nu_m - \Delta\nu$ in the high- and low- wavenumber wings, respectively, $\tilde{\alpha}^{0}_{qm}$ is the relative maximum intensity of a quadrupole-induced transition at $\nu = \nu_m$, and δ_q is the half-width at half height, measured to the high- wavenumber wing.

The profile analysis was repeated using a "symmetrized" dispersion line shape (cf. Mactaggart and Welsh 1973) for the quadrupole induced lines. In this case Eqs.(3-9) and (3-10) for the quadrupolar lines are modified as:

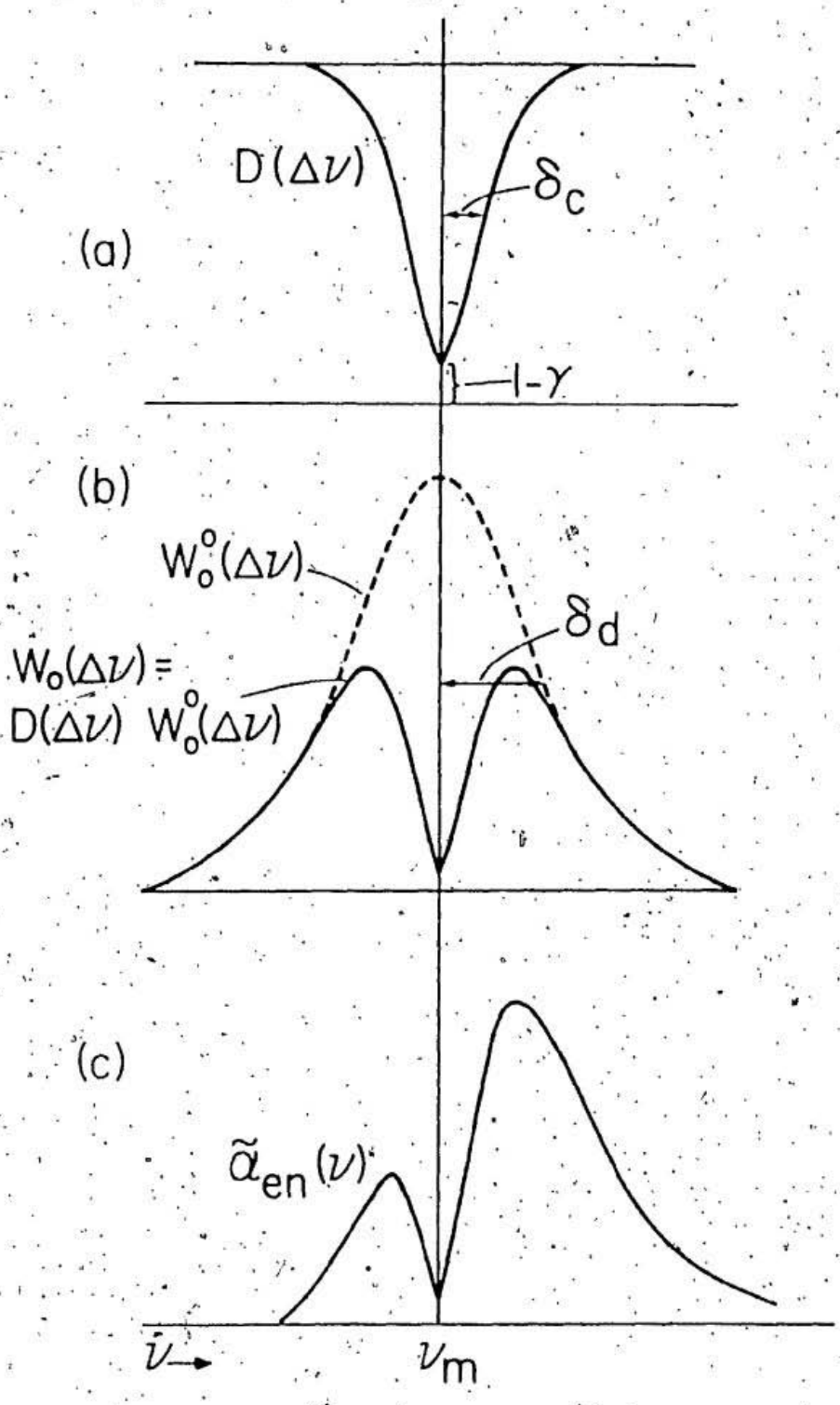

Fig. III-9. Line shape for an overlap-induced component: (a) intercollisional line form [Eq. (3-7)], (b) intracollisional line form [Eq. (3-8)] shown by dashed curve, and (c) the observed line form obtained by dividing the product of (a) and (b) by [1+exp(-hcΔν/kT)] [Eq. (3-5)].

$$\tilde{\alpha}_{en}(\nu) = \frac{\tilde{\alpha}^0_{q',m} W_1(\Delta\nu)}{[1 + \exp(-hc\Delta\nu/kT)]}$$

$$= \frac{\tilde{\alpha}^0_{q'm}[1+(\Delta\nu/\delta_{q'})^2]^{-1}}{[1 + \exp(-hc\Delta\nu/kT)]} \qquad (3\text{-}11)$$

The symmetrical line shape thus obtained represents the Fourier transform of the autocorrelation function of the dipole moment induced during a collision. Figure III-10 illustrates the line shapes described by Eqs. (3-9), (3-10), and (3-11).

(b) Relative Intensities

The intensities of the overlap-induced transitions and the quadrupole-induced transitions can be calculated from the general theory of Van Kranendonk (1958). For the overlap components $Q_1(J)$, the relative intensities are given by

$$\tilde{\alpha}^0_{om} = P_J \ , \qquad (3\text{-}12)$$

where P_J is the normalized Boltzmann factor for the rotational state J (note: $\Sigma_J P_J = 1$) and is given by

$$P_J = (1/Z)(2J + 1)\exp(-E_J/kT) \ . \qquad (3\text{-}13)$$

Here, Z is the rotational partition function. For the quadrupolar components $O_1(J)$, $Q_1(J)$ $(J\neq 0)$, and $S_1(J)$ of HD-inert gas mixtures, the intensities can be calculated in terms of the matrix elements of the quadrupole moment of the HD molecule, $\langle vJ|Q_{HD}|v'J'\rangle$, which were computed by Birnbaum and Poll (1969), and the polarizability α_p of the perturbing

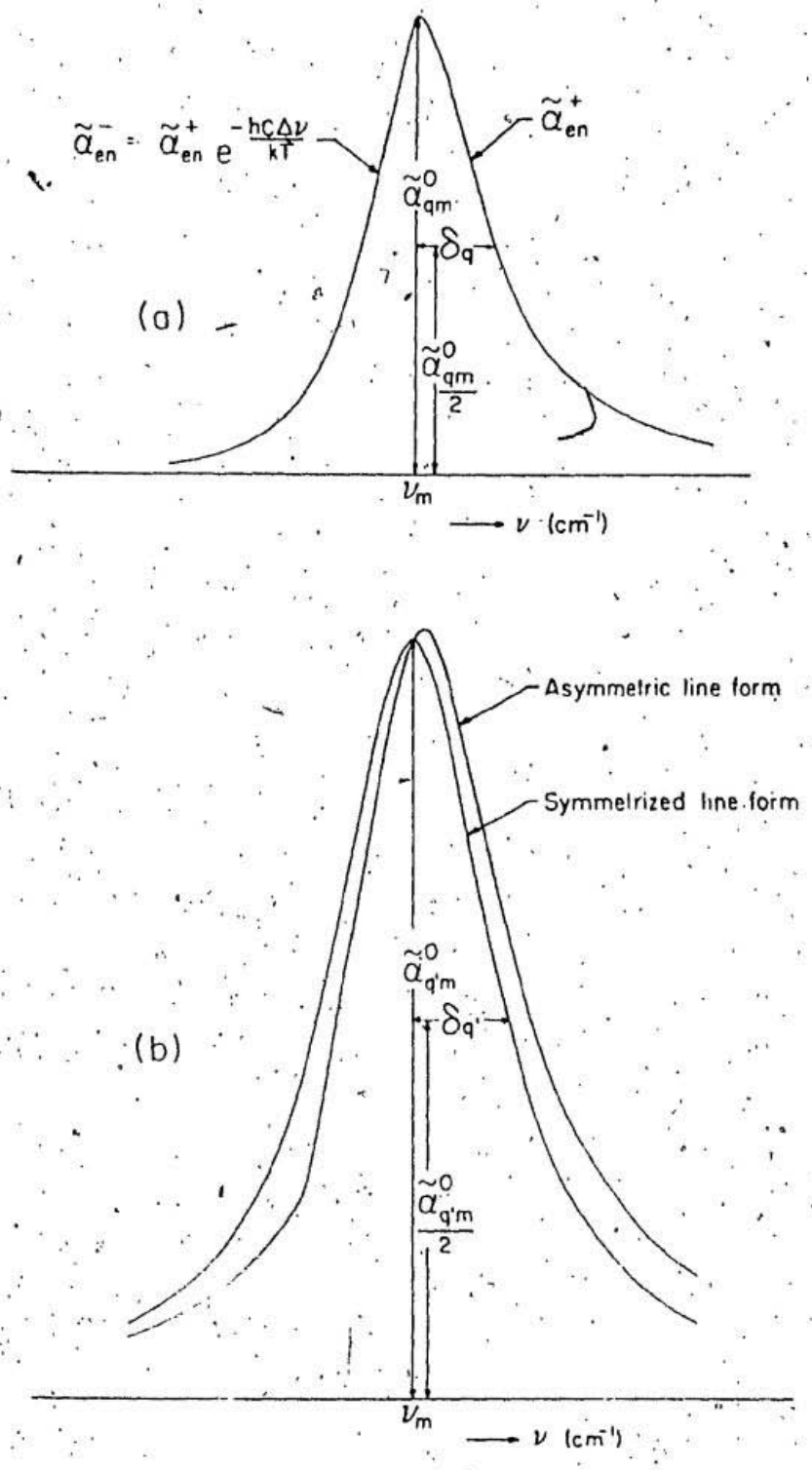

Fig. III-10. Line shapes for a quadrupole-induced component: (a) Boltzmann-modified dispersion line form [Eqs. (3-9) and (3-10)] and (b) symmetrized dispersion line form [Eq. (3-11)].

inert gas atom. Thus, the intensities of these components for the transitions in the fundamental band of HD (i.e., $v = 0$, $J \rightarrow v' = 1$, J') can be expressed as (see Poll 1970)

$$\tilde{\alpha}^{0}_{qm} = P_J C(J2J';00)^2 |\langle 0J|Q_{HD}|1J'\rangle|^2 \alpha_p^2 , \qquad (3\text{-}14)$$

where $C(J2J';00)$ is a Clebsch-Gordan coefficient.

Based on above considerations, the relative intensities of the overlap transitions were obtained in terms of the peak intensity of the most intense overlap component $Q_{1\ \text{overlap}}(1)$ and those of the quadrupolar components in terms of that of $S_1(1)$. These intensities are listed in Appendix A.

(c) Method of Computation

Analysis of the profiles of the enhancement of absorption was carried out by a program written for the IBM 370/155 computer. The two relative peak intensities of the overlap and quadrupolar components and their half-widths δ_c, δ_d, and δ_q (or $\delta_{q'}$), defined by Eqs. (3-7), (3-8), and (3-9) [or (3-11)], respectively, were the adjustable parameters in the program. Provision was also made in the computer program to adjust the molecular frequencies ν_m of the quadrupolar HD lines in order to account for any possible perturbations of the HD vibrational frequencies. A series of computations was carried out by the computer for different values of the adjustable parameters until the computed profile, which was the sum of the intensities of the individual transitions, gave the best nonlinear least-squares fit to the experimental

profile in the entire region of the band.

(d) Results of the Profile Analysis and Discussion

For each of the HD-inert gas binary mixtures, a number of profiles was analyzed. Figures III-11 to III-15 show the analysis of a typical profile of the HD fundamental band for each of HD-He, HD-Ne, HD-Ar, HD-Kr, and HD-Xe mixtures using a Boltzmann-modified dispersion line shape for the quadrupolar lines. The agreement between the experimental and synthetic profiles is reasonably good except for slight differences for a few in the wings. Profile analysis was also carried out using the symmetrized line shape for the quadrupolar lines. The agreement between the experimental and calculated profiles was equally good.

Results of the profile analysis are listed in Table III-4. The values of the half-widths δ_d, δ_q, and $\delta_{q'}$ for each of the mixtures within the range of the densities investigated are observed to remain constant. The overlap and quadrupolar collision durations τ_d (= $1/2\pi c\delta_d$) and τ_q (= $1/2\pi c\delta_q$) are also included in the table. On the basis of the profile analysis carried out, it is possible to estimate the contributions of the overlap and quadrupolar inductions to the integrated intensity of the HD-inert gas mixtures. These are listed in the same table. The overlap and the quadrupolar contributions vary from 86% and 14% for HD-He mixtures to 31% and 69% for HD-Xe mixtures.

Fig. III-11. Analysis of the enhancement absorption profile of the HD fundamental band in a mixture of HD with He at 298 K. The solid curve is the experimental profile. The dashed curves represent the individual overlap and quadrupolar components and the dots represent the summation of these. For the sake of clarity, the weaker quadrupolar components $Q_1(3)$, $Q_1(4)$, and $S_1(4)$ are not shown. Note that the quadrupolar component $Q_1(0)$ does not occur.

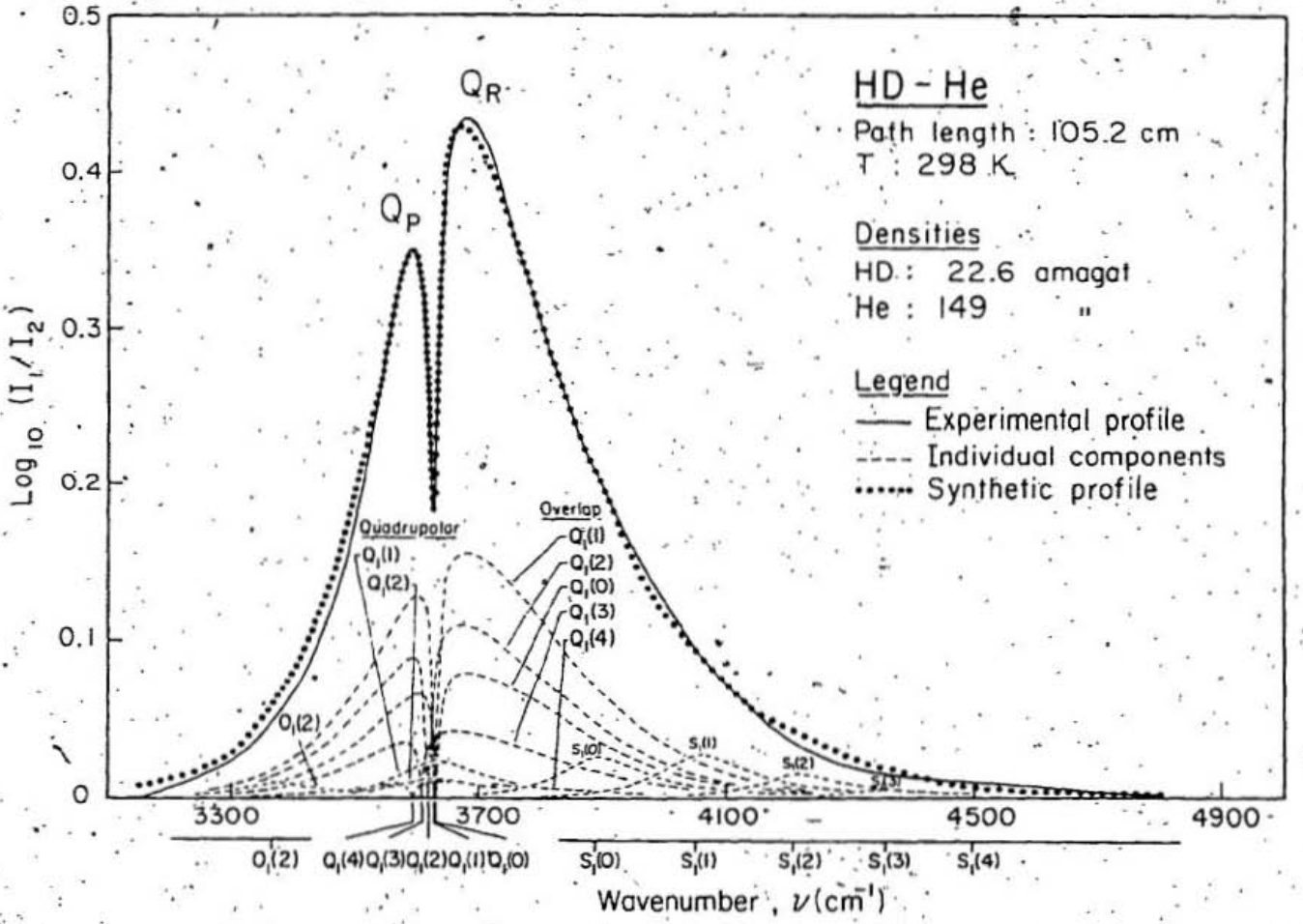
HD - He
Path length : 105.2 cm
T : 298 K
Densities
HD : 22.6 amagat
He : 149 "
Legend
Experimental profile
Individual components
Synthetic profile
Q_R
Q_P
Quadrupolar
Overlap
$Q_1(1)$
$Q_1(2)$
$Q_1(0)$
$Q_1(3)$
$Q_1(4)$
$S_1(0)$
$S_1(1)$
$S_1(2)$
$S_1(3)$
$S_1(4)$
$\log_{10}(I_1/I_2)$
0.5
0.4
0.3
0.2
0.1
0
3300
3700
4100
4500
4900
$O_1(2)$ $Q_1(4)Q_1(3)Q_1(2)O_1(1)O_1(0)$
Wavenumber , $\nu(cm^{-1})$

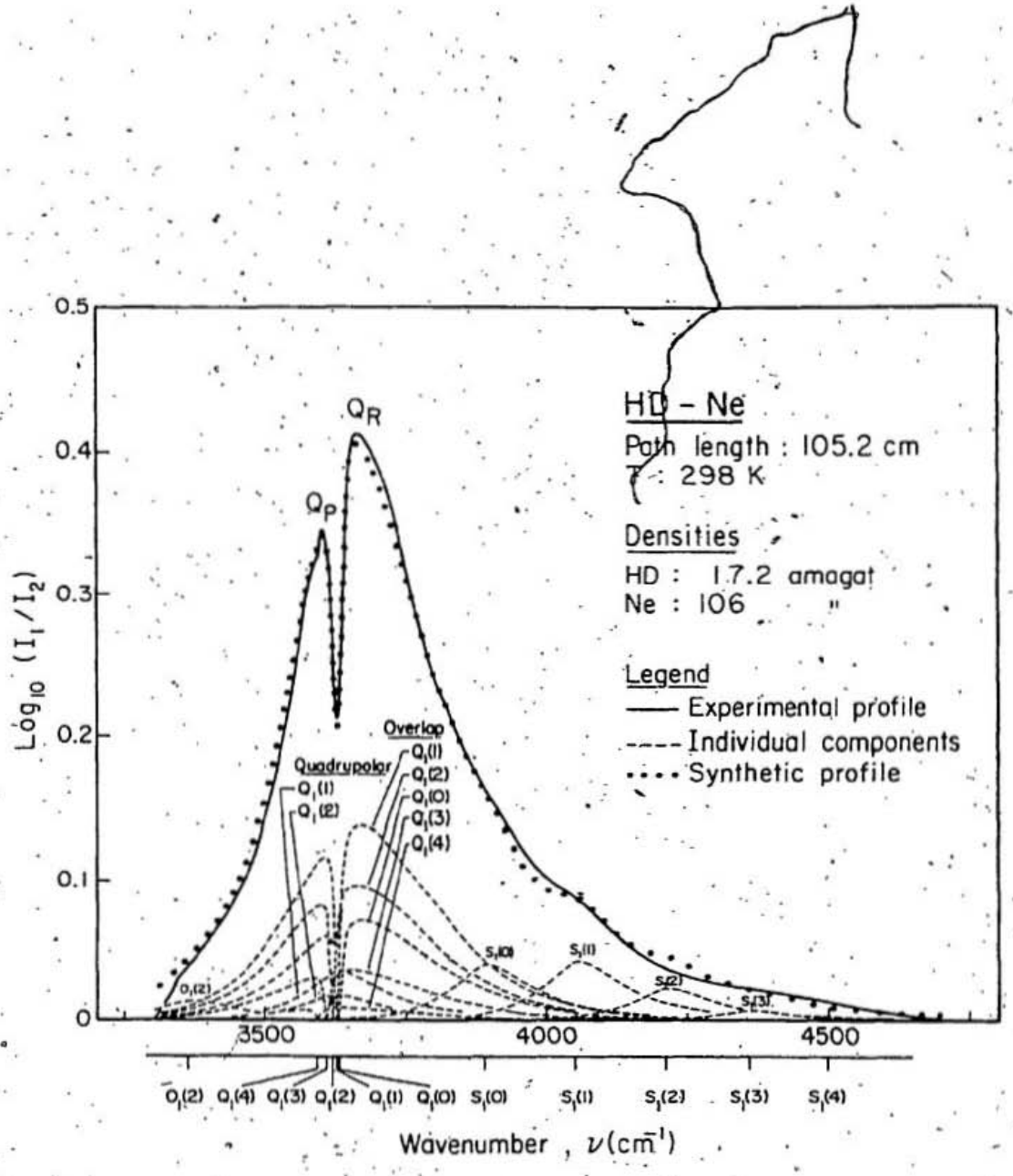

Fig. III-12. Analysis of the enhancement absorption profile of the HD fundamental band in an HD-Ne mixture at 298 K. See the caption of Fig. III-11 for other details.

Fig. III-13. Analysis of the enhancement absorption profile of the HD fundamental band in a mixture of HD with Ar at 298 K. The solid curve is the experimental profile. The dashed curves represent the individual overlap and quadrupolar components and the dots represent the summation of these. For the sake of clarity, the weaker quadrupolar component $Q_1(4)$ is not shown. Note that the quadrupolar component $Q_1(0)$ does not occur.

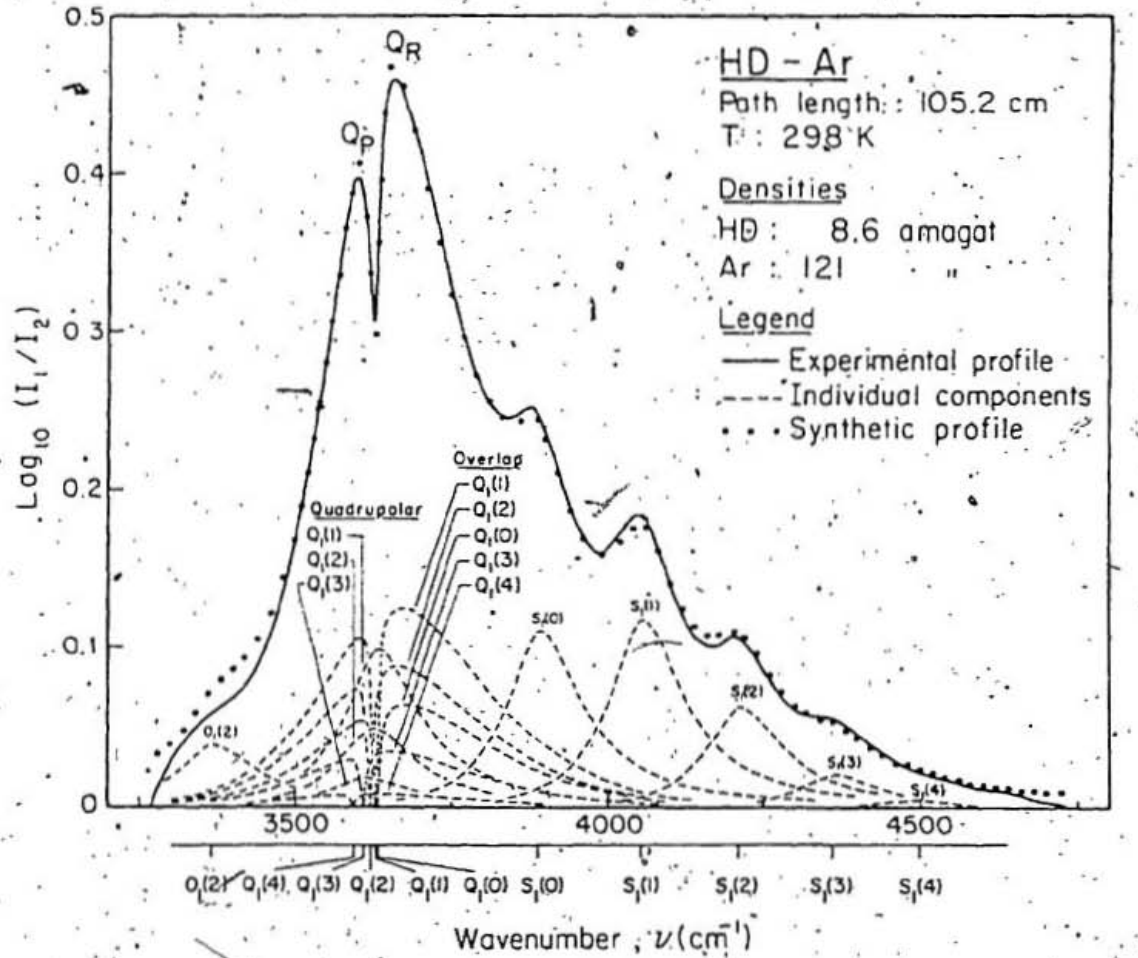
HD - Ar
Path length : 105.2 cm
T : 298 K
Densities
HD : 8.6 amagat
Ar : 121 "
Legend
Experimental profile
Individual components
Synthetic profile
Q_R
Q_P
Overlap
$Q_1(1)$
$Q_1(2)$
$Q_1(0)$
$Q_1(3)$
$Q_1(4)$
Quadrupolar
$Q_1(1)$
$Q_1(2)$
$Q_1(3)$
$S_1(0)$
$S_1(1)$
$S_1(2)$
$S_1(3)$
$S_1(4)$
$Q_1(2)$
$Log_{10}(I_1/I_2)$
0.5
0.4
0.3
0.2
0.1
0
3500
4000
4500
$Q_1(2)$ $Q_1(4)$ $Q_1(3)$ $Q_1(2)$ $Q_1(1)$ $Q_1(0)$ $S_1(0)$ $S_1(1)$ $S_1(2)$ $S_1(3)$ $S_1(4)$
Wavenumber , $\nu(cm^{-1})$

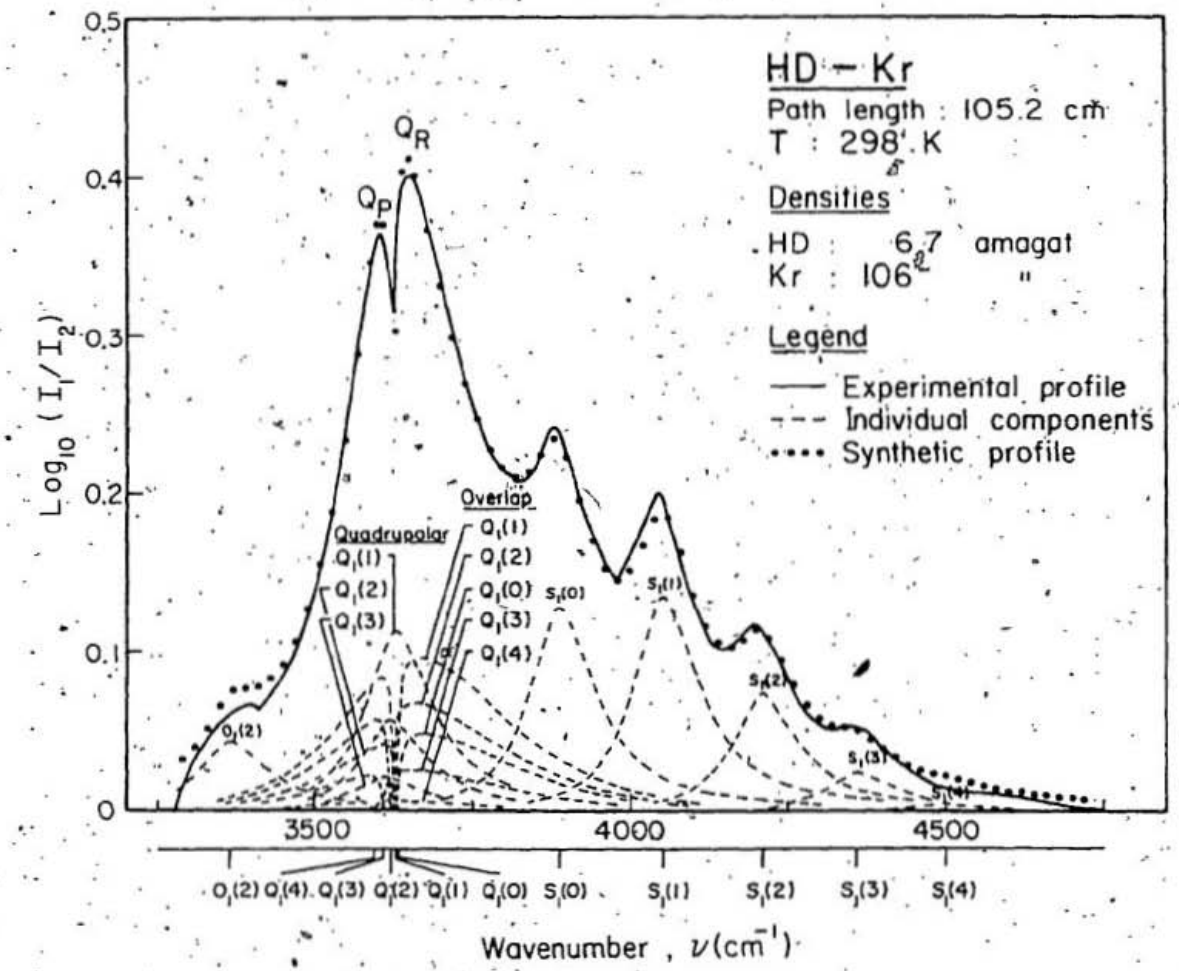

Fig. III-14. Analysis of the enhancement absorption profile of the HD fundamental band in an HD-Kr mixture at 298 K. See the caption of Fig. III-13 for other details.

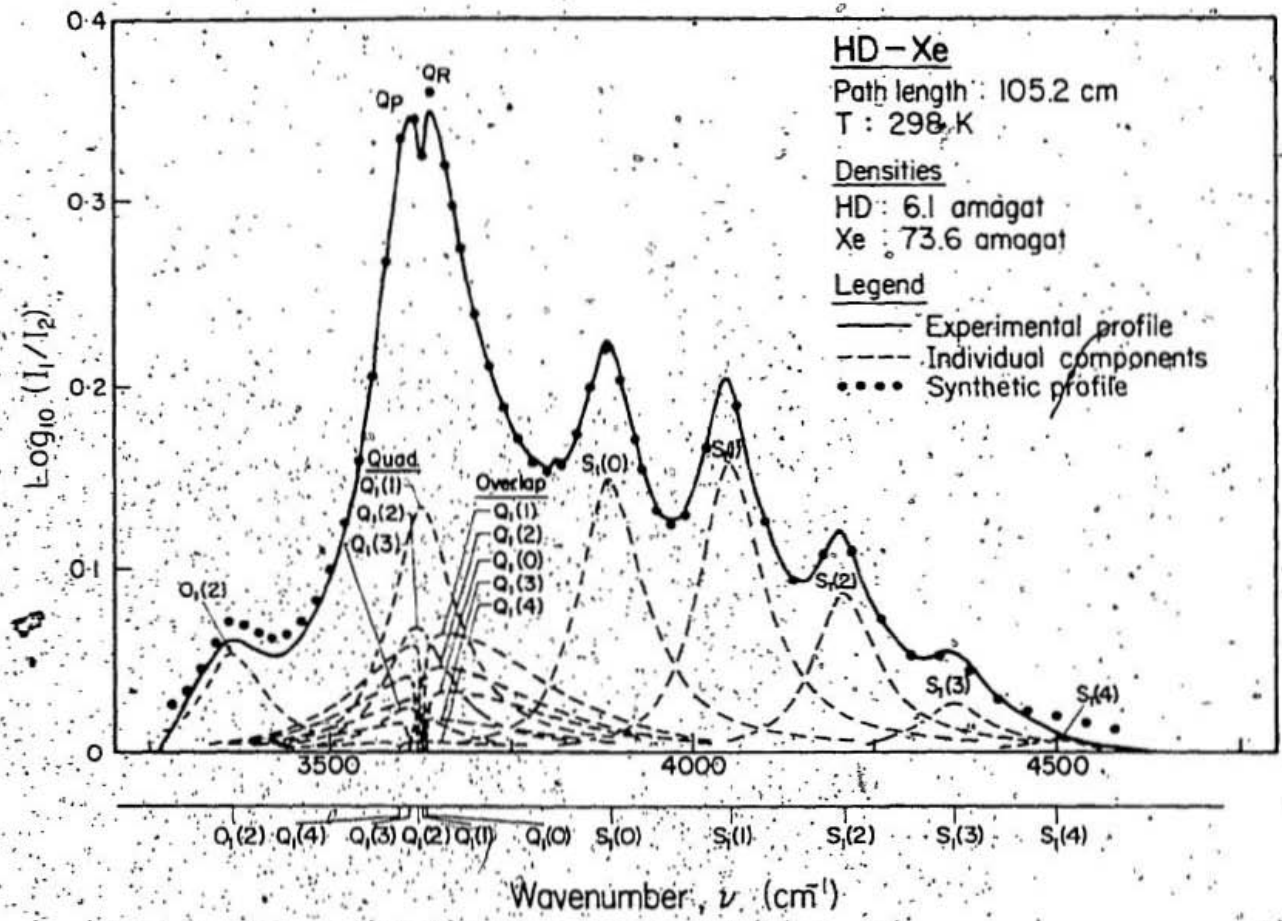

Fig. III-15. Analysis of the enhancement absorption profile of the HD fundamental band in an HD-Xe mixture at 298 K. See the caption of Fig. III-13 for other details.

TABLE III-4

Results of profile analysis

Mixture	Intracollisional half-width γ_d (cm^{-1})	Collision duration τ_d (10^{-14} s)	Quadrupolar half-width γ_q (cm^{-1})	Collision duration τ_q (10^{-14} s)	Quadrupolar half-width γ_q (cm^{-1}) (symmetrized)	Overlap contribution %	Quadrupolar contribution %
HD-He	177±2	3.0	95±10	5.6	77±3	86	14
HD-Ne	148±3	3.6	104±4	5.1	86±3	71	29
HD-Ar	148±1	3.6	78±2	6.8	66±2	50	50
HD-Kr	144±3	3.7	70±2	7.6	60±2	41	59
HD-Xe	135±3	3.9	60±3	8.8	55±2	31	69

The half-width δ_c of the intercollisional dip was found to increase with the perturbing gas density. It was observed that this quantity δ_c varied with the perturbing gas density ρ_b of the mixture linearly making a small intercept of less than one wavenumber within the range of the present experimental densities. In the case of HD-Ar mixtures, although δ_c varied linearly with Ar density, the intercept was negative. Plots of δ_c against ρ_b are shown in Figs. III-16 to III-18 and were found to be represented by

$$\delta_c = a_o + a\rho_b , \qquad (3-15)$$

where a_o and a are constants.

For the H_2 fundamental band Mactaggart and Welsh (1973) have found that $\delta_c = a\rho_b + b\rho_b^2$ fits well over a wide range of perturbing gas densities extending up to 1200 amagat so that their graphs pass through the origin for the zero perturbing gas density. The collision diameter σ_{12} and the coefficient a are related by (see Mactaggart and Welsh 1973 and Chapman and Cowling 1952)

$$a = (1 - \bar{\Delta})\sigma_{12}^2 n_0 / c(\pi m/2kT)^{1/2} , \qquad (3-16)$$

where $\bar{\Delta}$ is the mean persistence-of-velocity ratio, n_0 is the Loschmidt's number and m is the reduced mass of the colliding pair of molecules. To obtain a theoretical value of a from Eq. (3-16), one needs the values of the mean persistence-of-velocity ratio $\bar{\Delta}$ and the collision diameter

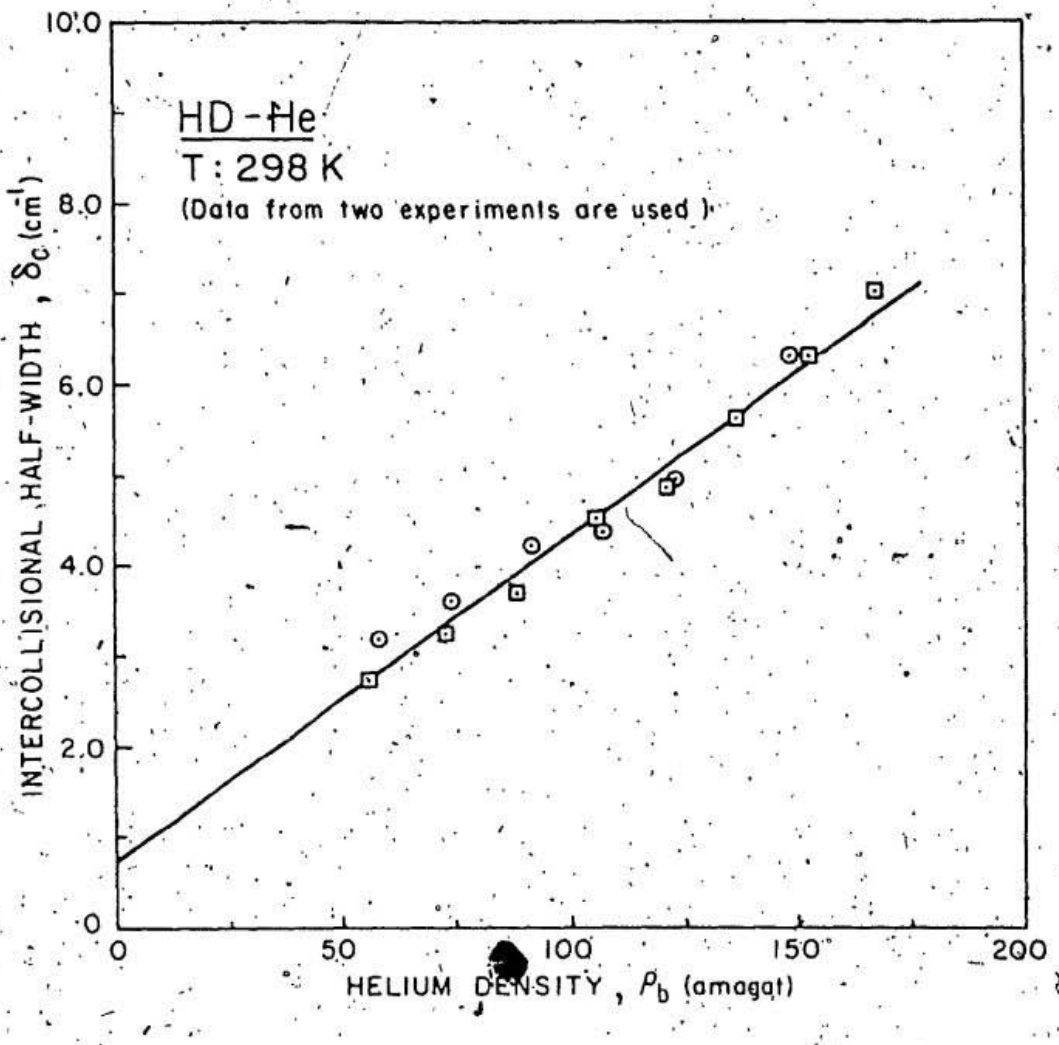

Fig. III-16. A plot of the intercollisional half-widths for HD-He at 298 K against the partial density ρ_b of helium. The experimental points are represented by the straight line given by $\delta_c = a_o + a\rho_b$.

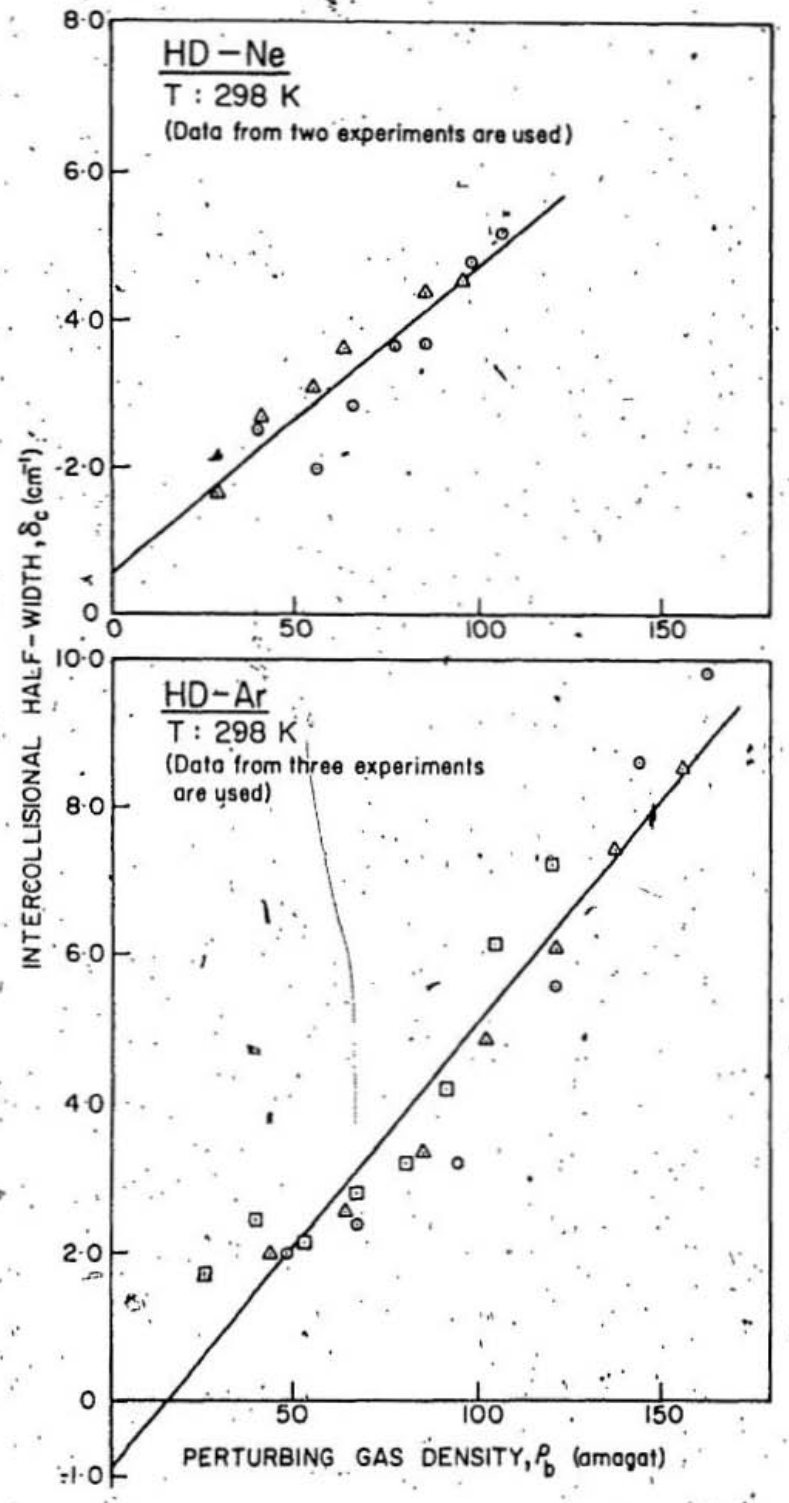

Fig. III-17. Plots of the intercollisional half-widths for HD-Ne and HD-Ar at 298 K against the partial densities ρ_b of neon and argon. The experimental points are represented by the straight line given by $\delta_c = a_o + a\rho_b$.

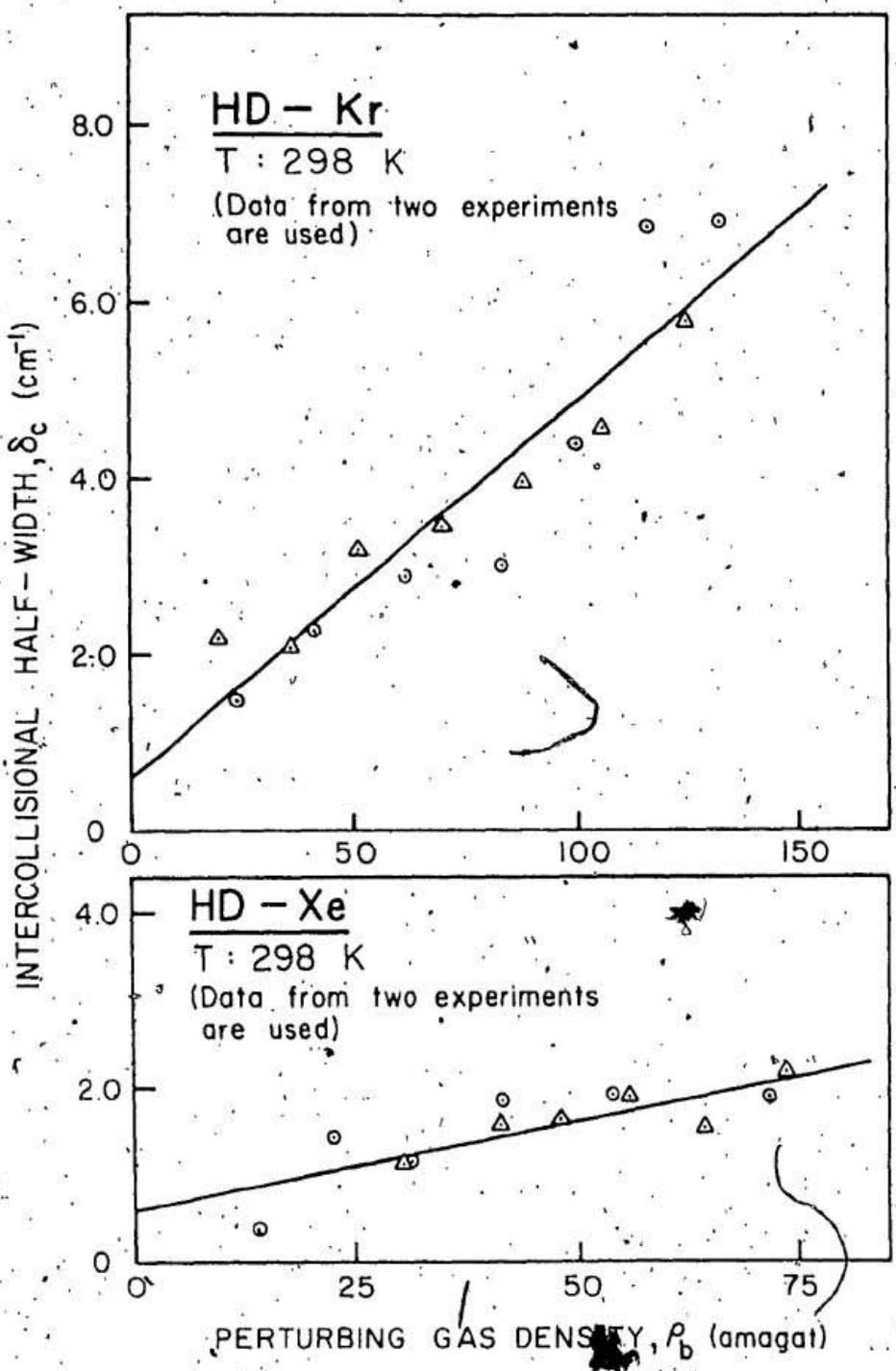

Fig. III-18. Plots of the intercollisional half-widths for HD-Kr and HD-Xe at 298 K against the partial densities ρ_b of krypton and xenon. The experimental points are represented by the straight line given by $\delta_c = a_o + a\rho_b$.

σ_{12} in addition to the values of the other quantities. The values of $\tilde{\Delta}$ calculated from the equation (see Chapman and Cowling 1952)

$$\tilde{\Delta} = \frac{M_1}{2} + \frac{M_1^2}{2\sqrt{M_2}} \ln\left(\frac{\sqrt{M_2} + 1}{\sqrt{M_1}}\right) \qquad (3\text{-}17)$$

are listed in Table III-5 for all the HD-inert gas collision pairs used in the present experiments. In Eq. (3-17), $M_1 = m_1/(m_1 + m_2)$ and $M_2 = m_2/(m_1 + m_2)$, m_1 and m_2 being the masses of the HD molecule and the perturbing gas atom, respectively. In the calculation of a, the Lennard-Jones diameter σ_{12}^{LJ} was used instead of the collision diameter σ_{12}. Values of the quantities a_o, a (both experimental and theoretical), and the Lennard-Jones diameter σ_{12}^{LJ} are listed for all the HD-inert gas mixtures in Table III-6. Values of the Lennard-Jones diameter σ_{12}^{LJ} were obtained from the combination rule $\sigma_{12}^{LJ} = \frac{1}{2}[\sigma_1^{LJ} + \sigma_2^{LJ}]$ successively, first from those of H_2 and D_2 to get that of HD, and then from those of HD and the perturbing gas. It may be noted that the values of the quantity a obtained experimentally are smaller than those obtained theoretically for all the HD-inert gas mixtures. This difference is relatively large for HD-Kr and HD-Xe mixtures, which may be understood from the fact that the HD-Kr and HD-Xe experiments were limited only to low partial densities of Kr and Xe.

TABLE III-5

The mean persistence-of-velocity ratio $\tilde{\Delta}$ for various gas mixtures

Mixture	$\tilde{\Delta}$
HD-He	0.33
HD-Ne	0.081
HD-Ar	0.042
HD-Kr	0.019
HD-Xe	0.012

TABLE III-6

Values of the coefficients a_o and a in the equation $\delta_c = a_o + a\rho_b$ for various gas mixtures at 298 K

Mixture	Intercept a_o (cm^{-1})	Experimental value of a (10^{-2} cm^{-1} $amagat^{-1}$)	Calculated* value of a (10^{-2} cm^{-1} $amagat^{-1}$)	σ_{12}^{LJ}† (A^o)
HD-He	0.7±0.2	3.6±0.2	4.3	2.742
HD-Ne	0.6±0.4	4.2±0.5	5.1	2.839
HD-Ar	-0.9±0.4	6.0±0.4	6.5	3.167
HD-Kr	0.6±0.4	4.3±0.5	6.9	3.26
HD-Xe	0.6±0.2	2.0±0.5	8.0	3.514

* From Eq. (3-16).

† Obtained from the combination rule $\sigma_{12}^{LJ} = \frac{1}{2}[\sigma_1^{LJ} + \sigma_2^{LJ}]$.

As mentioned earlier, in the computer program for the profile analysis, provision was made to adjust the molecular wavenumbers ν_m of HD. For HD-He, HD-Ne, and HD-Ar spectra, the best fits of the calculated profiles to the observed profiles were obtained for unshifted wavenumbers. However, for the profiles of HD-Kr and HD-Xe, it was necessary to shift the wavenumbers of the quadrupolar lines to the lower values. Within the range of the experimental densities of Kr in HD-Kr mixtures the maximum wavenumber shift was $\sim 3 cm^{-1}$ and it was not possible to study the density dependence of these wavenumber shifts. However, for HD-Xe experiments, a study of the density dependence of wavenumber shifts could be made. Figure III-19 shows a plot of the wavenumber shift as a function of the density of Xe in HD-Xe mixtures. The wavenumber shifts plotted in Fig. III-19 were obtained from the profile analysis where a Boltzmann-modified dispersion line form was used for the quadrupolar lines. The wavenumber shifts were also obtained from the profile analysis with the symmetrized dispersion line form and were found to be almost the same as those obtained by the previous method. The wavenumber shifts are negative over the entire density range and increase linearly with increasing density. These shifts for a given density of the mixture were found to be the same for all the HD quadrupolar transitions. This observation indicates that the observed perturbation is due primarily to a change

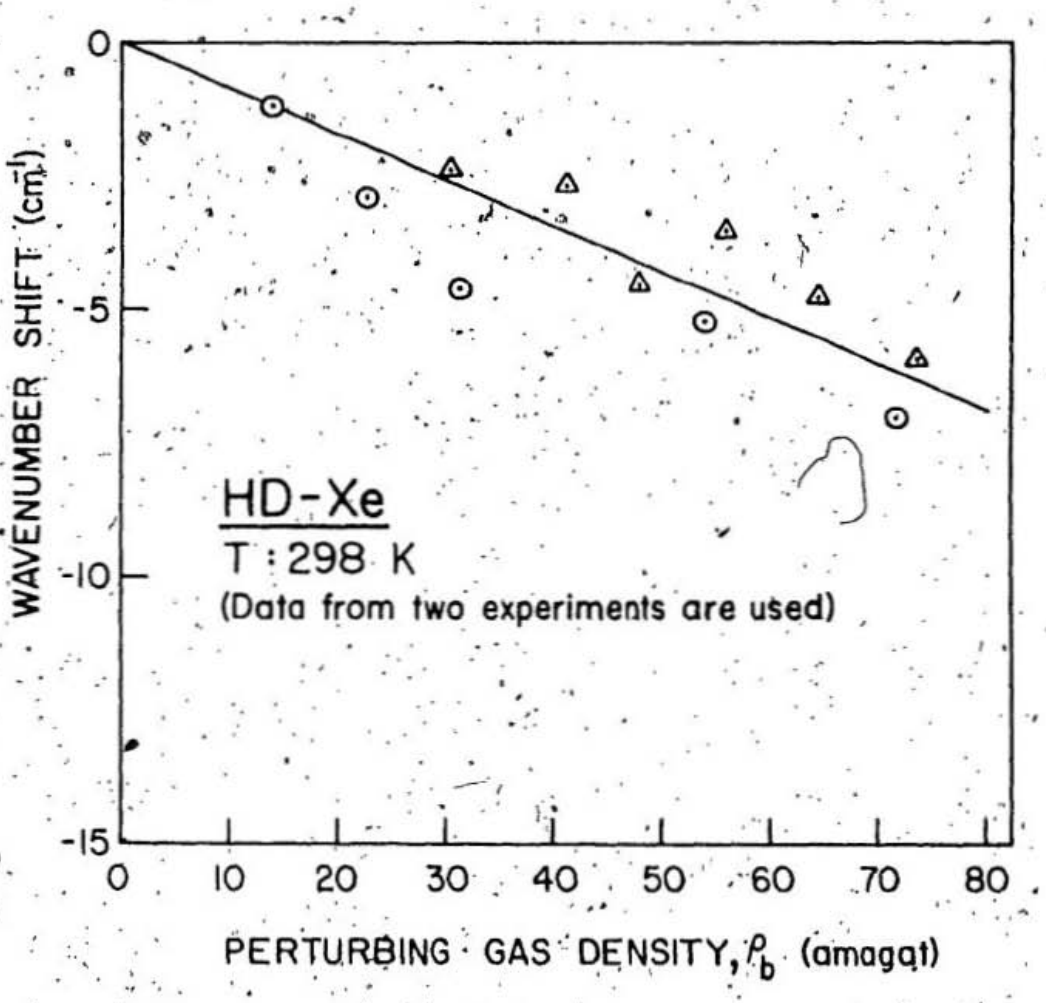

Fig. III-19. The wavenumber shifts of the quadrupolar components in the enhancement profiles of HD-Xe at 298 K. The experimental points are represented by $\Delta\nu = a'\rho_b$, where a' is negative.

in the vibrational frequency of the HD molecule. It is evident from Fig. III-19 that the wavenumber shifts $\Delta\nu$ may be expressed as a linear function of the density ρ_b of Xe, i.e., $\Delta\nu = a'\rho_b$, where a' is negative. Similar observations were made by Mactaggart (1971) for H_2-Xe mixtures for a similar range of partial densities of xenon at room temperature (see also Varghese et al. 1972).

In a study of the wavenumber shifts of the Raman lines of the fundamental band of the hydrogen gas at densities up to 800 amagat, May, Degen, Stryland, and Welsh (1961) and May, Varghese, Stryland, and Welsh (1965) expressed the wavenumber shifts $\Delta\nu$ by the relation $\Delta\nu = a'\rho + b'\rho^2$. According to these authors, the linear coefficient a' can be expressed as

$$a' = K_{rep}I_1 - K_{att}I_2. \qquad (3\text{-}18)$$

Here K_{rep} and K_{att} are positive constants representing the wavenumber shift due to repulsive and attractive intermolecular forces, respectively. The quantities I_1 and I_2 are temperature-dependent integrals involving the pair distribution function and the intermolecular potential. If a similar equation is assumed to be applicable to the present result, the observed negative value of a' for HD-Xe mixtures indicates that the attractive forces predominate over the repulsive forces.

CHAPTER IV

INTRACOLLISIONAL INTERFERENCE EFFECT IN THE INFRARED ABSORPTION SPECTRA OF HD-Kr AND HD-Xe MIXTURES.

The usual collision-induced features of the O, Q, and S branches, corresponding to the selection rule $\Delta J = -2$, 0, and +2, of the enhancement spectra of the HD fundamental band in binary mixtures of HD in He, Ne, Ar, Kr, and Xe at room temperature have been analyzed and discussed in detail in Chapter III. In addition to these usual broad features, a new special feature has been observed in the enhancement spectra of the fundamental band of HD in HD-Kr and HD-Xe mixtures. This is the observation of a narrow absorption peak at the transition frequency of the $R_1(1)$ line of the free HD molecule corresponding to the selection rule $\Delta J = +1$. In this chapter, the experimental results associated with this new feature will be presented in Section 1; in Section 2 a brief account of the theory proposed by Poll et al. (1976) to explain this observation in terms of an "intracollisional interference effect" will be given and a comparison of the experimental binary absorption coefficients of the observed $R_1(1)$ line due to this effect will be made with the corresponding values calculated from the theory.

1. The Experimental Observation and Results

Representative profiles of the enhancement of absorption of the fundamental band of HD in binary mixtures HD-Kr and HD-Xe have been shown in Figs. III-4 and III-5. For the sake of completeness a typical profile of the enhancement of absorption of the fundamental band of HD in a HD-Kr mixture for a base density of 6.7 amagat of HD and for a partial density of 70 amagat of Kr is presented in Fig. IV-1. The enhancement spectrum is obtained by subtracting the absorption due to pure HD gas at the base density from the total absorption due to HD-Kr mixture. Thus, this enhancement spectrum is due to the interaction of HD molecules with Kr atoms. In Fig. IV-1, in addition to the well known broad features of the O, Q, and S branches, a sharp feature marked by an arrow at the position of the $R_1(1)$ line is seen. This feature is due neither to the allowed $R_1(1)$ line arising from the free HD molecules nor to any impurity. These conclusions are based on the facts that the contribution of HD gas at the base density was subtracted (in fact, the base density of HD used is so small that the allowed $R_1(1)$ line was not observable under the present experimental conditions) and that careful experimentation with Kr alone did not show any impurity in the spectrum around the region of the $R_1(1)$ line. The sharp feature of the observed $R_1(1)$ line is therefore interpreted as due to an intracollisional interference which will be discussed in Section 2. This feature

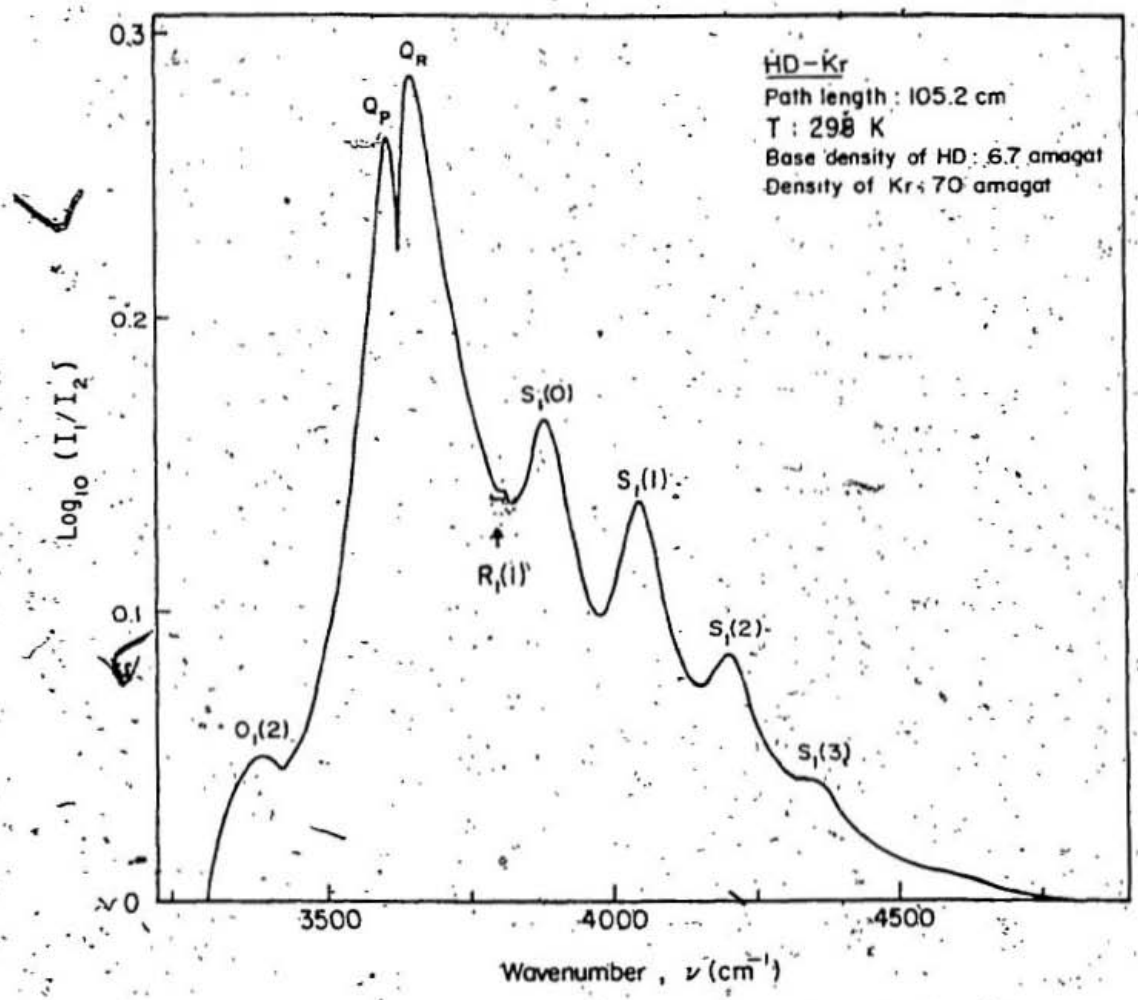

Fig. IV-1. A typical profile of the enhancement of absorption of the collision-induced fundamental band of HD in an HD-Kr mixture at 298 K.

can also be seen in the enhancement absorption profiles of HD-Kr at other densities in Fig. III-4 and in those of HD-Xe in Fig. III-5.

An enlarged version of a typical enhancement spectrum of HD-Kr in the region 3770-3850 cm^{-1} where the $R_1(1)$ due to intracollisional interference occurs is shown in Fig. IV-2. The intensity due to the intracollisional interference line alone is determined by subtracting from the experimental profile the contribution of the Q and S branches, which is obtained by extending smoothly the high wavenumber wing of the Q branch and the low wavenumber wing of the S branch. Plots of $(1/\rho_{HD}\nu)\int\alpha_{en}(\nu)d\nu$ (cm^{-1} $amagat^{-1}$) vs the partial densities ρ_{Kr} and ρ_{Xe} are shown respectively in Figs. IV-3 and IV-4. The slopes of the straight lines obtained by a linear least-squares analysis give the binary absorption coefficients (in the unit of cm^{-1} $amagat^{-2}$). The experimental values of the binary absorption coefficients of the intracollisional $R_1(1)$ line in HD-Kr and HD-Xe are $(5\pm3)\times10^{-10}$ and $(9\pm3)\times10^{-10}$ cm^{-1} $amagat^{-2}$, respectively.

2. Theoretical Binary Absorption Coefficient for the Intracollisional Interference Line

It is well known that a free HD molecule has a small oscillating electric dipole moment of the order of 10^{-3} Debye (McKellar 1973) which gives rise to the allowed P and R lines (selection rule $\Delta J = \pm1$) in its vibration-rotation spectrum. Such an allowed infrared spectrum was first predicted by

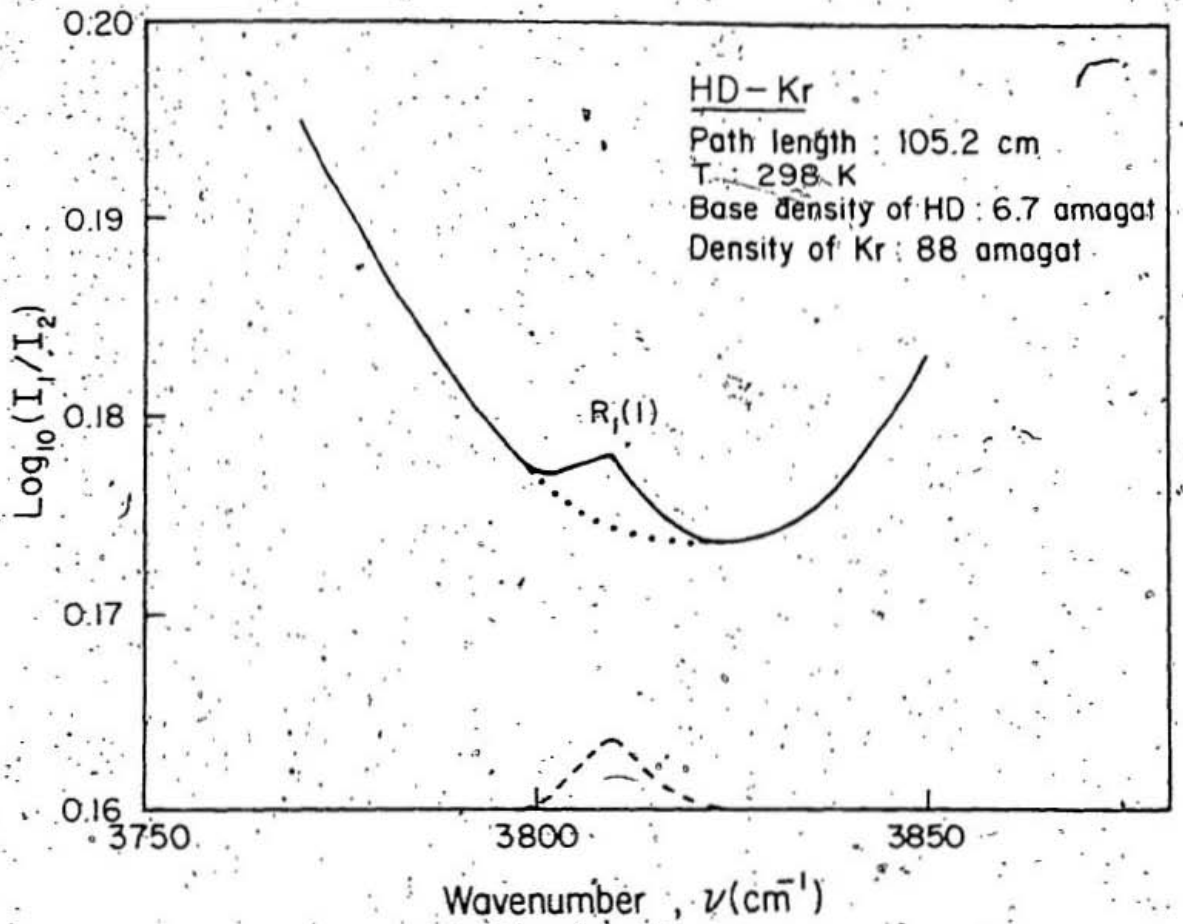

Fig. IV-2. An enlarged portion of the enhancement spectrum of an HD-Kr mixture in the region 3770 - 3850 cm^{-1}. The solid curve is the experimental profile. The dotted curve is obtained by extending smoothly the high-wavenumber wing of the Q branch and the low-wavenumber wing of S branch. The dashed curve at the bottom represents the $R_1(1)$ line obtained from the difference between the solid and the dotted profiles.

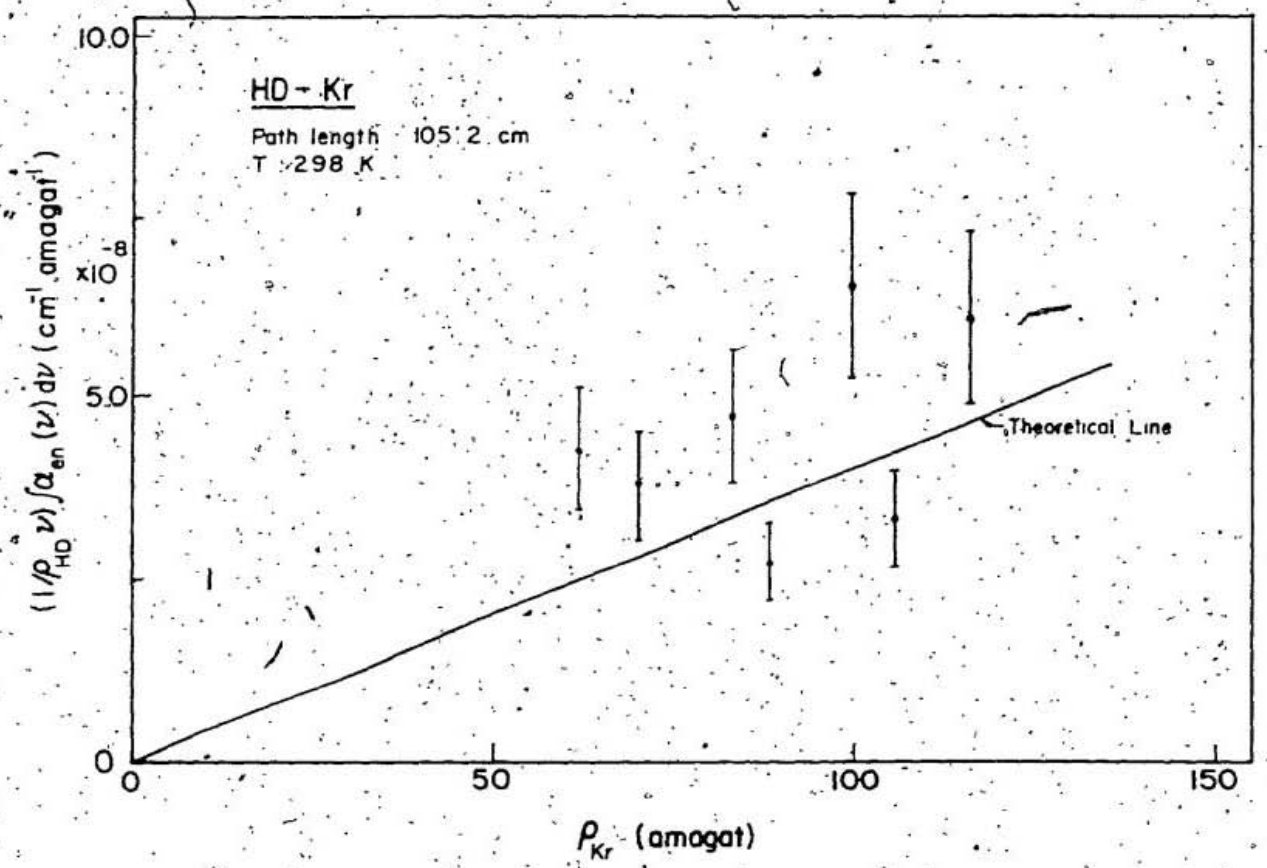

Fig. IV-3. A plot of the integrated absorption coefficient per unit density of HD vs the density of Kr for the $R_1(1)$ line at 298 K.

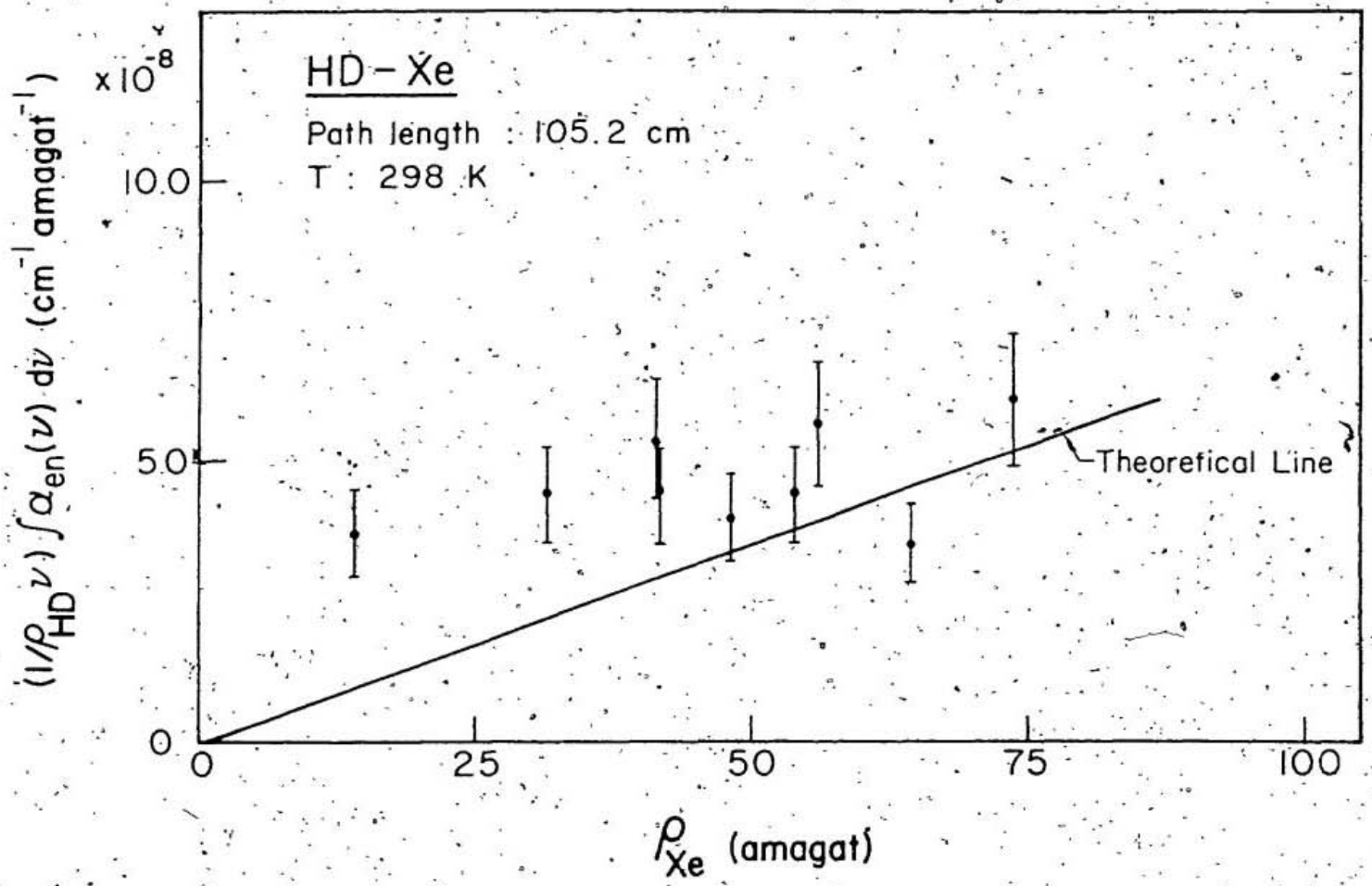

Fig. IV-4. A plot of the integrated absorption coefficient per unit density of HD vs the density of Xe for the $R_1(1)$ line at 298 K.

Wick (1935) and first observed by Herzberg (1950). Subsequent studies of the allowed vibration-rotation spectra of HD were made by Durie and Herzberg (1961), McKellar (1973, 1974), and Bejar and Gush (1974). The allowed pure rotational R_0 lines were first observed by Trefler and Gush (1968).

Generally speaking, for HD gas the selection rule for induced spectra is $\Delta J = 0, \pm 1, \pm 2, \ldots$. Thus in its collision-induced spectra, in addition to the usual O, Q, and S transitions, induced P and R transitions are expected to occur. The collision-induced spectra occur as a result of dipole moments induced during collisions between molecules. Therefore, for a dipole gas such as HD, the possibility of an interference between the allowed dipole of HD and the induced dipole in its colliding partner should be considered. Such an interference takes place only during the collisions and the resulting effect will be referred to as "intracollisional interference," which must be distinguished from the "intercollisional interference" (Van Kranendonk 1968), that arises from the interference of collision-induced dipoles in successive collisions. Intercollisional interference is always destructive and gives rise to a dip in the collision-induced spectrum at the transition wavenumber of the free molecule; the width of the dip is given by $\delta_c = 1/2\pi c\tau_c$, where τ_c is the time between collisions. On the other hand, the intracollisional

interference can be either constructive or destructive and also occurs at the transition frequency of the molecule; its width, however, is of the same order of magnitude as that of the allowed lines.

According to Poll et al. (1976) (for details see Appendix B), the integrated intensities of the $R_1(1)$ transition in a dipole gas arising from the allowed dipole, collision-induced dipole, and intracollisional interference are respectively

$$\int \alpha(\nu)\nu^{-1}d\nu = (4\pi^2/3)\, n_a\, a_0^2\, \alpha_F\, P_1\, C(112;00)^2 \times \langle 01|P_A|12\rangle^2 \quad \text{(allowed)} \tag{4-1}$$

$$\int \alpha_{en}(\nu)\nu^{-1}d\nu = (4\pi^2/3)\, n_a\, a_0^2\, \alpha_F\, P_1\, C(112;00)^2 \times n_b\, a_0^3\, 4\pi \int_0^\infty \langle 01|P_I|12\rangle^2\, g(R)R^2dR, \quad \text{(pure induced)} \tag{4-2}$$

$$\int \alpha_{en}(\nu)\nu^{-1}d\nu = (4\pi^2/3)\, n_a\, a_0^2\, \alpha_F\, P_1\, C(112;00)^2 \times 2\, n_b\, a_0^3\, \langle 01|P_A|12\rangle\, 4\pi \int_0^\infty \langle 01|P_I|12\rangle\, g(R)R^2dR \quad \text{(intracollisional interference)} \tag{4-3}$$

where $\alpha(\nu)$ is the absorption coefficient, $\alpha_{en}(\nu)$ is the enhancement absorption coefficient, n_a ($= \rho_a n_0$) and n_b ($= \rho_b n_0$) (n_0 being the Loschmidt's number) are the number densities of the absorbing and perturbing gas molecules, respectively, a_0 is the Bohr radius, α_F is the fine structure constant, P_1 is the probability for the rotational state corresponding to $J = 1$ (note: $\Sigma_J P_J = 1$), $C(112;00)$ is the Clebsch-Gordan coefficient, $g(R)$ is the pair correlation function for the absorber-perturber pair, and the quantities

$\langle 01|P_A|12\rangle$ and $\langle 01|P'_I|12\rangle$ are the matrix elements of the allowed and induced dipole moments, respectively.

In the present case n_a is the number density of HD and n_b is the number density of Kr or Xe. In order to estimate the intensity of the $R_1(1)$ line due to the intra-collisional interference (Eq. (4-3)), values of the matrix elements $\langle 01|P_A|12\rangle$ and $\langle 01|P_I|12\rangle$ must be known. McKellar (1974) obtained a value of 2.17 ± 10^{-5} a.u. for the matrix element $\langle 01|P_A|12\rangle$ from the allowed $R_1(1)$ of HD. The values of the matrix elements $\langle 01|P_I|12\rangle$ for HD-Kr and HD-Xe are not readily available. Values of $\langle 01|P_I|12\rangle$ can be estimated in terms of the induced dipole moments of H_2-Kr and H_2-Xe pairs. This is because, apart from the negligibly small nonadiabatic effects, the electronic charge distributions for H_2-Kr and H_2-Xe are the same as those of HD-Kr and HD-Xe, respectively. On the basis of this and on the assumption that the spherical component of the induced dipole is an exponentially decreasing function of the intermolecular separation R (for details see Appendix B), the induced dipole P_I for HD-Kr or HD-Xe can be expressed as

$$P_I = \frac{x}{3}\,(2/R - 1/\rho)\, m(r)\, \exp[-(R-\sigma)/\rho], \qquad (4\text{-}4)$$

where $x = r/6$, r being the internuclear distance for HD, ρ is a range parameter, σ is the Lennard-Jones parameter, and $m(r)$ is the strength of the induced moment at $R = \sigma$. The

values of $\langle 01|m(r)|12\rangle$ and ρ/σ obtained by a reasonable fit to the induced spectra of H_2-Kr are 2×10^{-3} a.u. and 0.12, respectively. For H_2-Xe the corresponding values are 2.2×10^{-3} a.u. and 0.12, respectively. The value of $\langle 01|m(r)|12\rangle$ for H_2-Xe was obtained by multiplying the corresponding quantity for H_2-Kr by the factor $\mu_{overlap}^{H_2\text{-}Xe}(\sigma) / \mu_{overlap}^{H_2\text{-}Kr}(\sigma)$, where $\mu_{overlap}(\sigma) = \lambda e\sigma$ is the overlap-induced dipole moment at $R = \sigma$ and λ is an overlap parameter (for details see Chapter V). Values of λ for H_2-Kr and H_2-Xe were obtained from Reddy (1975). Using these results for P_A and P_I, we obtain from Eq. (4-3) the intracollisional interference contributions to the binary absorption coefficient of the $R_1(1)$ line, $(1/\rho_a\rho_b)\int\alpha_{en}(\nu)\nu^{-1}d\nu$ for HD-Kr and HD-Xe at room temperature as 4×10^{-10} and 7×10^{-10} cm^{-1} $amagat^{-2}$, respectively. The lines corresponding to these theoretical values are shown in Figs. III-3 and III-4.

The theoretical values are compared with the experimental values in Table IV-1. In view of the difficulty in obtaining the accurate values of the small integrated intensities of the $R_1(1)$ line as a function of density of the perturbing gas, it may be concluded that the agreement between the theoretical and experimental values of the binary absorption coefficients of the intracollisional $R_1(1)$ line is reasonable.

TABLE IV-1

Binary absorption coefficients of the $R_1(1)$ line due to intracollisional interference effect at 298 K

Mixture	$(1/\rho_a\rho_b)\int\alpha_{en}(\nu)\nu^{-1}d\nu$ (cm^{-1} $amagat^{-2}$)	
	Theoretical	Experimental*
HD-Kr	4×10^{-10}	$(5\pm3)\times10^{-10}$
HD-Xe	7×10^{-10}	$(9\pm3)\times10^{-10}$

*Values obtained from a linear least-squares fit of the experimental points.

The observation of the line arising from the intracollisional interference effect has some astrophysical importance. As can be seen from Eqs. (4-1), (4-2), and (4-3), the ratio of the intensity due to the intracollisional interference to that due to the induced absorption is independent of densities but the ratio with respect to the intensity of the allowed line is proportional to the density of the perturbing gas. At 300 K, this ratio works out to be $0.04\ \rho_{Kr}$. This means that for $\rho_{Kr} > 25$ amagat, the intensity due to the intracollisional interference will dominate over the intensity of the allowed line. Therefore, one must take this effect into account in the analysis of the line strengths at high densities in planetary atmospheres.

Since the observed intracollisional interference effect is constructive, the sign of $\langle 01|P_I|12\rangle$ should be positive because there is evidence for $\langle 01|P_A|12\rangle$ to be positive (Blinder 1960 a, 1960 b, 1961).

CHAPTER V

COLLISION-INDUCED ABSORPTION OF THE FUNDAMENTAL BAND OF HD IN THE PURE GAS AT DIFFERENT TEMPERATURES

In Chapter III experimental profiles of the enhancement of absorption of the collision-induced fundamental band of HD in binary mixtures of HD with He, Ne, Ar, Kr, and Xe at room temperature were presented and the absorption coefficients of the band and the results of profile analysis carried out for all the mixtures were given. In the present chapter results of the work on this band in the pure HD gas at three temperatures will be presented. In general, the collision-induced vibration-rotation spectra of pure gases are more complex than the corresponding enhancement spectra of the gases because of a large number of double transitions. For example, the enhancement spectrum of the HD fundamental band in HD-Ar at room temperature has 5 overlap- and 11 quadrupole-induced transitions whereas the spectrum of the same band at room temperature in pure gas has 5 overlap-induced transitions and more than 60 quadrupole-induced transitions. The fundamental band of HD was studied in the pure gas at temperatures 77, 196, and 298 K with 1 m and 2 m absorption cells and data were obtained for several densities up to 60 amagat.

Table V-1 summarizes the conditions under which the experiments were performed. The present work on the band at 77 K is complementary to that of McKellar (1973).

TABLE V-1

Summary of the experimental conditions

Temperature (K)	Sample path length of the cell (cm)	Maximum density of the HD gas (amagat)	Number of profiles analyzed
77	194.9	41	13
196	195.1	45	12
298	105.2	49	18

The main purpose of studying the collision-induced fundamental band of HD in the pure gas at different temperatures and analyzing the absorption profiles is to separate the contributions of the overlap and quadrupolar interactions to the total intensity of the band, to study their variation with temperature, and to obtain certain overlap parameters for the HD-HD collision pairs from a theoretical fit of the overlap binary absorption coefficient to experimental values as a function of temperature. In Section 1 of this chapter the experimental absorption profiles of the band and the absorption coefficients will be presented. An analysis of the absorption profiles using the line shapes derived from the most recent theories

will be given in Section 2. In Section 3, the data for the overlap contribution obtained from the profile analysis will be used to derive certain overlap parameters for the HD-HD collision pairs.

1. Absorption Profiles and Absorption Coefficients

Typical absorption profiles of the HD fundamental band in the pure HD gas at 77, 196, and 298 K are shown in Figs. V-1, V-2, and V-3, respectively, by plotting the quantity $\log_{10} [I_0(\nu)/I(\nu)]$ against wavenumber ν (see Chapter II, Section 3 for the definitions of $I_0(\nu)$ and $I(\nu)$). Three absorption profiles corresponding to different densities of the gas are chosen at each temperature in order to illustrate the main features. The positions of the collision-induced single transitions $O_1(J)$, $Q_1(J)$, and $S_1(J)$ for the appropriate J values obtained from the constants of the free HD molecule are marked along the wavenumber axis. At 77 K only the lowest rotational states $J = 0$, 1, and 2, whereas at 196 and 298 K states $J = 0$, 1, 2, and 3 and $J = 0$, 1, 2, 3, and 4, respectively, were taken into account. In the spectra of the HD fundamental band in the pure gas, in addition to the single transitions, a large number of double transitions of the types $Q_1(J) + Q_0(J)$ and $Q_1(J) + S_0(J)$ is expected to occur. In a double transition of the former type, one of the colliding pair of molecules makes a vibrational transition $Q_1(J)$

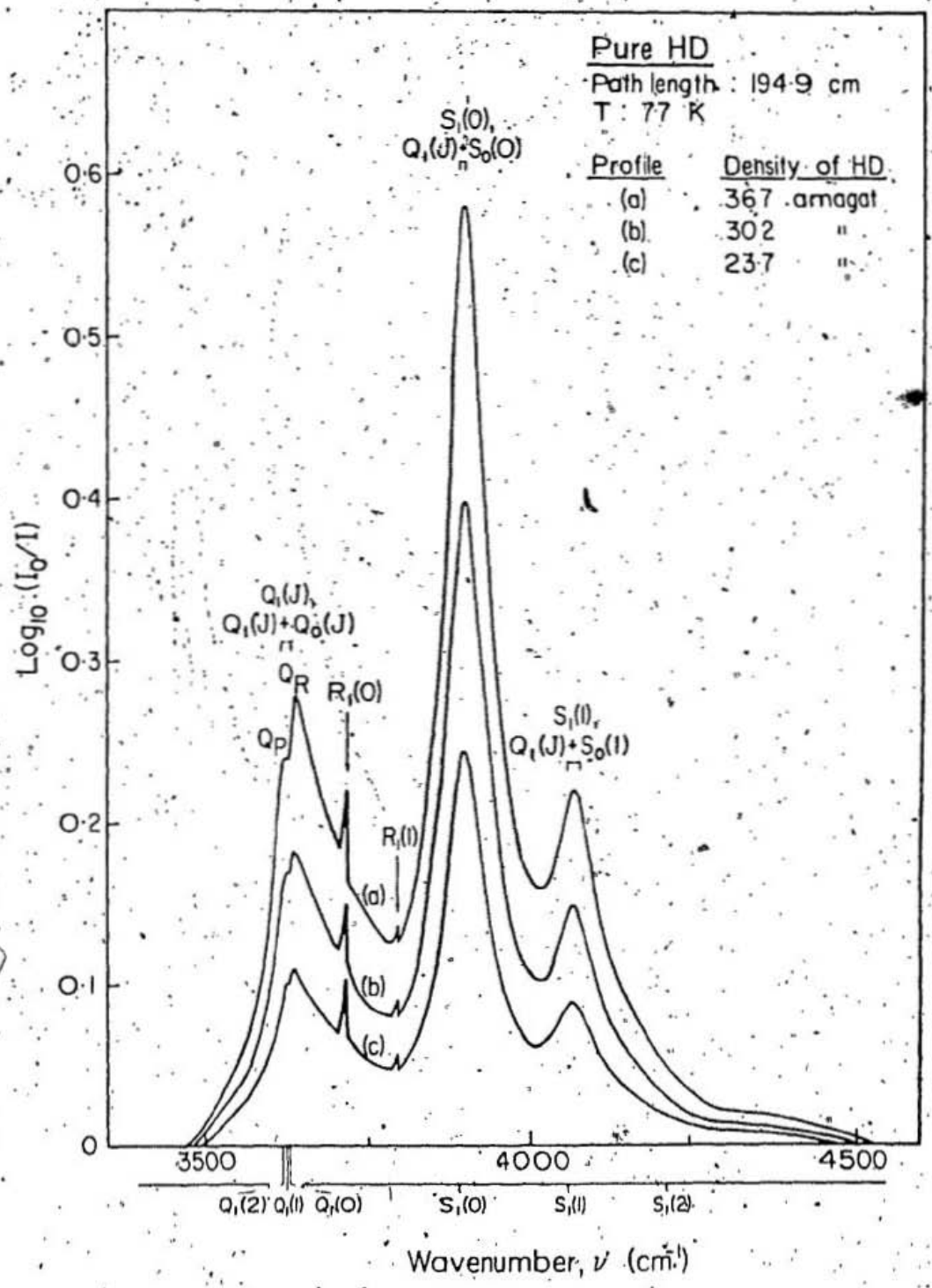

Fig. V-1. Absorption profiles of the collision-induced fundamental band of HD in the pure gas for various densities at 77 K.

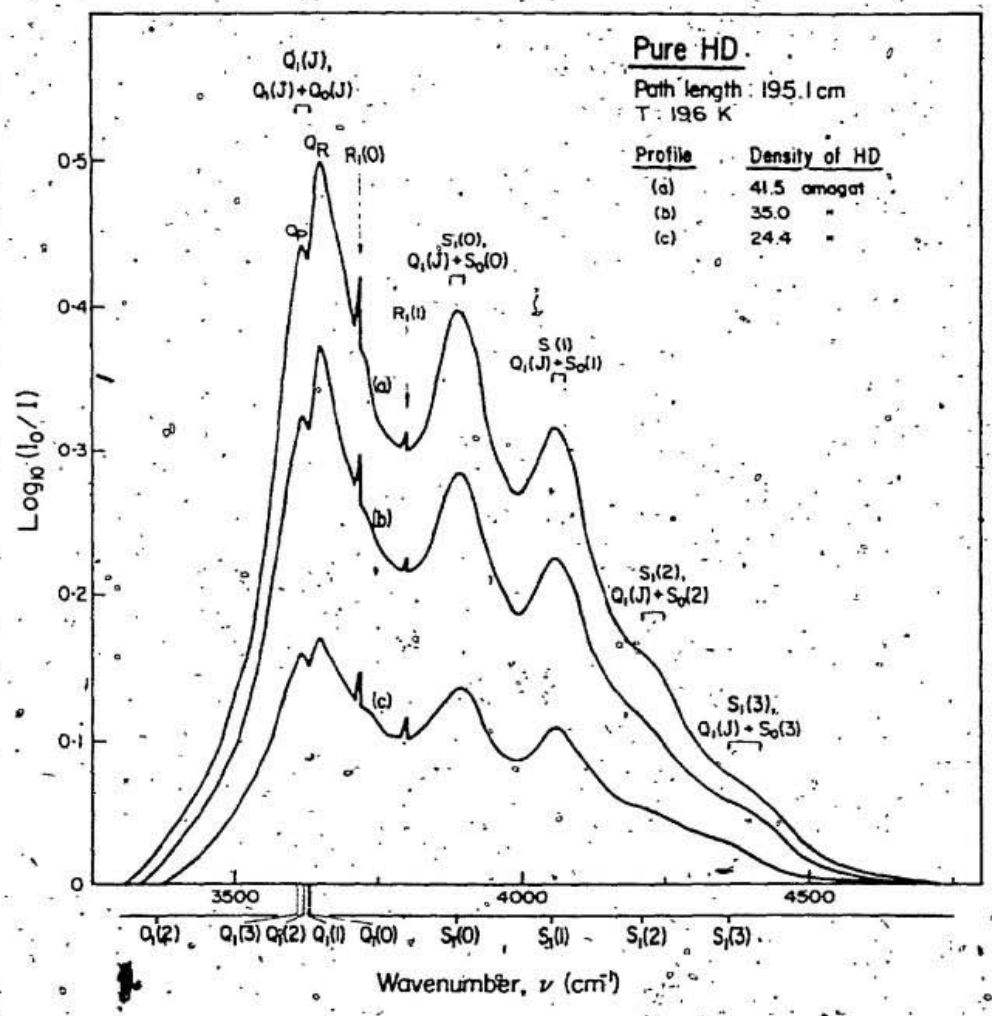

Fig. V-2. Absorption profiles of the collision-induced fundamental band of HD in the pure gas for various densities at 196 K.

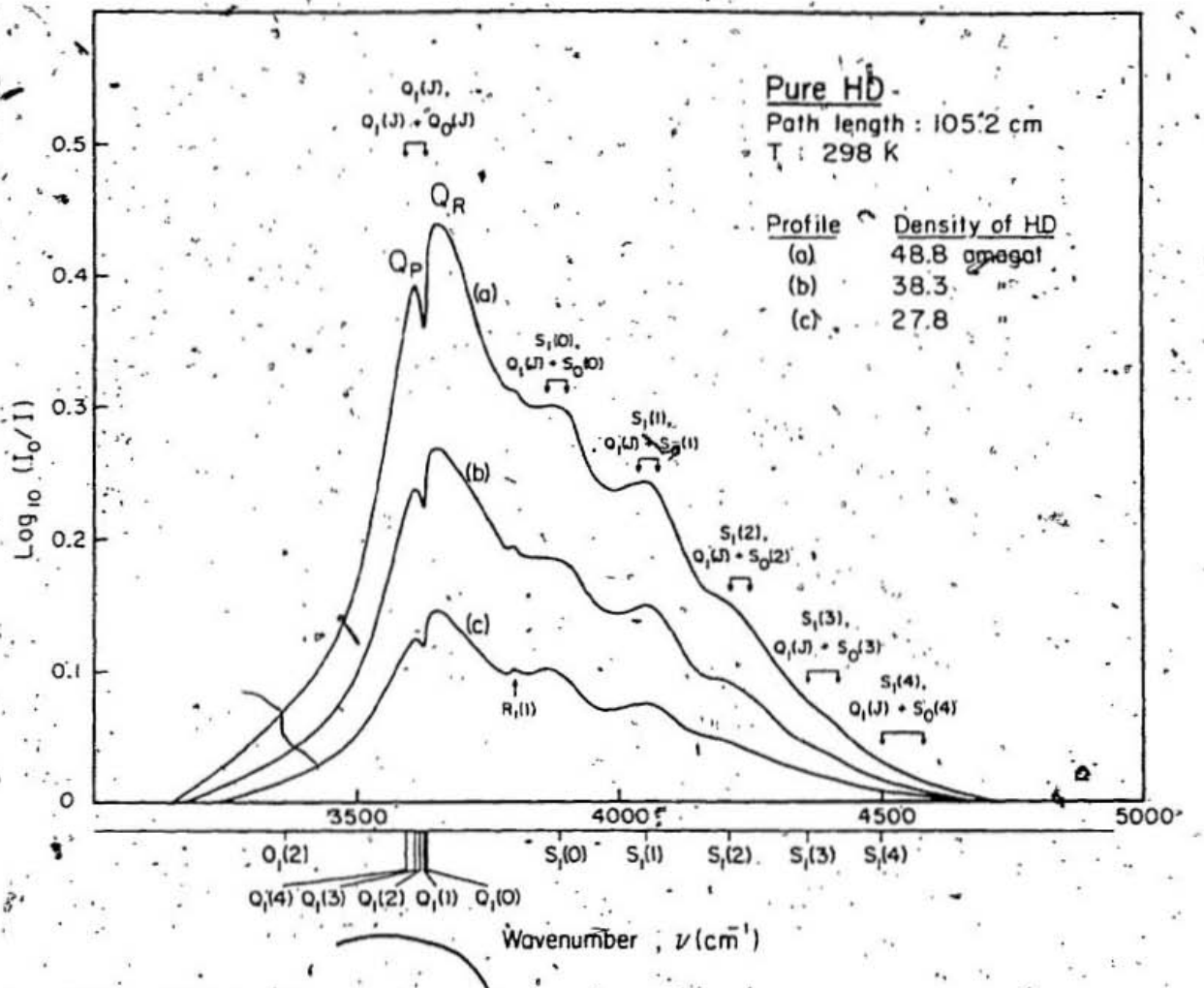

Fig. V-3. Absorption profiles of the collision-induced fundamental band of HD in the pure gas for various gas densities at 298 K.

while the other simultaneously undergoes an orientational transition $Q_0(J)$ $(J\neq 0)$ without any frequency change. In a double transition of the latter type one molecule of the colliding pair makes a vibration-rotation transition $Q_1(J)$ while the other simultaneously makes a pure rotational transition $S_0(J)$. In Figs. V-1 to V-3 the extents of different single and double transitions are marked over the absorption peaks. In these figures a marked dip in the Q branch which occurs at the position of $Q_1(0)$ line ($3632\ cm^{-1}$) at 77 K, and at the position of $Q_1(1)$ line ($3628\ cm^{-1}$) at 196 and 298 K, of the free HD molecule, is similar to the ones observed in the collision-induced spectra of H_2 and D_2. As mentioned earlier in this thesis, the occurrence of the dip was explained by Van Kranendonk (1968) in terms of an intercollisional interference effect due to negative correlations existing between the overlap dipole moments in successive collisions. The separations $\Delta\nu_{PR}^{max}$ between the peaks of the low- and high- frequency components Q_P and Q_R of the Q branch dip increase with increasing density of the gas. In collision-induced spectra at higher temperatures the individual lines are broad because the relative translational energy of the colliding pairs of molecules is large and hence the duration of collision is small. At low temperatures, the lines are in general sharper. This effect of low temperature on the spectra is clearly seen in the absorption profiles at 77 K

(Fig. V-1). One characteristic feature of the absorption profiles is the appearance of the transitions $R_1(0)$ (3717.4 cm^{-1}) and $R_1(1)$ (3798.3 cm^{-1}) at 77 and 196 K and $R_1(1)$ at 298 K, which by virtue of their narrow-band widths are interpreted as "allowed" transitions. In principle one expects intracollisional interference effect (cf. Chapter IV) in a binary collision between two HD molecules. A noticeable feature of R(J) lines is their asymmetry on the low wavenumber side. This asymmetry has been explained by McKellar (1973) as a resonant interference between the discrete dipole transitions and the collision-induced continuum.

The integrated absorption coefficients $\int\alpha(\nu)\,d\nu$ (where $\alpha(\nu) = (1/\ell)\ln[I_0(\nu)/I(\nu)]$) for the collision-induced band of HD were obtained from the areas under the experimental profiles. These can be represented in terms of density ρ_a (in amagat units) of HD gas by the relation

$$\int\alpha(\nu)d\nu = \alpha_{1a}\rho_a^2 + \alpha_{2a}\rho_a^3 + \ldots, \qquad (5\text{-}1)$$

where α_{1a} (cm^{-2} $amagat^{-2}$) and α_{2a} (cm^{-2} $amagat^{-3}$) are the binary and the ternary absorption coefficients of the pure gas, respectively. Plots of $(1/\rho_a^2)\int\alpha(\nu)d\nu$ vs ρ_a for the profiles at the three experimental temperatures are shown

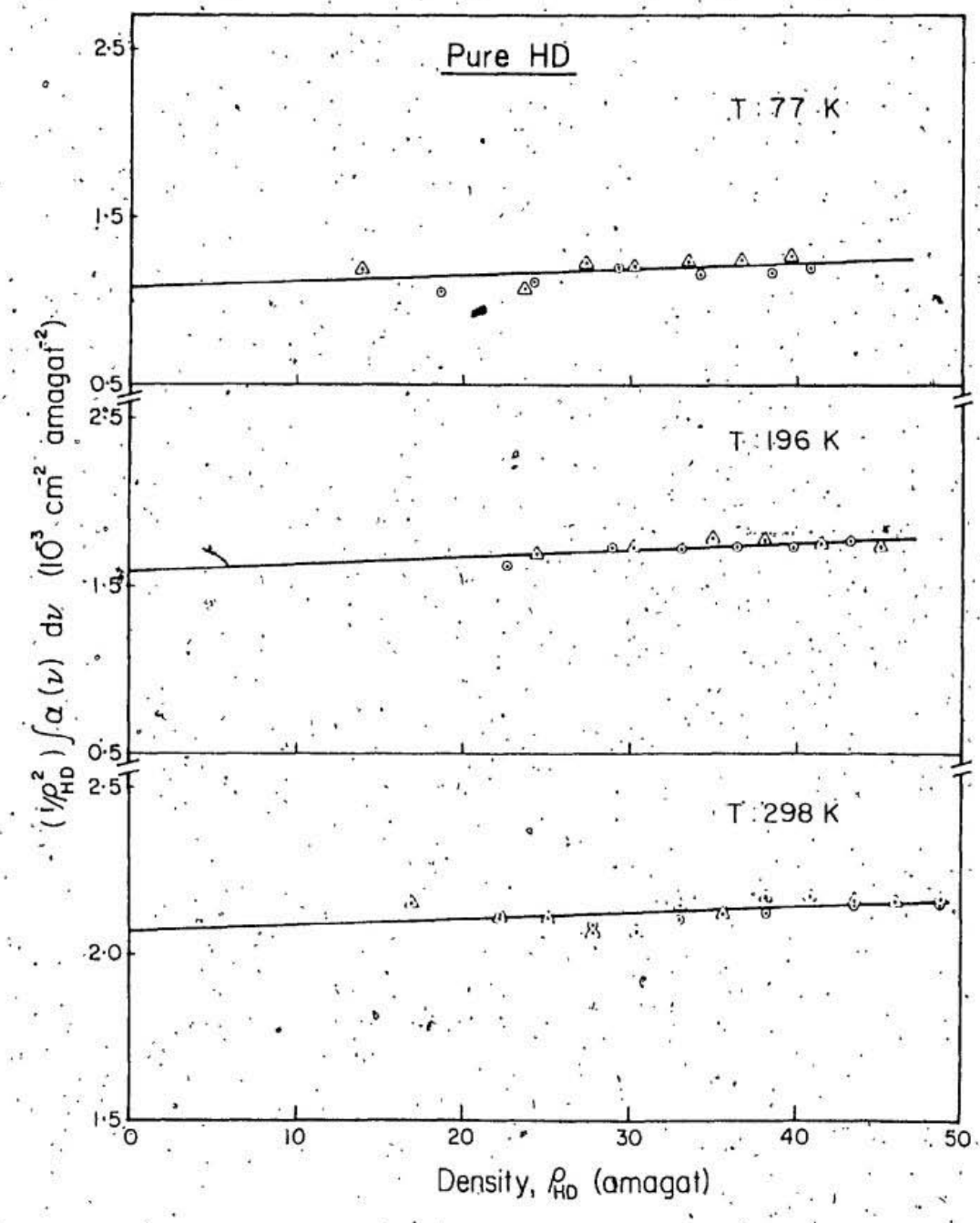

Fig. V-4. Plots of $(1/\rho_{HD}^2)\int\alpha(\nu)\,d\nu$ vs ρ_{HD} for the profiles of pure HD gas at 77, 196, and 298 K.

in Fig. V-4 and are found to be straight lines. The intercepts and the slopes of the straight lines, which give the binary and the ternary absorption coefficients, respectively, were calculated by a least-squares fit of the experimental data and their values are listed in Table V-2. While deriving the absorption coefficients, the contribution to the integrated intensity of the absorption profiles in the pure gas by the allowed $R_1(J)$ and $P_1(J)$ transitions (see Bejar and Gush 1974 and McKellar 1973 for the data at 298 and 77 K, respectively) was considered, but was found to be several orders of magnitude smaller than the contribution of the collision-induced transitions.

TABLE V-2

Absorption coefficients* of the fundamental band of HD

T (K)	Binary absorption coefficient (10^{-3} cm^{-2} amagat^{-2})	Binary absorption coefficient (10^{-35} cm^6 s^{-1})	Ternary absorption coefficient (10^{-6} cm^{-2} amagat^{-3})
77	α_{1a}: 1.07±0.06	$\tilde{\alpha}_{1a}$: 1.15±0.06	α_{2a}: 3.8±1.9
196	: 1.58±0.05	: 1.71±0.07	: 4.2±1.4
298	: 2.14±0.05	: 2.32±0.05	: 3.7±1.5

*Ranges of error indicated are standard deviations.

At all the experimental temperatures, the ternary absorption coefficients are very small compared to the binary absorption coefficients. This means, under the experimental conditions used in the present work, most of

the intensity arises from the binary collisions. The integrated absorption coefficient can be represented by the equation

$$c\int\tilde{\alpha}(\nu)\,d\nu = \tilde{\alpha}_{1a}\rho_a^2 n_0^2 + \tilde{\alpha}_{2a}\rho_a^3 n_0^3 + \ldots , \qquad (5\text{-}2)$$

where c is the speed of light, $\tilde{\alpha}(\nu) = \alpha(\nu)/\nu$, and n_0 is the Loschmidt's number. The new binary and ternary absorption coefficients $\tilde{\alpha}_{1a}(cm^6\ s^{-1})$ and $\tilde{\alpha}_{2a}(cm^9\ s^{-1})$ can be expressed as

$$\tilde{\alpha}_{1a} = \frac{(c/n_0^2)\alpha_{1a}}{\bar{\nu}} , \quad \tilde{\alpha}_{2a} = \frac{(c/n_0^3)\alpha_{2a}}{\bar{\nu}} , \qquad (5\text{-}3)$$

where the band center $\bar{\nu}$ is given by

$$\bar{\nu} = \int\alpha(\nu)\,d\nu / \int\alpha(\nu)\,\nu^{-1}d\nu \qquad (5\text{-}4)$$

The average values of $\bar{\nu}$ for the band at 77, 196, and 298 K are 3876, 3854, and 3821 cm^{-1}, respectively. The values of $\tilde{\alpha}_{1a}$ are also included in Table V-2. The binary absorption coefficient when expressed in units of cm^{-1} $amagat^{-2}$ was found to be 2.77×10^{-7} which compares favourably with 2.66×10^{-7}, the value obtained by McKellar (1973).

2. Profile Analysis and its Results

The collision-induced fundamental band of HD in the pure gas consists of a superposition of several overlap-induced Q lines with their characteristic dips occurring at the frequencies of the free HD molecules and two types of quadrupole-induced lines, arising from single- as well as double- transitions.* In Chapter III, Section 3, a detailed

*In the profile analysis it was assumed that the intensities of the O and S lines are completely due to the quadrupolar induction.

account of the analysis of the profiles of enhancement of absorption of the HD fundamental band in binary mixtures of HD with inert gases is given. Equations for the line shapes of the overlap and the quadrupolar transitions (Eqs. (3-5) to (3-11)) and for the relative intensities of the overlap transitions (Eqs. (3-12) and (3-13)) are in fact applicable in the present analysis as well. The only change that has to be made in the notation in Eqs. (3-5), (3-9), (3-10), and (3-11) is to delete the subscript in $\tilde{\alpha}_{en}$, $\tilde{\alpha}^{+}_{en}$, and $\tilde{\alpha}^{-}_{en}$ because in the present case one is concerned with the total absorption rather than the enhancement of absorption. We assume here that the quadrupole-induced single and double transitions have the same line shapes. The relative intensities of these single and double transitions in the fundamental band of HD are given by the following relations (see Poll 1970):

Single transitions

$$\tilde{\alpha}^{0}_{qm} = P_{J_1} P_{J_2} C(J_1 2 J_1'; 00)^2 C(J_2 0 J_2'; 00)^2 \times |\langle 0 J_1 | Q_1 | v_1' J_1' \rangle|^2 |\langle 0 J_2 | \alpha_2 | v_2' J_2' \rangle|^2 \qquad (5\text{-}6)$$

Double transitions

$$\tilde{\alpha}^{0}_{qm} = P_{J_1} P_{J_2} C(J_2 2 J_2'; 00)^2 C(J_1 0 J_1'; 00)^2 \times |\langle 0 J_2 | Q_2 | v_2' J_2' \rangle|^2 |\langle 0 J_1 | \alpha_1 | v_1' J_1' \rangle|^2 \qquad (5\text{-}7)$$

where the subscripts 1 and 2 refer to the two colliding molecules and vJ and v'J' are the initial and final vibrational and rotational quantum numbers. The factors P_{J_1} and P_{J_2} are the normalized Boltzmann factors defined in the same way as in Eq. (3-13) and $C(J\lambda J';00)$ with $\lambda = 0$ and 2, is a Clebsch-Gordan coefficient. For the fundamental band one has $v_1' = 1$ and $v_2' = 0$. Thus the intensities of the single transitions are proportional to $\langle 0J|Q|1J'\rangle^2 \langle 0J|\alpha|0J\rangle^2$ and those of the double transitions are proportional to $\langle 0J|Q|0J'\rangle^2 \langle 0J|\alpha|1J'\rangle^2$. The relative intensities of various transitions of the fundamental band of HD at 77, 196, and 298 K calculated from the theoretical matrix elements $\langle vJ|Q_{HD}|v'J'\rangle$ and $\langle vJ|\alpha_{HD}|v'J'\rangle$ obtained by Birnbaum and Poll (1969) and Poll (1975a), respectively, are listed in Appendix A. The method of computation using a program written for the IBM 370/155 computer which was used for the profiles of the enhancement of absorption in Chapter III remained essentially the same. The computation thus gave the half-width parameters δ_d and δ_c for the overlap-induced lines and δ_q (of the Boltzmann-modified dispersion line shape) or $\delta_{q'}$ (of the symmetrized dispersion line shape) of the quadrupole-induced lines.

An example of the result of the profile analysis of the HD fundamental band at 77 K using the Boltzmann-modified dispersion line shape for the quadrupolar lines for a density of 34.2 amagat of HD is shown in Fig. V-5. As the number of components is not very large at this temperature all the

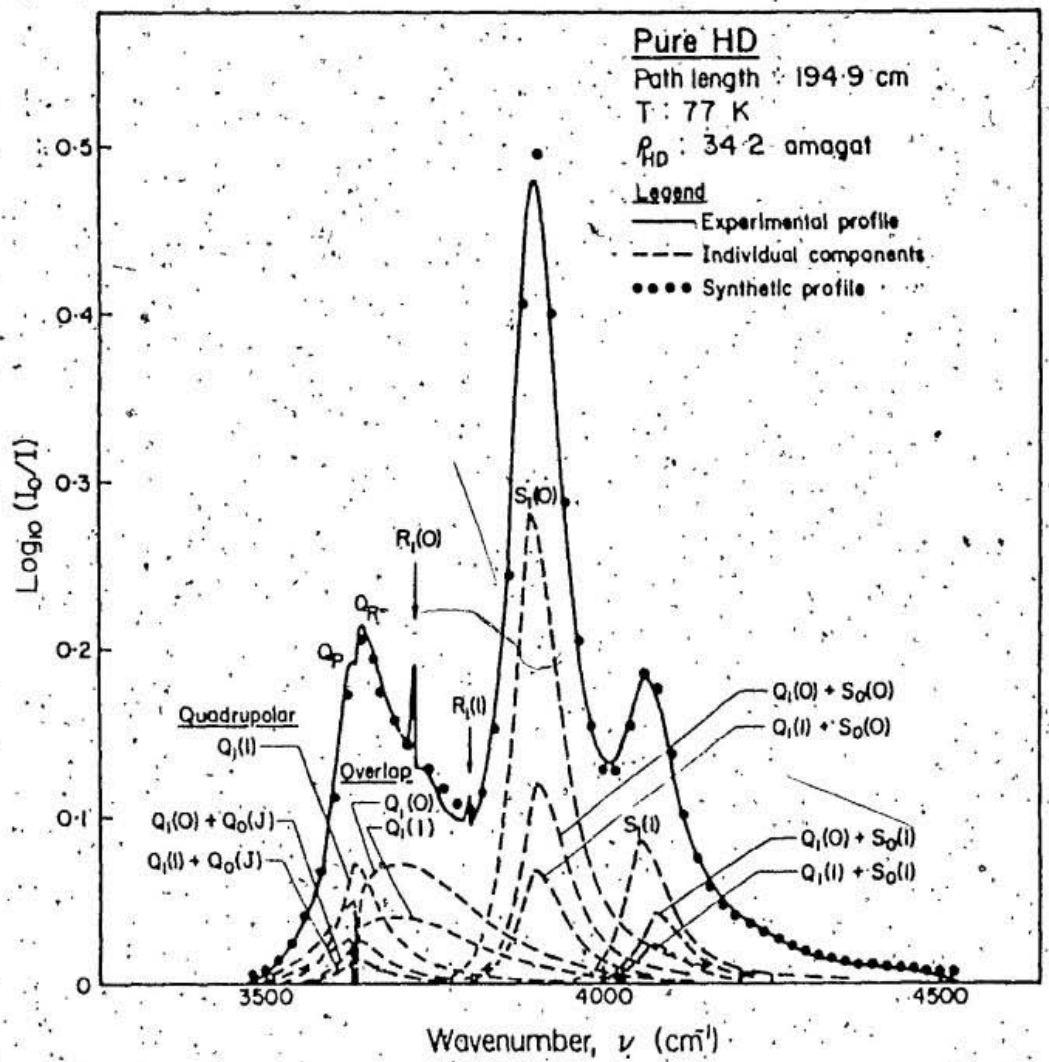

Fig. V-5. Analysis of an absorption profile of the HD fundamental band in the pure gas at 77 K. The solid curve is the experimental profile. The dashed curves represent the individual overlap and quadrupolar components and the dots represent the summation of these. For the sake of clarity, the weaker components with J = 2 are not shown. Note that the quadrupolar components $Q_1(0)$ and $Q_1(J) + Q_0(0)$ do not occur.

individual overlap and quadrupolar components have been shown. The agreement between the experimental and the synthetic profiles is reasonably good in the entire region of the band. It must be mentioned here that for the purpose of the profile analysis, the experimental curves under the allowed sharp $R_1(0)$ and $R_1(1)$ transitions were smoothed out. It means that the fit has been obtained only for the induced spectrum consisting of O, Q, and S transitions. It may be seen from Fig. V-5 that there is no unexplained absorption in the observed spectrum which could be ascribed to the broad collision-induced P and R transitions. However, induced $R_0(0)$ and $R_0(1)$ lines in the pure rotational band of HD and induced $R_1(0)$ line in the fundamental band of solid HD have been reported by Trefler et al. (1969) and Crane and Gush (1966), respectively. Results of similar profile analysis of the HD fundamental band at 196 and 298 K are shown in Figs. V-6 and V-7. For reasons of clarity, individual components have not been shown. As can be seen, the agreement between the experimental profile and the synthetic profile in each case is very good in almost the entire region of the fundamental band. An analysis performed with a symmetrized line shape for the quadrupole-induced lines gave equally good agreement between the observed and the synthetic profiles at all the three termperatures.

From the profile analysis it is possible to separate the contributions of the overlap and quadrupolar parts from the

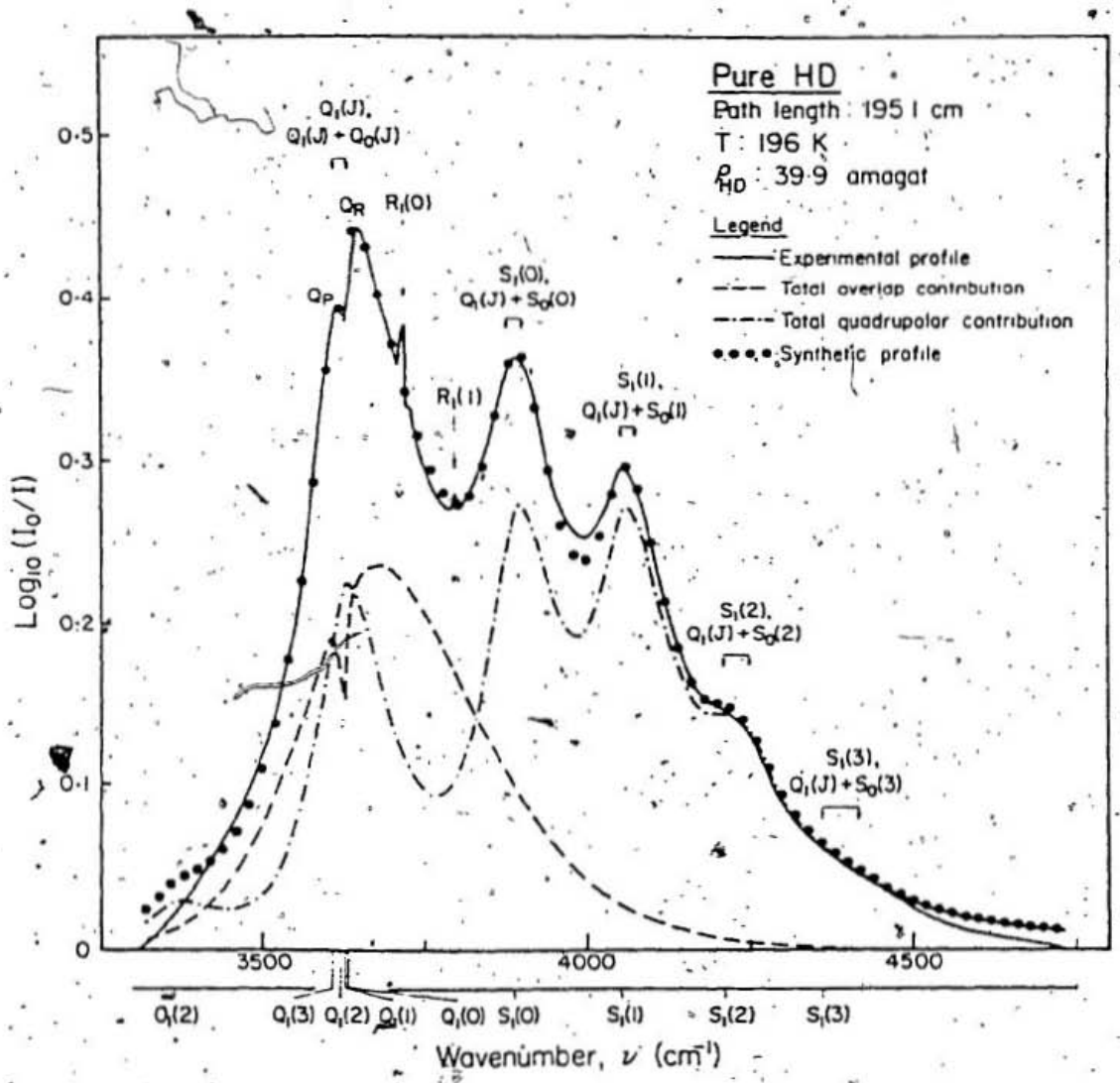

Fig. V-6. Analysis of an absorption profile of the HD fundamental band in the pure gas at 196 K. Here J takes the values 0 - 3. For other details see the caption of Fig. V-5.

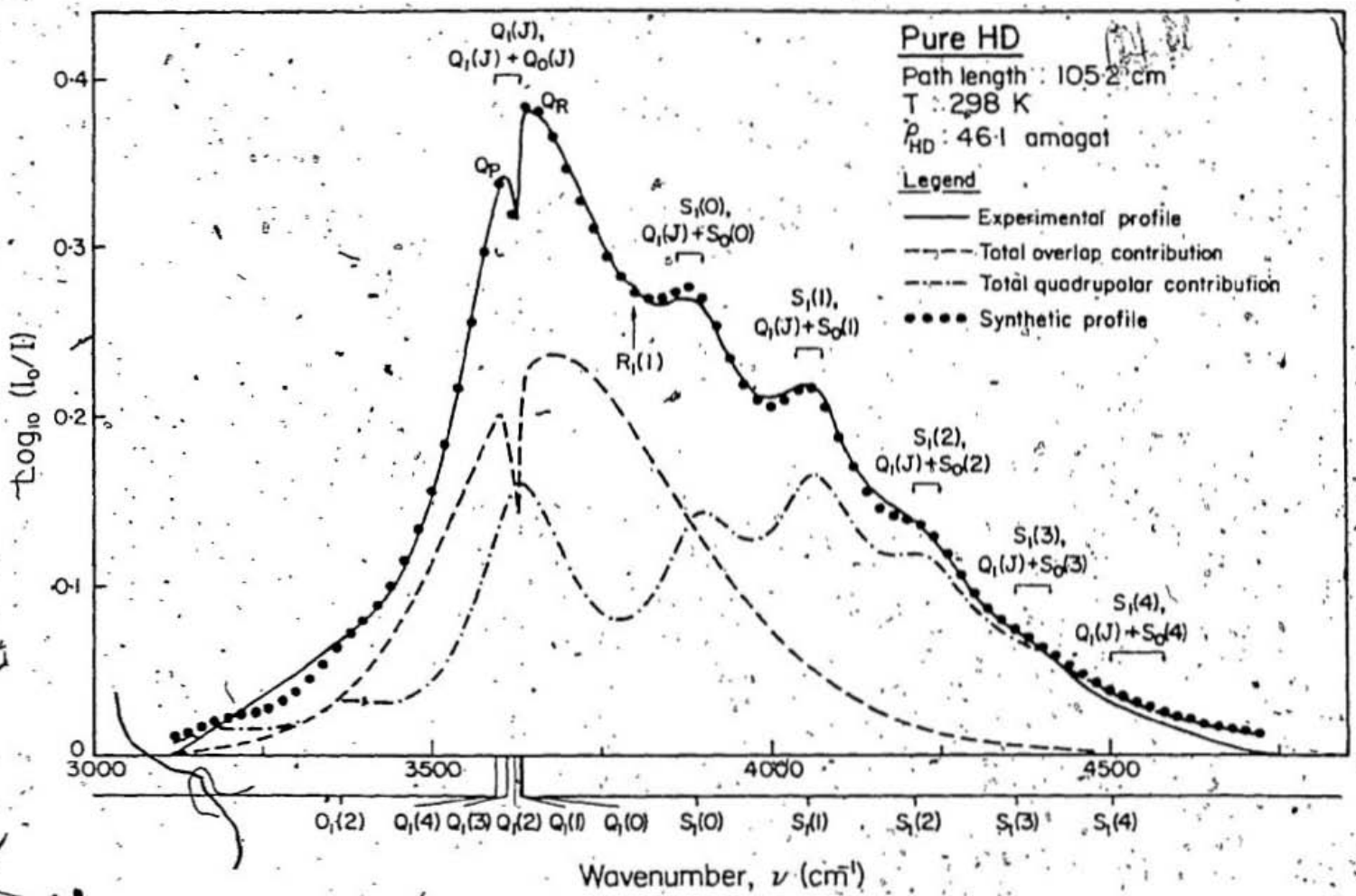

Fig. V-7. Analysis of an absorption profile of the HD fundamental band in the pure gas at 298 K. Here J takes the values 0 - 4. For other details see the caption of Fig. V-5.

total intensity of the band. In Table V-3 the results of the profile analysis are presented. As the temperature varies from 77 to 298 K, the overlap contribution increases from 27% to 46% and the quadrupolar contribution decreases from 73% to 54%. The half-width parameters δ_d, δ_q, and $\delta_{q'}$, obtained at 77 K in the present work compare well with the corresponding parameters at the same temperature obtained by McKellar (1973) (see Table V-3).

Although δ_d, δ_q, and $\delta_{q'}$ are independent of density (within the range of densities used), they show a characteristic temperature dependence. In Fig. V-8 average values of δ_d, δ_q, and $\delta_{q'}$ have been plotted against the square root of temperature (K). It may be seen that δ_d increases approximately linearly with $\sqrt{T}$ in a manner similar to that obtained for H_2-inert gas mixtures (Mactaggart and Welsh 1973). The intercept of the line gives a value of 88 cm^{-1} which corresponds to the value of δ_d for T = 0. This large value of δ_d at T = 0 indicates that the duration of collision ($\tau_d = 1/2\pi c\delta_d$) at T = 0 is still relatively short because the overlap-induction takes place mainly in the region of the strong repulsion of the colliding pair of molecules. The quadrupolar half-widths δ_q and $\delta_{q'}$ vary as $\sqrt{T}$ and are given by $\delta_q = 5.81\sqrt{T}$ and $\delta_{q'} = 4.65\sqrt{T}$. The half-widths vary as $\sqrt{T}$ and are thus proportional to the average relative velocity of the colliding pair of molecules.

TABLE V-3

Results of the profile analysis for the HD fundamental band

T (K)	Intracollisional half-width δ_d (cm^{-1})	Collision duration τ_d (s) (10^{-14} s)	Quadrupolar half-width δ_q (cm^{-1})	Collision duration τ_q (s) (10^{-14} s)	Quadrupolar half-width (symmetrized) $\delta_{q'}$	Overlap contribution %	Quadrupolar contribution %	Reference
77	145±6	3.7	51±1	10.4	38±1	27	73	This work
	142±4		55±1		39			McKellar (1973)
196	162±2	3.3	83±1	6.4	66±1	36	64	This work
298	199±2	2.7	99±3	5.4	81±2	46	54	"

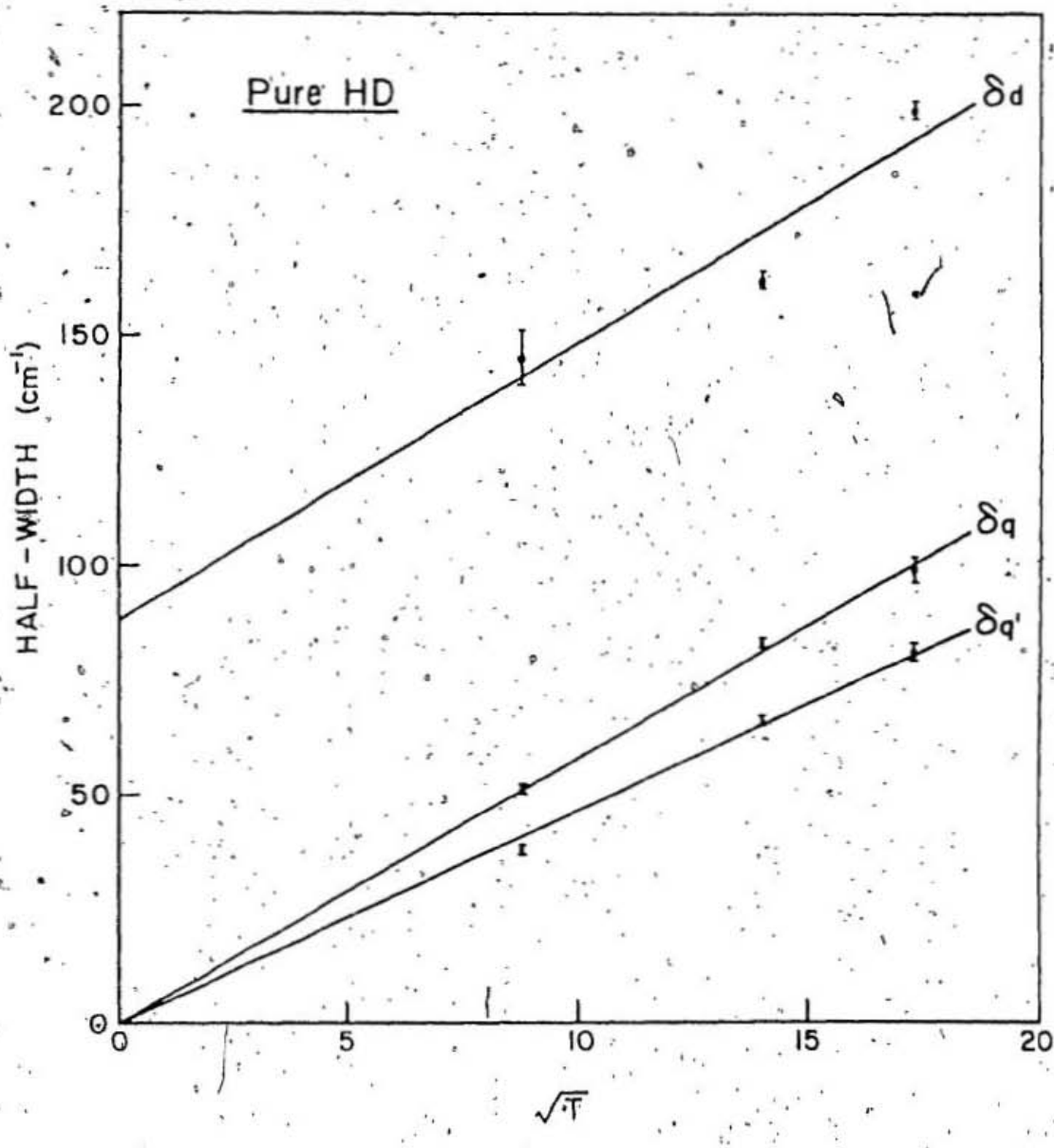

Fig. V-8. Plots of the half-width parameters δ_d, $\delta_{q'}$ and δ_q, against the square root of the absolute temperature T.

The intercollisional half-width δ_c increases with increasing density. Thus it shows a clear density dependence at each of the temperatures investigated. Since experiments with pure HD gas have been limited only up to 50 amagat at each of the temperatures, no definite expression for density dependence could be obtained. The values of δ_c were less than 1, 1.5 and 1.8 cm^{-1} at 77, 196, and 298 K, respectively, for the maximum experimental densities of the gas. In order to obtain a reliable density-dependent relation for δ_c experiments must be extended to higher densities.

3. Overlap Parameters for the HD-HD Molecular Pairs

The values of the overlap integrated absorption coefficient $\int \alpha_{overlap}(\nu)d\nu$ derived from the profile analysis can be represented by the relation which is similar to the one represented by the Eq. (5-1)

$$\int \alpha_{overlap}(\nu)d\nu = \alpha_{1a\ overlap}\rho_a^2 + \alpha_{2a\ overlap}\rho_a^3 + \ldots, \quad (5\text{-}8)$$

Plots of $(1/\rho_a^2)\int \alpha_{overlap}(\nu)d\nu$ vs ρ_a are shown in Fig. V-9 for the data for all the three experimental temperatures and are found to be straight lines. The overlap binary and ternary absorption coefficients $\alpha_{1a\ overlap}(cm^{-2}\ amagat^{-2})$ and $\alpha_{2a\ overlap}(cm^{-2}\ amagat^{-3})$ were obtained respectively from the intercepts and slopes, which were calculated from the linear least-squares fits. The values of these coefficients and those of the new binary absorption coefficients

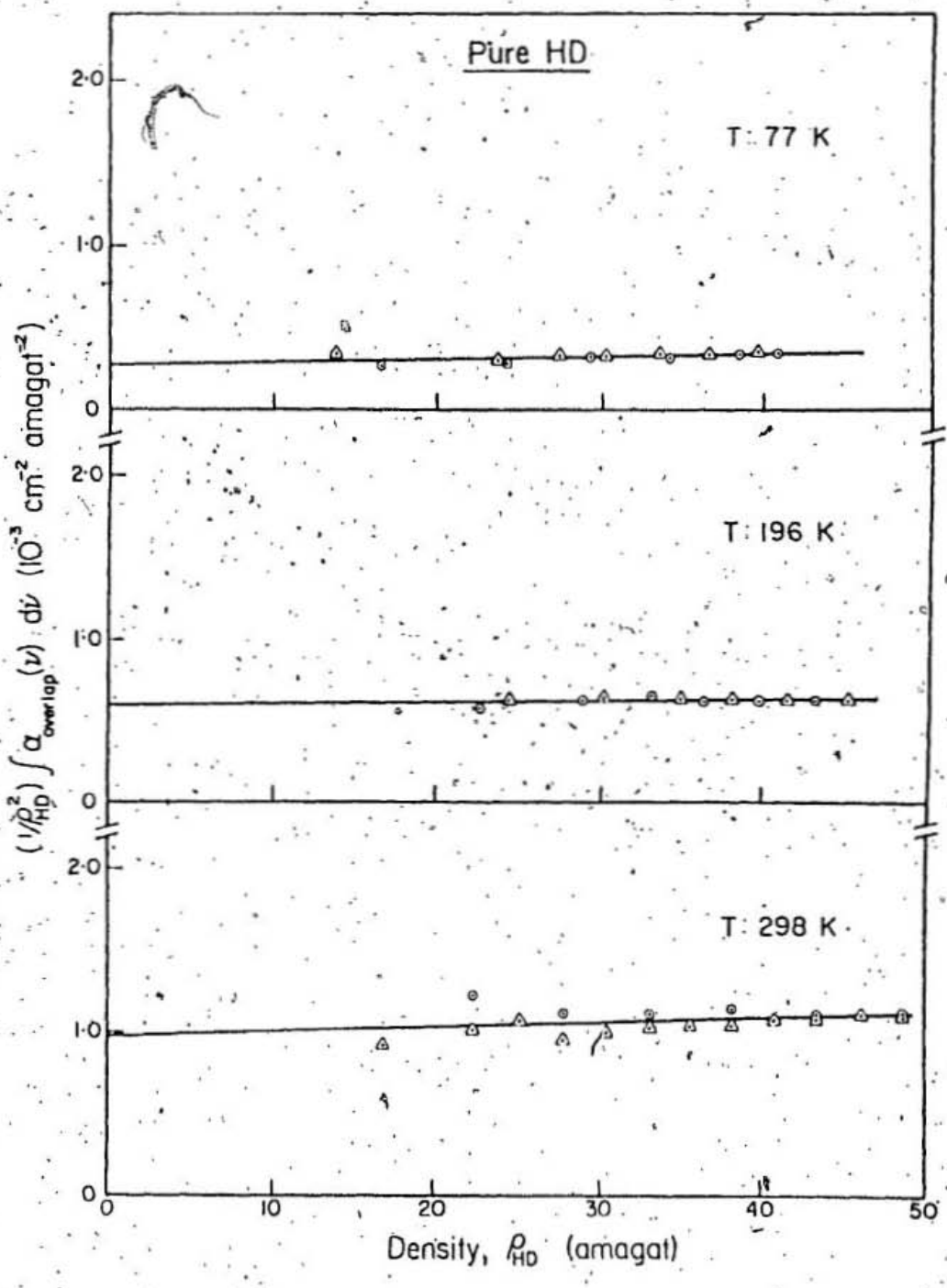

Fig. V-9. Plots of $(1/\rho_{HD}^2)\int \alpha_{overlap}(\nu)\, d\nu$ vs ρ_{HD}^a for the profiles of pure HD gas at 77, 196, and 298 K.

$\tilde{\alpha}_{\text{la overlap}}(\text{cm}^6\ \text{s}^{-1})$ calculated from the relation $\tilde{\alpha}_{\text{la overlap}} = (c/\pi_0^2) \times (\alpha_{\text{la overlap}}/\bar{\nu})$, $\bar{\nu}$ being the center of the overlap profile (see Eq. (5-4)), are listed in Table V-4.

Theoretical Expression for the Overlap Binary Absorption Coefficient

According to Van Kranendonk (1958), the overlap binary absorption coefficient $\tilde{\alpha}_{\text{la overlap}}$ of the fundamental band can be written as

$$\tilde{\alpha}_{\text{la overlap}} = (8\pi^3/3h)\ \kappa_1^2 \int |\{\vec{M}(\vec{R})\}_{\text{overlap}}|^2\ g_0(\vec{R})\, d\vec{R}, \quad (5\text{-}9)$$

where $\vec{M} = \langle(\partial\vec{\mu}/\partial r_1)_0\rangle$ is the expectation value of the rate of change of $\vec{\mu}$ with respect to r_1 at the internuclear separation r_0 and $\kappa_1 = \langle 0|(r-r_0)|1\rangle$. The quantity $g_0(\vec{R})$ is the low density limit of the pair distribution function. Equation (5-9) may be rewritten as

$$\tilde{\alpha}_{\text{la overlap}} = (8\pi^3/3h)\ \kappa_1^2 \int |\vec{M}_0(\vec{R})|^2\ g_0(\vec{R})\, d\vec{R}. \quad (5\text{-}10)$$

The quantity $M_0(R)$ is assumed to decrease exponentially with the intermolecular separation R and is expressed as

$$M_0(R) = \xi \exp(-R/\rho) = \lambda e \exp[-(R-\sigma)/\rho], \quad (5\text{-}11)$$

where the dimensionless quantity $\lambda = (\xi/e) \exp(-\sigma/\rho)$. Here λe is the amplitude of the oscillating overlap induced moment when the molecular separation is σ corresponding to the Lennard-Jones intermolecular potential $V(\sigma) = 0$ (Note: $\mu_{\text{overlap}}(\sigma) = \lambda e \sigma$). The quantities ξ and ρ give respectively the magnitude and the range of the oscillating part of the overlap induced moment. Equation (5-10) now becomes

TABLE V-4

Absorption coefficients* of the overlap part of the HD fundamental band

T (K)	Binary absorption coefficient (10^{-3} cm^{-2} amagat^{-2})		Binary absorption coefficient (10^{-35} cm^{6} s^{-1})		Ternary absorption coefficient (10^{-6} cm^{-2} amagat^{-3})	
77	$\alpha_{1a\ overlap}$	0.28±0.03	$\tilde{a}_{1a\ overlap}$	0.31±0.03	$\alpha_{2a\ overlap}$	1.5±0.8
196		0.60±0.03		0.67±0.03		0.8±0.8
298		0.97±0.06		1.08±0.06		2.8±1.7

* Ranges of error indicated are standard deviations.

$$\tilde{\alpha}_{1a\ \text{overlap}} = (8\pi^3/3h)\,|\langle 0|(r-r_0)|1\rangle|^2 \int |\vec{M}_0(\vec{R})|^2\, g_0(\vec{R})\, d\vec{R}$$

$$= \lambda^2 \frac{8\pi^3}{3h} e^2\sigma^3 |\langle 0|(r-r_0)|1\rangle|^2 \times 4\pi \int_0^\infty \exp[-2(x-1)(\sigma/\rho)]\, g_0(x)\, x^2 dx$$

$$= \lambda^2 I \tilde{\gamma}, \qquad (5\text{-}12)$$

in which $x = R/\sigma$. The quantity $\tilde{\gamma} = \frac{8\pi^3}{3h} e^2\sigma^3 |\langle 0|(r-r_0)|1\rangle|^2$ has the dimensions of the binary absorption coefficient $\tilde{\alpha}_{1a}$ and the temperature-dependent dimensionless integral $I(T^*)$, where $T^* = kT/\varepsilon$, is represented by the relation

$$I(T^*) = 4\pi \int_0^\infty \exp[-2(x-1)(\sigma/\rho)]\, g_0(x)\, x^2 dx. \qquad (5\text{-}13)$$

Actually $I(T^*)$ represents the average R-dependence of $M_0(R)$. At high temperatures where quantum effects can be neglected $g_0(x)$ can be calculated by the classical expression

$$g_0(x) = \exp[-V^*(x)/T^*], \qquad (5\text{-}14)$$

where $V^*(x) = V(x)/\varepsilon$, $V(x)$ being the Lennard-Jones intermolecular potential given by

$$V(x) = 4\varepsilon[x^{-12} - x^{-6}]. \qquad (5\text{-}15)$$

At intermediate temperatures, $g_0(x)$ may be expanded as an asymptotic series in terms of the reduced mean de Broglie wavelength Λ^* $[= (h^2/2m_{00}\varepsilon\sigma^2)^{\frac{1}{2}}]$, m_{00} being the reduced mass of the colliding pair of molecules. The resulting expression for I is

$$I = I_{cl} - \Lambda^{*2} I^{(2)} + \Lambda^{*(4)} I^{(4)} \ldots \qquad (5\text{-}16)$$

To obtain the experimental values of $\lambda^2 I$ for the HD-HD pairs, values of $\tilde{\alpha}_{1a\ overlap}$ were divided by the value of $\tilde{\gamma}$ at each of the temperatures. In order to calculate the value of $\tilde{\gamma}$ (see Table V-5 for the values of the molecular constants used in the calculations), the value of the matrix element $\langle 00|(r-r_0)|10\rangle$ (Poll 1975b) was used. Fig. V-10 shows the plot of the experimental values of $\lambda^2 I$ against absolute temperature T. The integral I in Eq. (5-13) depends on the factor σ/ρ which occurs in the exponential. The most probable value of σ/ρ for the HD-HD pairs was determined by a procedure similar to the one described by Reddy and Chang (1973) and the details are as follows: The values of I_{cl} were computed for a series of values of ρ/σ in the range 0.070 to 0.140 at intervals of 0.002 at reduced temperatures T* in the range 0.5 to 20.0 at intervals of 0.5. Appropriate values of I were obtained by applying the quantum corrections $I^{(2)}$ and $I^{(4)}$ (see Eq. (5-16)) taken either directly or extrapolated from the data given by Van Kranendonk and Kiss (1959). For a particular value of σ/ρ, λ^2 which is assumed to be independent of temperature was calculated from the value of $\lambda^2 I$ at one of the temperatures using the corresponding value of I. The values of $\lambda^2 I$ at the other two experimental temperatures were in turn calculated and compared with the corresponding experimental values. This procedure was repeated for a

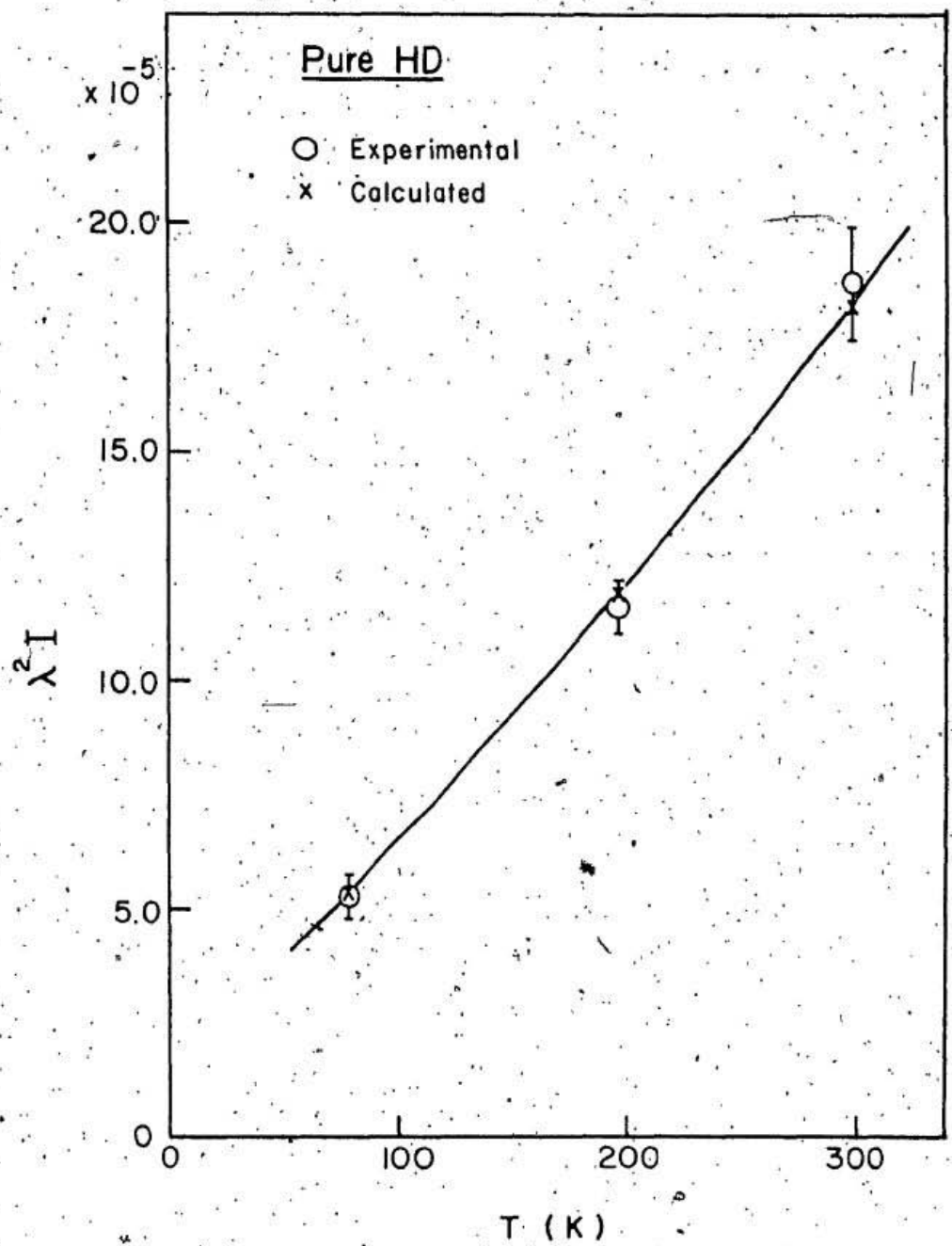

Fig. V-10. Variation of $\lambda^2 I$ with the absolute temperature T for the pure HD gas.

series of values of σ/ρ until the calculated values of $\lambda^2 I$ at the three temperatures agreed closely with the corresponding experimental values. The criterion used for the best fit of the curve $\lambda^2 I$ vs T was that $\sum_i \delta_i^2$ be a minimum, where δ_i are the deviations of the calculated values of $\lambda^2 I$ from the corresponding experimental values. The calculated values of $\lambda^2 I$ for the best fit are also shown in Fig. V-10. The values of ρ/σ and λ for HD-HD obtained from the best fit are given in Table V-6. Also included in the table are the values of ρ, σ, and $\mu(\sigma)$ (the induced dipole moment corresponding to the Lennard-Jones diameter σ). A comparison of the values of the overlap parameters of HD-HD pairs with those of H_2-H_2 pairs will be made in the next chapter.

TABLE V-5

Molecular constants for the pure HD gas

ε/k (K)	σ (Å)	$\bar{\gamma}$ (10^{-32} cm^6 s^{-1})	A^*
37.00	2.928	5.767	1.414

TABLE V-6

Overlap parameters for the pure HD gas

ρ/σ	λ	σ (Å)	ρ (Å)	$\mu(\sigma)$ (10^{-3} ea_0)
0.084	5.13×10^{-3}	2.928	0.25	28.4

CHAPTER VI

COLLISION-INDUCED ABSORPTION OF THE FUNDAMENTAL BAND OF H_2 IN THE PURE GAS AT DIFFERENT TEMPERATURES

1. Introduction

The collision-induced fundamental band of gaseous H_2 first observed by Welsh et al. (1949) has been the subject of numerous investigations under a variety of experimental conditions in the last twenty-six years. The band was studied at the McLennan Laboratory, University of Toronto, by Welsh and his collaborators in pure H_2 and in binary mixtures H_2-He, H_2-Ar, H_2-N_2, H_2-Kr, and H_2-Xe at sample path lengths ranging from a fraction of a cm to 13.6 m, at pressures in the range 1 to 5000 atm, and at temperatures in the range 18 to 376 K (cf., Chisholm and Welsh 1954, Gush, Nanassy, and Welsh 1957, Hare and Welsh 1958, Hunt 1959, Hunt and Welsh 1964, Watanabe and Welsh 1965, 1967, Watanabe 1971, De Remigis et al. 1971, Mactaggart and Welsh 1973, and Mactaggart et al. 1973). There have also been several experimental studies on this band in our laboratory. These were the studies of the band in H_2-Ne and H_2-Kr (Reddy and Lee 1968), H_2-O_2 and H_2-Xe (Varghese and Reddy 1969), para H_2-Ar, para H_2-Kr, and para H_2-Xe (Varghese

et al. 1972) at room temperature and in H_2-He and H_2-Ne (Reddy and Chang 1973) at different temperatures in the range 77 to 298 K. In these studies, the band was investigated with absorption cells with sample path lengths 1/4 m and 1 m at total gas densities up to ~500 amagat. Because of space limitations we do not include here references on the spectra of the induced fundamental band of H_2 in the solid and liquid states, in H_2 dissolved in liquids of inert gases and other substances and in H_2-X van der Waals complexes (where X stands for H_2 or other perturbing gas molecules), and those on the spectra of the U ($\Delta J = +4$) transitions.

A general survey of the previous work on the profile analysis of the collision-induced spectra with a special emphasis on that of the spectra of H_2 is given in Chapter I. The reader is referred to Chapter I for the details of the previous work on the profile analysis of the H_2 fundamental band in the pure gas, at 78, 195, and 300 K by Hunt and Welsh (1964), and at a number of temperatures in the range 18 to 77 K by Watanabe and Welsh (1967), and on the revised profile analysis of the band at 18, 20.4, and 24 K by Watanabe (1971). The reader is also referred to the same chapter for details of the theoretical expression derived for the intracollisional line form applicable to the overlap Q components by Levine and Birnbaum (1967) and of the dispersion type line form obtained for the dips of the Q

components by Van Kranendonk (1968). We also remind the reader that the enhancement profiles of the H_2 fundamental band in H_2-inert gas mixtures were satisfactorily analyzed by Mactaggart and Welsh (1973) and Mactaggart et al. (1973) using the theoretical line shapes of Levine and Birnbaum and Van Kranendonk.

Prior to the present work the new theoretical line shapes of Levine and Birnbaum and Van Kranendonk have not been applied to the profiles of the H_2 fundamental band in the pure gas. In the present work the profiles of the fundamental band of H_2 in the pure gas were recorded for densities up to 60 amagat at 77 and 196 K in the 2 m absorption cell and at 298 K in the 1 m and 2 m absorption cells. The overlap contribution to the total intensity of the band at the three temperatures was separated, just as in the case of the HD fundamental band in the pure gas in Chapter V, by the method of the profile analysis making use of the new line shapes of Levine and Birnbaum (1967) and Van Kranendonk (1968) for the overlap components, and the Boltzmann-modified dispersion line form as well as the symmetrized dispersion line form for the quadrupolar components. The overlap parameters λ, ρ, and $\mu(\sigma)$ (defined in Chapter V) for the H_2-H_2 collision pairs are then derived from the overlap binary absorption coefficients using the theory of Van Kranendonk (1958). Table VI-1 gives a summary of the experiments in the present work on the collision-induced fundamental band of

H_2 in the pure gas whose results are described in the rest of this chapter.

TABLE VI-1

Summary of the experiments on the H_2 fundamental band

T (K)	Sample path length (cm)	Maximum density of the gas (amagat)	Number of gas densities studied
77	194.9	45	13
196	195.1	47	14
298	105.2, 195.3	58	20

2. Absorption Profiles and Absorption Coefficients

The experimental arrangements and the experimental procedure for the study of the H_2 fundamental band are the same as those for the HD fundamental band and are described in detail in Chapter II. The absorption profiles of the H_2 fundamental band in the pure gas are well known from the earlier works and typical profiles obtained in the present study at 77, 196, and 298 K are shown in Figs. VI-1, VI-2, and VI-3, respectively. The positions of the single transitions $O_1(J)$, $Q_1(J)$, and $S_1(J)$ for the appropriate J values obtained from the constants of the free H_2 molecule (Stoicheff 1957) are marked along the wavenumber axis. At 77 K only two rotational states J = 0 and J = 1 are populated and at 196 and 298 K states J = 0, 1, and 2 and J = 0, 1, 2, and 3, respectively, are populated. One should of

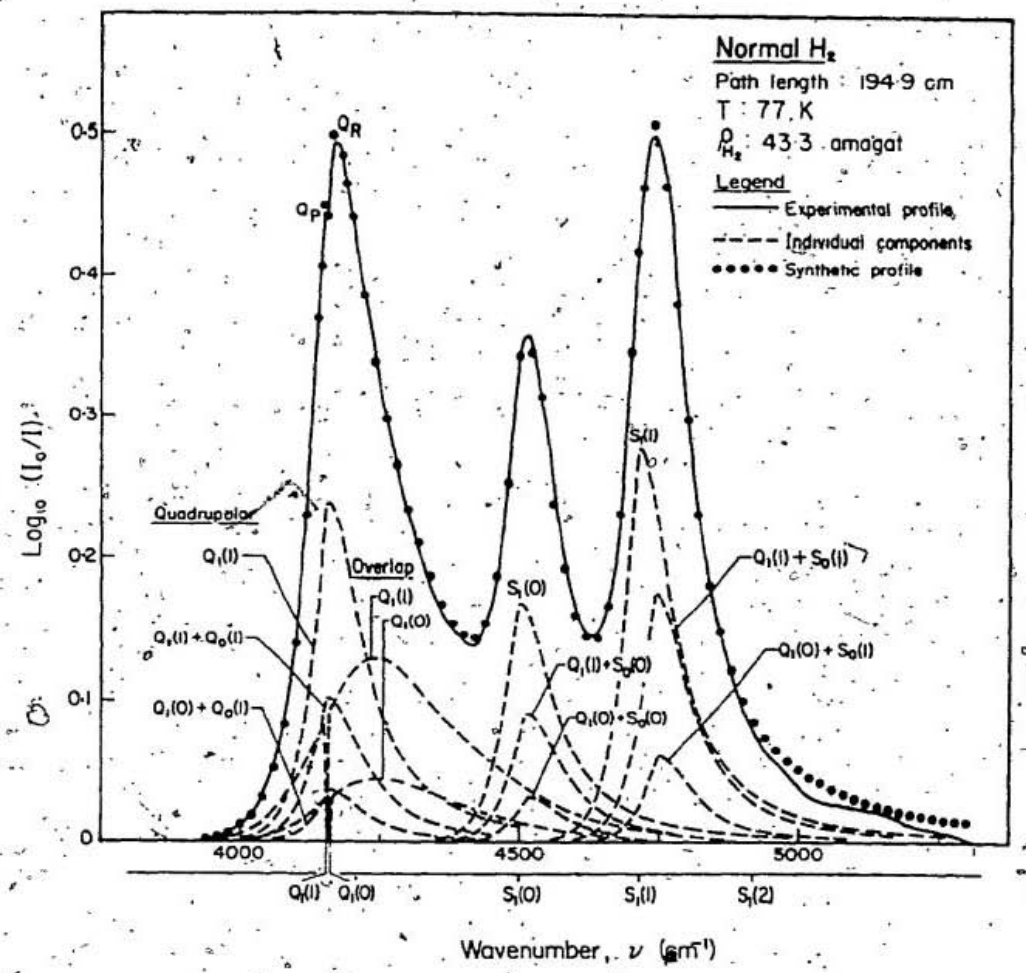

Fig. VI-1. Analysis of an absorption profile of the H_2 fundamental band in the normal gas at 77 K. The solid curve is the experimental profile. The dashed curves represent the overlap and quadrupolar components and the dots represent the summation of these. Note that the quadrupolar component $Q_1(0)$ does not occur.

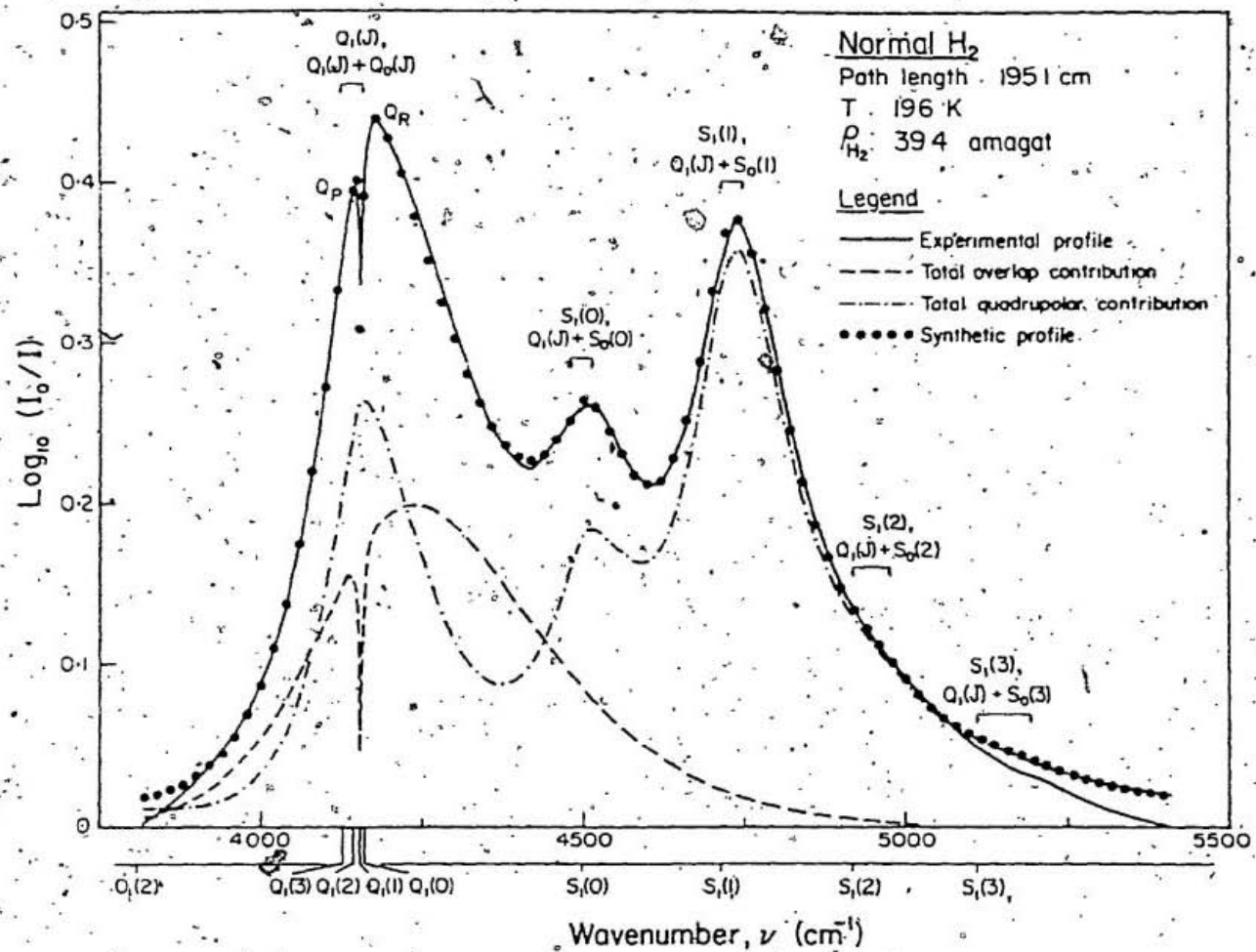

Fig. VI-2. Analysis of an absorption profile of the H_2 fundamental band in the normal gas at 196 K. Here J takes the values 0 - 3. See the caption of Fig. VI-1 for other details.

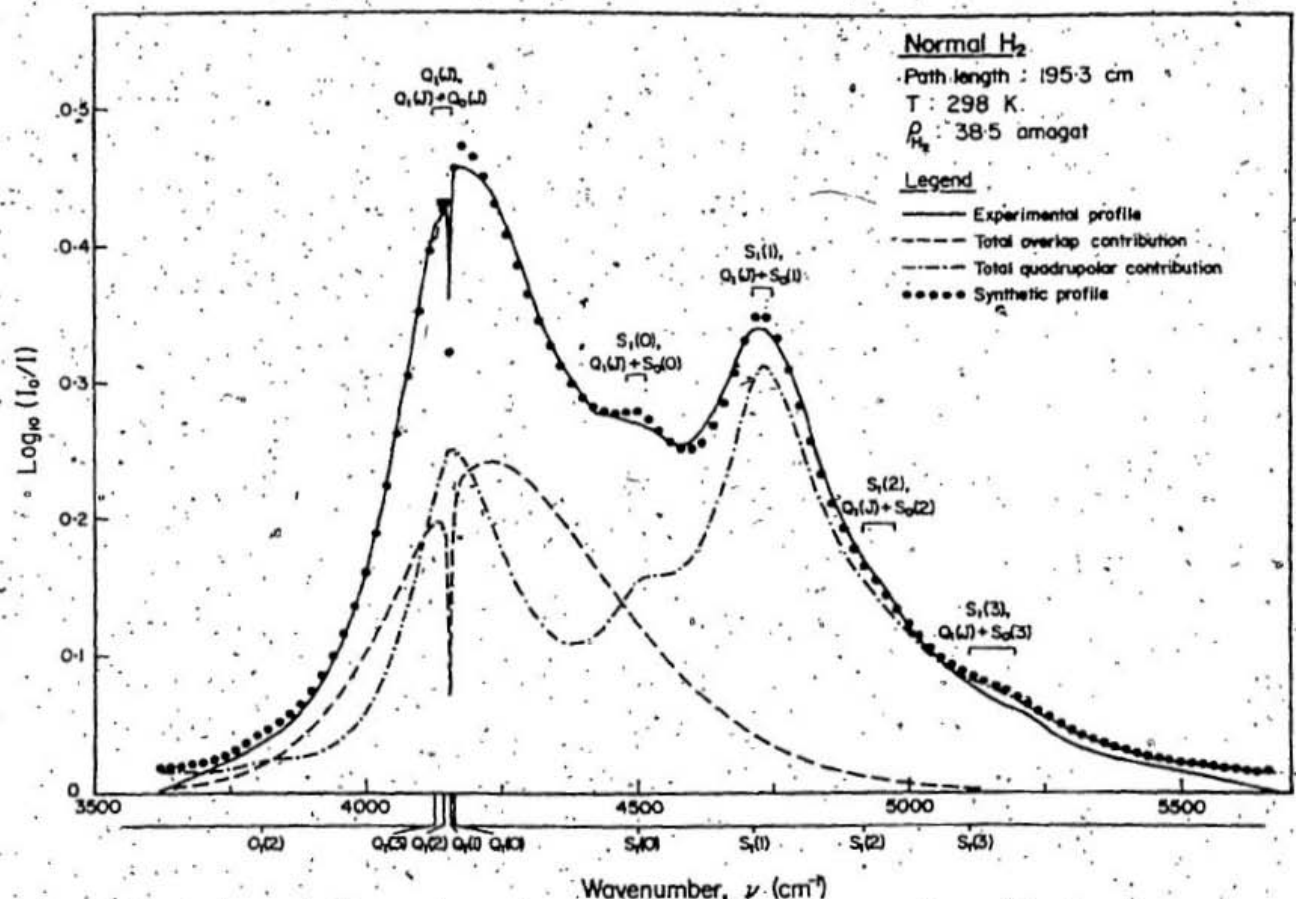

Fig. VI-3. Analysis of an absorption profile of the H_2 fundamental band in the normal gas at 298 K. Here J takes the values 0 - 3. See the caption of Fig. VI-1 for other details.

course note that for H_2 the even and odd J levels correspond to the para and ortho modifications, respectively. The pure gas fundamental band of H_2 is comprised of, in addition to the single transitions, many double transitions of the types $Q_1(J) + Q_0(J)$ ($J \neq 0$ for the orientational transition) and $Q_1(J) + S_0(J)$. The occurrence of the dip at the position of the $Q_1(1)$ line (4155 cm^{-1}) of the free H_2 molecule, the increase of separation $\Delta\nu_{PR}^{max}$ between the Q_P and Q_R maxima of the Q branch with increasing density of the gas, and the effect of the temperature on the profiles of the band are well known from the work of the earlier researchers.

By integrating the areas under the experimental profiles, the integrated absorption coefficients $\int\alpha(\nu)d\nu$ of the band were determined and these can be expressed in terms of density by Eq. (5-1). Plots of $(1/\rho_a^2)\int\alpha(\nu)d\nu$ vs ρ_a at the three experimental temperatures are shown in Fig. VI-4. The binary and ternary absorption coefficients were obtained from, respectively, the intercepts and slopes of these lines. The values of the binary absorption coefficients α_{1a} (cm^{-2} $amagat^{-2}$) and $\tilde{\alpha}_{1a}$ (cm^6 s^{-1}) (cf. Eq. (5-3)) and ternary absorption coefficient α_{2a} (cm^{-2} $amagat^{-3}$) for the experiments at all the three temperatures are listed in Table VI-2. The centers $\bar{\nu}$ of the band at 77, 196, and 298 K are 4483, 4466, and 4444 cm^{-1}, respectively. For the purpose of comparison,

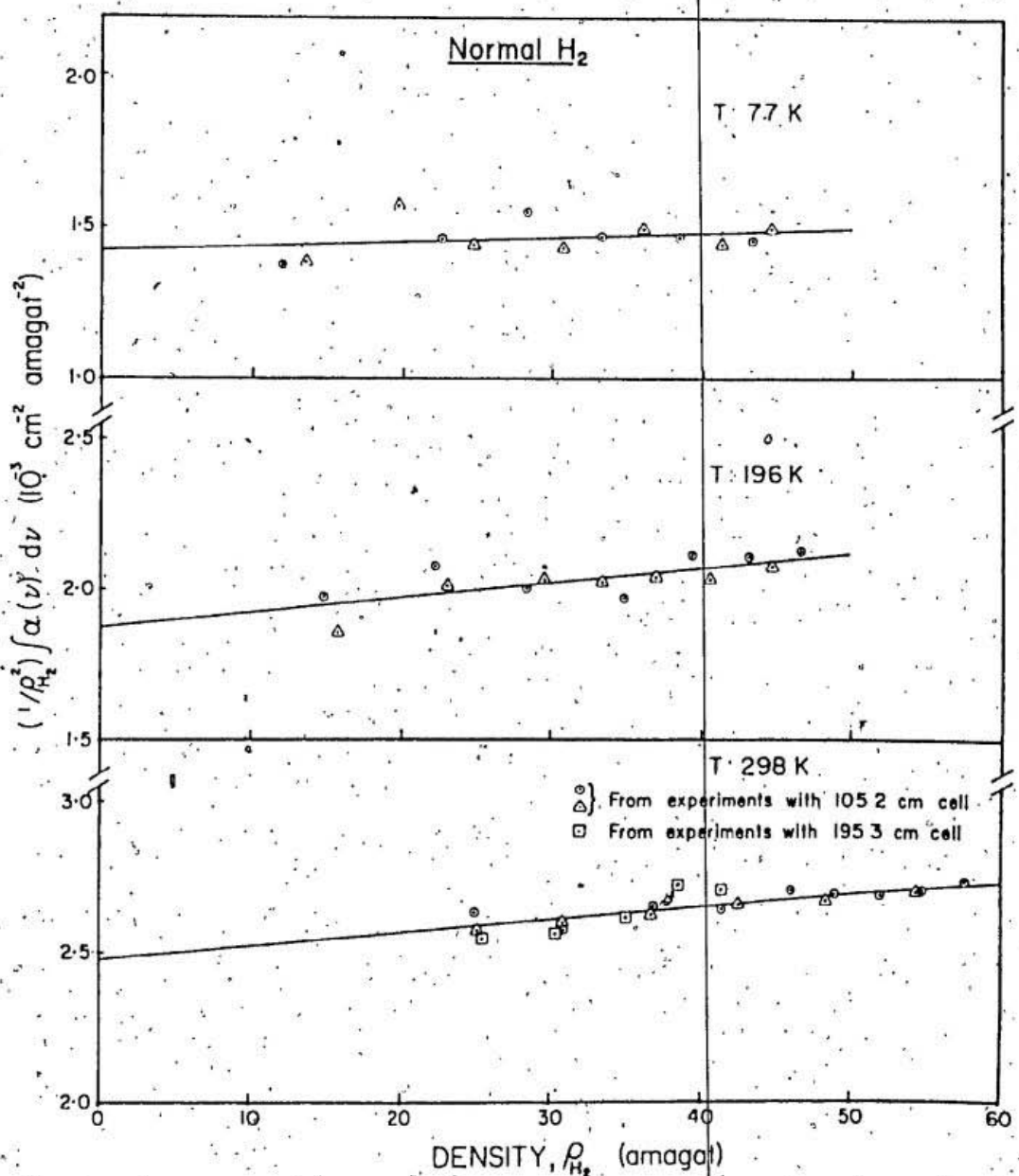

Fig. VI-4. Plots of $(1/\rho_{H_2}^2)\int\alpha(\nu)\,d\nu$ vs ρ_{H_2} for the profiles of normal H_2 gas at 77, 196, and 298 K.

TABLE VI-2

Absorption coefficients* of the fundamental band of normal H_2 at 77, 196, and 298 K

T (K)	Binary absorption coefficient α_{1a} (10^{-3} cm^{-2} amagat^{-2})	Binary absorption coefficient $\tilde{\alpha}_{1a}$ (10^{-35} cm^{6} s^{-1})	Ternary absorption coefficient α_{2a} (10^{-6} cm^{-2} amagat^{-3})	References
77	1.42±0.05	1.32±0.05	1.5±1.5	Present work
	1.44	1.37		Hunt (1959)
		1.32±0.02		Watanabe and Welsh (1965)
196	1.87±0.05	1.74±0.05	4.9±1.3	Present work
	2.04	1.89		Hunt (1959)
298	2.46±0.03	2.30±0.03	4.7±0.7	Present work
	2.5		2.0	Chisholm and Welsh (1954)
	2.4		1.1	Hare and Welsh (1958)
	2.42	2.24		Hunt (1959)

* Ranges of error indicated in the present work are standard deviations.

the values of the absorption coefficients obtained by earlier researchers are also listed in the same table. The present values of the absorption coefficients at 77 and 298 K compare very well with the corresponding values obtained by earlier researchers. However, the present values of the absorption coefficient at 196 K are somewhat smaller than those obtained by Hunt (1959).

3. Profile Analysis and Results

The method of profile analysis used for the absorption profiles of the HD fundamental band in the pure gas, which was described in Chapter V, Section 2, is applicable in its entirety to the profiles of the H_2 fundamental band. The reader is therefore referred to that chapter for details of the method. For the H_2 fundamental band the relative intensities of the overlap components expressed in terms of the intensity of the Q_1 overlap(1) component and those of the quadrupolar components expressed in terms of that of the $S_1(1)$ line are listed in Appendix C. In the calculation of the relative intensities, the theoretical matrix elements of the quadrupole moment $\langle vJ|Q_{H_2}|v'J'\rangle$ calculated by Birnbaum and Poll (1969) and of the polarizability $\langle vJ|\alpha_{H_2}|v'J'\rangle$ calculated by Poll (1970) were used. Just as for the profiles of the HD fundamental band in Chapters III and V, the profile analysis was carried out with a program written for the IBM 370/155 computer. The computation thus provided the half-width parameters

δ_q and δ_c of the overlap-induced components and δ_q (of the Boltzmann-modified dispersion line form) or $\delta_{q'}$ (of the symmetrized dispersion line form) of the quadrupole-induced lines. For the best fit of the computed profiles with the synthetic profiles, the computer also gave the overlap and quadrupolar contributions to the intensity of the band separately. An example of the results of the analysis for an absorption profile of the H_2 fundamental band at 77 K using the Boltzmann-modified dispersion line shape for the quadrupolar lines is shown in Fig. VI-1. As the individual components contributing to the intensity of the band are only 11 at 77 K, these are shown separately in this figure. As can be seen from this figure, the agreement between the experimental and the synthetic profiles is very good over the entire region of the band. Results of similar profile analysis for the H_2 fundamental band at 196 and 298 K are shown in Figs. VI-2 and VI-3. As the number of individual components at these temperatures are too many (29 at 196 K and 34 at 298 K) these are not shown separately in these figures; however, the total overlap and quadrupolar contributions are shown separately. An analysis performed with a symmetrized line shape for the quadrupole-induced lines gave equally good agreement between the computed and calculated profiles at all the three temperatures.

The results of the profile analysis are presented in Table VI-3. It is seen from Table VI-3 that the overlap

TABLE VI-3

Results of profile analysis for normal H_2 gas

T (K)	Intracollisional half-width δ_d (cm^{-1})	Collision duration τ_d (10^{-14} s)	Quadrupolar half-width δ_q (cm^{-1})	Collision duration τ_q (10^{-14} s)	Symmetrized Quad. half-width $\delta_{q'}$ (cm^{-1})	Overlap contribution %	Quadrupolar contribution %
77	192±5	2.8	74±2	7.2	53±1	23	77
196	211±6	2.5	112±2	4.7	86±1	31	69
298	248±3	2.1	135±2	3.9	107±2	38	62

contribution increases from 23% to 38% as the temperature increases from 77 to 298 K; equivalently, the quadrupolar contribution decreases from 77% at 77 K to 62% at 298 K. Within the range of the densities used in the present experiments, δ_d, δ_q, and $\delta_{q'}$ are found to be independent of density at each of the temperatures. Figure VI-5 gives a plot of the average values of δ_d, δ_q, and $\delta_{q'}$ against $\sqrt{T}$, the square root of absolute temperature. The half-width parameter δ_d which varies linearly with $\sqrt{T}$, when extrapolated to T = 0 has a value of 133 cm^{-1}, which indicates that even at T = 0 the duration of collision τ_d (= $1/2\pi c\delta_d$) is still relatively short because the overlap induction occurs mainly in the region of the strong repulsive forces (see also Mactaggart and Welsh 1973). The quadrupolar half-widths δ_q and $\delta_{q'}$ are found to satisfy the linear relations $\delta_q = 7.97\sqrt{T}$ and $\delta_{q'} = 6.16\sqrt{T}$. The intracollisional half-width δ_c increases with increasing density of the H_2 gas. As the present experiments with pure H_2 gas were limited to densities up to 60 amagat only, it was not possible to derive a definite expression for the density dependence of δ_c. The values of δ_c for the maximum experimental densities of the gas at 77, 196, and 298 K were less than 0.4, 3.0, and 3.5 cm^{-1}, respectively.

4. Overlap Parameters for the H_2-H_2 Molecular Pairs

The procedure adopted to derive the overlap parameters of the HD-HD molecular pairs is given in Chapter V,

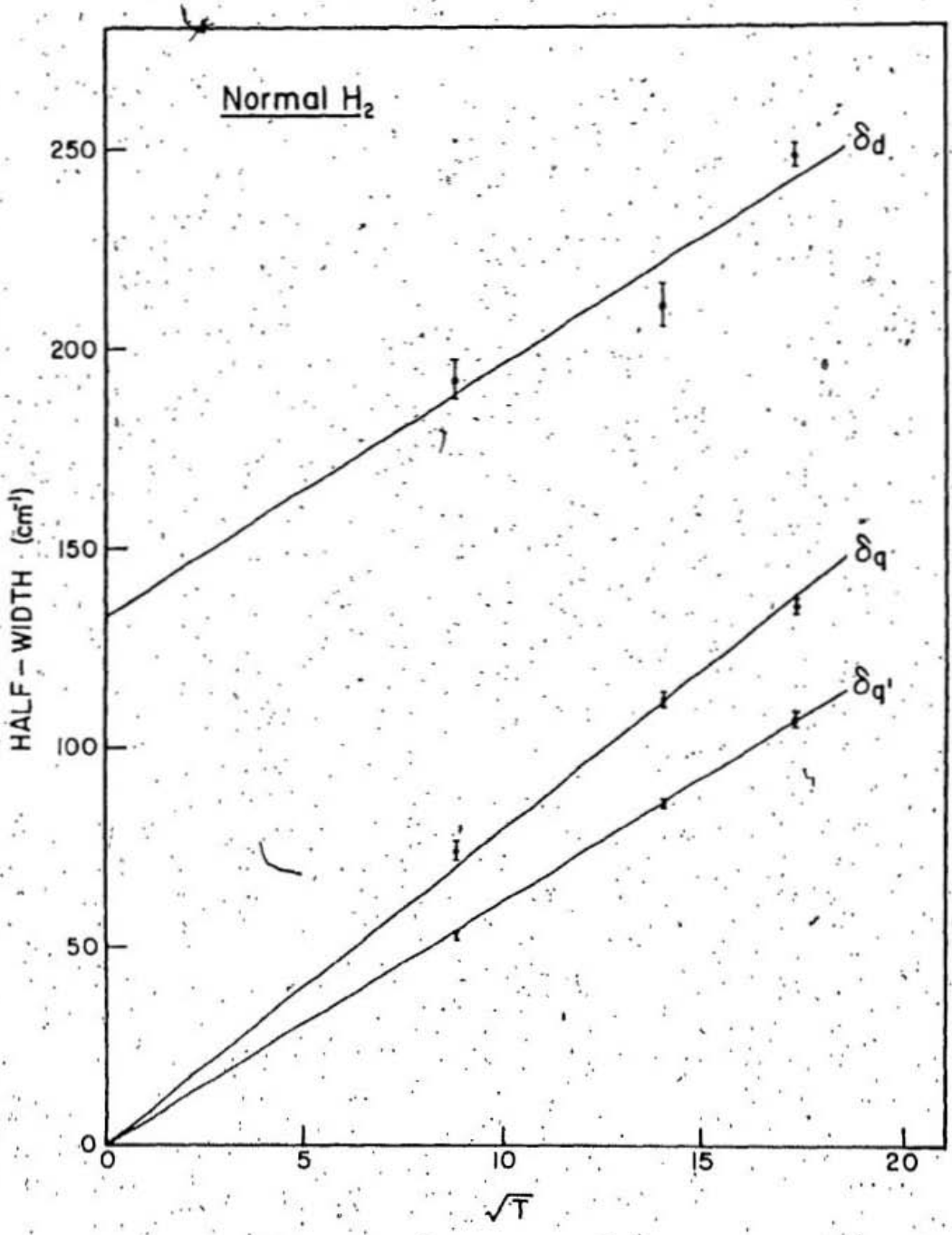

Fig. VI-5. Plots of the half-width parameters δ_d, δ_q, and $\delta_{q'}$ against the square root of the absolute temperature T.

Section 3. In order to derive the overlap parameters for the H_2-H_2 molecular pairs the same procedure was used. The overlap integrated absorption coefficients $\int \alpha_{overlap}(\nu)d\nu$ derived from the profile analysis were expressed in terms of density of the gas by Eq. (5-8). The intercepts and the slopes obtained from the plots of $(1/\rho_a^2)\int \alpha_{overlap}(\nu)d\nu$ vs ρ_a gave, respectively, the overlap binary and ternary absorption coefficients at each of the experimental temperatures. These plots are shown in Fig. VI-6 and the values of the absorption coefficients are listed in Table VI-4. By equating the overlap binary absorption coefficient to $\lambda^2 I\tilde{\gamma}$ at each temperature, values of $\lambda^2 I$ as a function of temperature T were obtained. The value of $\tilde{\gamma}$ was calculated from the value of the matrix element $\langle 00|(r-r_0)|10\rangle$ as given by Poll (1975b) (see Table VI-5 for the values of $\tilde{\gamma}$ and other constants). A plot of the experimental values of $\lambda^2 I$ as a function of temperature T is shown in Fig. VI-7. The integral I depends on σ/ρ (cf. Eq. (5-13)), where σ is the Lennard-Jones diameter and ρ is a range parameter. The most probable value of σ/ρ for the H_2-H_2 pairs was determined by a procedure similar to the one used by Reddy and Chang (1973) and described in detail in Chapter V, Section 3. The calculated values of $\lambda^2 I$ for the best fit are also shown in Fig. VI-7. The values of ρ/σ, λ, σ, ρ, and $\mu(\sigma)$ (the induced dipole moment at a molecular separation σ) are listed in Table VI-6. For the purpose of comparison, values of the overlap parameters for the pure HD gas obtained in

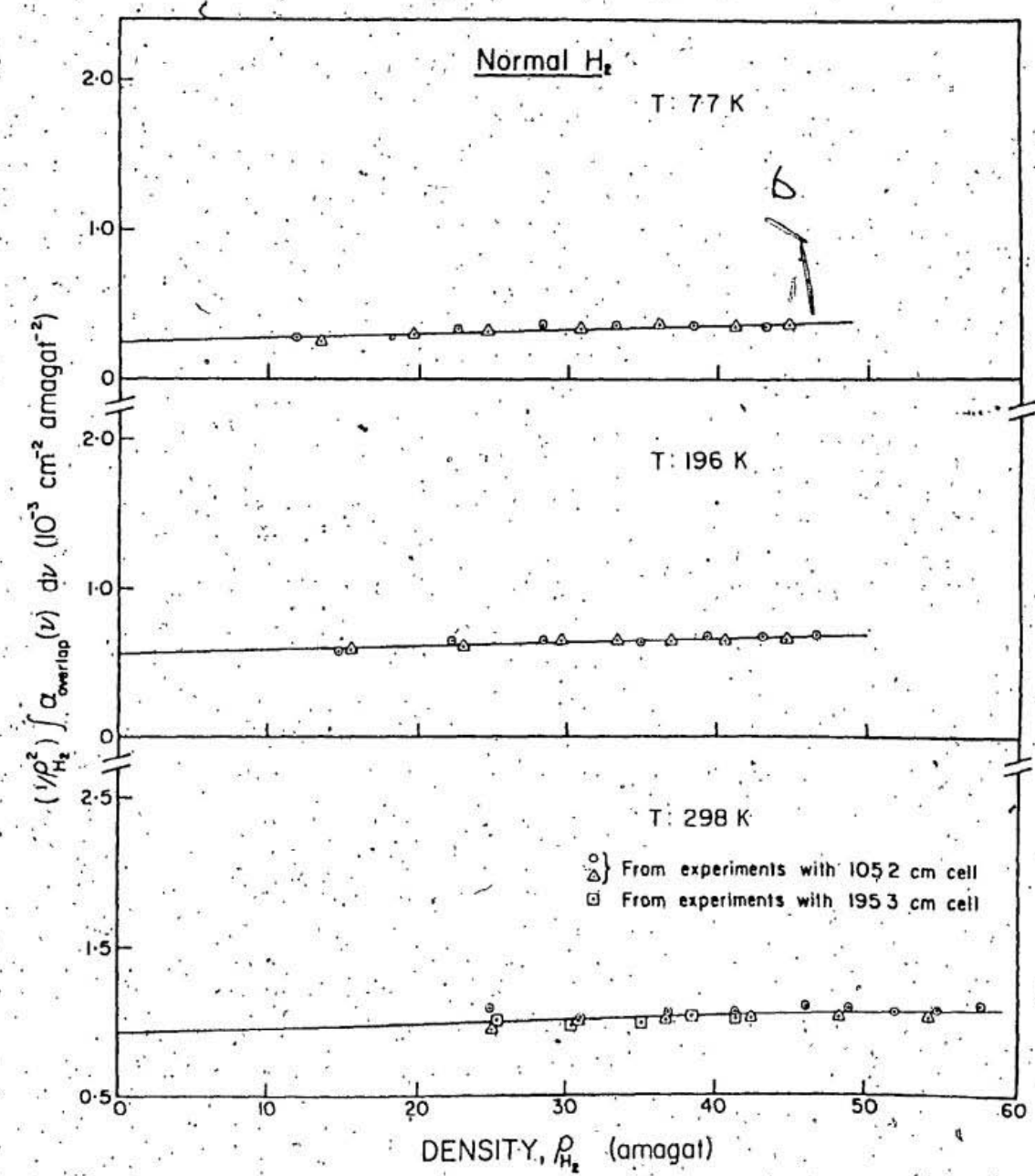

Fig. VI-6. Plots of $(1/\rho_{H_2}^2)\int \alpha_{overlap}(\nu)\, d\nu$ vs ρ_{H_2} for the profiles of normal H_2 gas at 77, 196, and 298 K.

TABLE VI-4

Absorption coefficients* of the overlap part of the fundamental band of normal H_2 at three different temperatures

T (K)	Binary absorption coefficient		Ternary absorption coefficient
	$\alpha_{1a\ \text{overlap}}$	$\tilde{\alpha}_{1a\ \text{overlap}}$	$\alpha_{2a\ \text{overlap}}$
	$(10^{-3}\ \text{cm}^{-2}\ \text{amagat}^{-2})$	$(10^{-35}\ \text{cm}^{6}\ \text{s}^{-1})$	$(10^{-6}\ \text{cm}^{-2}\ \text{amagat}^{-3})$
77	0.25 ± 0.02	0.24 ± 0.02	3.0 ± 0.5
196	0.56 ± 0.02	0.54 ± 0.02	2.5 ± 0.5
298	0.93 ± 0.04	0.90 ± 0.04	2.6 ± 0.8

* Ranges of error indicated are standard deviations.

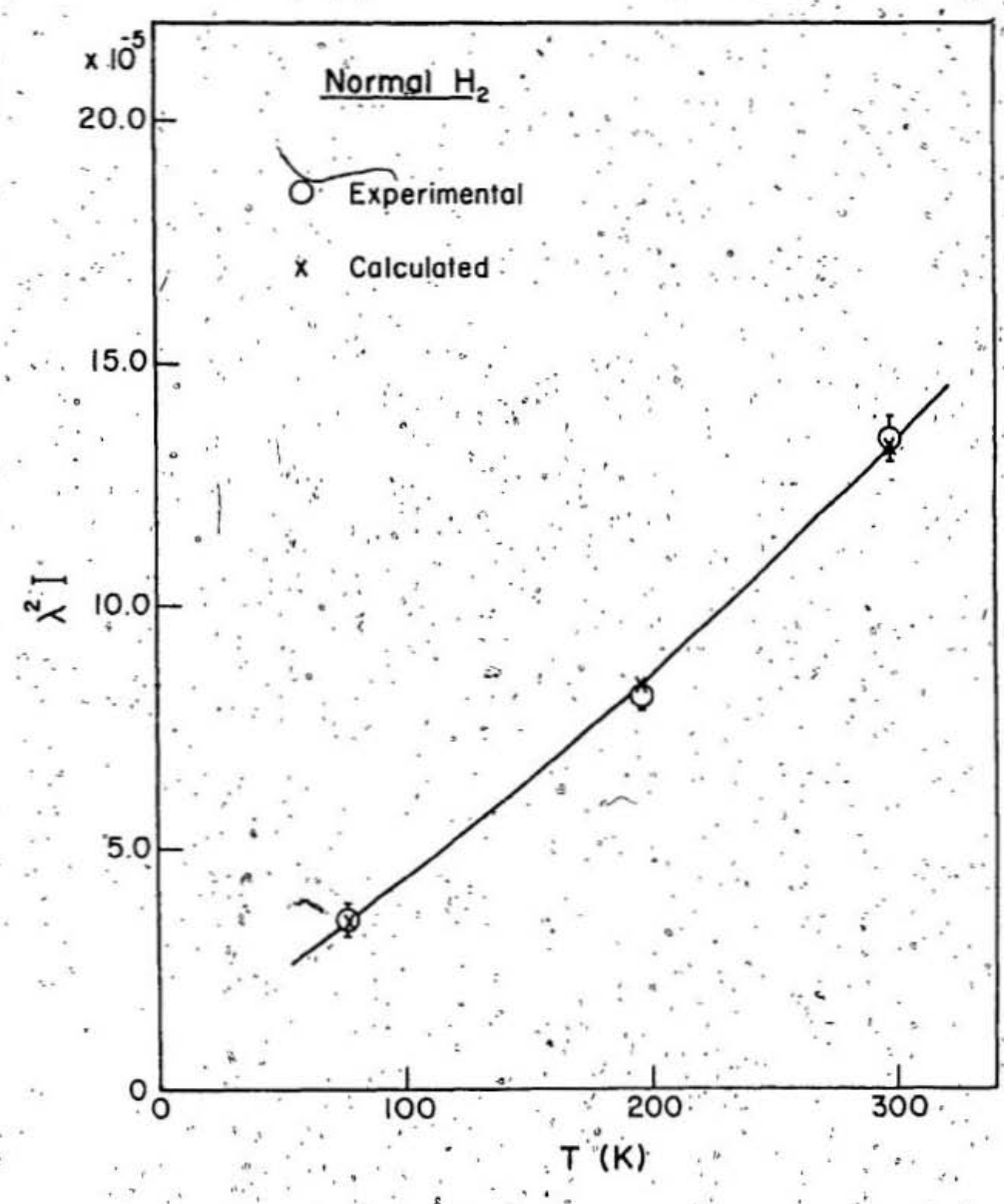

Fig. VI-7. Variation of $\lambda^2 I$ with the absolute temperature T for the normal H_2 gas.

TABLE VI-5

Molecular constants for normal H_2 gas

ϵ/k (K)	σ (Å)	$\tilde{\gamma}$ (10^{-32} cm^6 s^{-1})	Λ^*
37.00	2.928	6.678	1.731

TABLE VI-6

Overlap parameters for H_2-H_2 and HD-HD molecular pairs

Molecular pairs	ρ/σ	λ	σ (Å)	ρ (Å)	$\mu(\sigma)$ (10^{-3} ea_0)
H_2-H_2	0.080	4.15×10^{-3}	2.928	0.23	23.0
HD-HD	0.084	5.13×0^{-3}	2.928	0.25	28.4

the last chapter are also listed in the same table. It may be seen from this table that the values of the corresponding quantities for the H_2-H_2 and HD-HD molecular pairs are reasonably close. This seems reasonable since the charge distributions in the H_2-H_2 and HD-HD molecular pairs are very similar. Hunt (1959) obtained a value of 0.126 for ρ/σ for the H_2-H_2 molecular pairs, which is about one and a half times higher than the value obtained in the present work. The higher value of ρ/σ obtained by Hunt may be understood on the basis of the following reasons: (i) He ignored the Q branch splitting, which is rather a dominant feature of the absorption profile at higher temperatures, and analyzed only the high frequency wing of the band; (ii) he also ignored the double-transition quadrupolar components $Q_1(J) + Q_0(J)$ of the Q branch as well as several, double transition lines of the S branch; and (iii) the new theoretical line shapes were developed by Levine and Birnbaum (1967) and Van Kranendonk (1968) subsequently.

NOTE: In principle the absolute intensity of the quadrupole-induced lines arising from the binary collisions can be calculated from the theoretical expressions (see for example Poll 1970). For example, for the $S_1(1)$ line of the H_2 fundamental band at 77 K, the theoretical value of the binary absorption coefficient is found to be 0.43×10^{-7} cm^{-1} $amagat^{-2}$. The value of the corresponding

quantity obtained experimentally is $(0.53\pm0.01)\times10^{-7}$ cm^{-1} amagat^{-2}. The experimental value was obtained from the profile analysis where a Boltzmann-modified dispersion line form was used for the quadrupole-induced lines with the assumption that the intensities of the O and S lines were completely due to the quadrupolar induction. One must note that the calculated values of the binary absorption coefficient of the quadrupole-induced lines are very sensitive to small uncertainties in the value of the Lennard-Jones diameter σ of the colliding pair of molecules, which occurs in the fifth power in the theoretical expressions. A simple calculation shows that a mere 4% decrease in the value of σ will account for this large difference of $\sim$23% in the theoretical and experimental values of the binary absorption coefficient. On account of this, the entire difference can not be attributed with any degree of certainty to the anisotropic overlap contribution to the S lines. A similar situation exists for the case of pure HD. For the $S_1(0)$ line of the HD fundamental band at 77 K, the theoretical and experimental values of the binary absorption coefficient are found to be 0.62×10^{-7} and $(0.78\pm0.03)\times10^{-7}$ cm^{-1} amagat^{-2}, respectively. An argument similar to the one made for H_2 is applicable for HD as well.

APPENDIX A

TABLE A-1

Relative intensities* of the overlap and quadrupolar transitions of the fundamental band of HD

Transitions	Wavenumber (cm^{-1})	Temperature (K)		
		77	196	298
		Overlap Transitions		
$Q_1(5)$	3575.14	-	-	0.0098
$Q_1(4)$	3593.97	-	0.0088	0.0650
$Q_1(3)$	3609.16	0.0003	0.0903	0.2748
$Q_1(2)$	3620.63	0.0340	0.4517	0.7062
$Q_1(1)$	3628.30	0.5662	1.0000	1.0000
$Q_1(0)$	3632.15	1.0000	0.6417	0.5128
		Quadrupolar Transitions		
$O_1(4)$	3004.67	-	0.0071	0.0646
$O_1(3)$	3185.25	0.0001	0.0590	0.2210
$O_1(2)$	3365.08	0.0099	0.2053	0.3950
$Q_1(4)$	3593.97	-	0.0044	0.0399
$Q_1(4)+Q_0(J)$	"	-	0.0024	0.0235
$Q_1(3)$	3609.16	0.0001	0.0460	0.1724
$Q_1(3)+Q_0(J)$	"	-	0.0246	0.0986
$Q_1(2)$	3620.63	0.0119	0.2457	0.4728

TABLE A-1 (continued)

Transitions	Wavenumber (cm^{-1})	Temperature (K)		
		77	196	298
$Q_1(2)+Q_0(J)$	3620.63	0.0034	0.1223	0.2512
$Q_1(1)$	3628.30	0.2760	0.7594	0.9348
$Q_1(1)+Q_0(J)$	"	0.0572	0.2699	0.3547
$Q_1(0)$	3632.15	0	0	0
$Q_1(0)+Q_0(J)$	"	0.1007	0.1727	0.1813
$Q_1(4)+S_0(0)$	3861.04	-	0.0028	0.0173
$Q_1(3)+S_0(0)$	3876.23	0.0001	0.0284	0.0726
$Q_1(2)+S_0(0)$	3887.70	0.0146	0.1411	0.1849
$S_1(0)$	3887.70	1.0000	1.0000	0.9836
$Q_1(1)+S_0(0)$	3895.37	0.2423	0.3116	0.2610
$Q_1(0)+S_0(0)$	3899.22	0.4266	0.1993	0.1335
$Q_1(4)+S_0(1)$	4037.02	-	0.0027	0.0204
$Q_1(3)+S_0(1)$	4052.21	0.0001	0.0268	0.0855
$S_1(1)$	4052.21	0.2952	0.8124	1.0000
$Q_1(2)+S_0(1)$	4063.68	0.0050	0.1328	0.2178
$Q_1(1)+S_0(1)$	4071.35	0.0829	0.2932	0.3074
$Q_1(0)+S_0(1)$	4075.20	0.1459	0.1876	0.1572
$Q_1(4)+S_0(2)$	4209.93	-	0.0010	0.0125
$S_1(2)$	4209.93	0.0131	0.2710	0.5214

TABLE A-1 (continued)

Transitions	Wavenumber (cm^{-1})	Temperature (K) 77	196	298
$Q_1(3)+S_0(2)$	4225.12	-	0.0105	0.0523
$Q_1(2)+S_0(2)$	4236.59	0.0003	0.0519	0.1331
$Q_1(1)+S_0(2)$	4244.26	0.0043	0.1147	0.1880
$Q_1(0)+S_0(2)$	4248.11	0.0076	0.0734	0.0961
$S_1(3)$	4359.85	0.0001	0.0428	0.1602
$Q_1(4)+S_0(3)$	4378.68	-	0.0002	0.0046
$Q_1(3)+S_0(3)$	4393.87	-	0.0020	0.0191
$Q_1(2)+S_0(3)$	4405.34	-	0.0097	0.0486
$Q_1(1)+S_0(3)$	4413.01	-	0.0215	0.0686
$Q_1(0)+S_0(3)$	4416.86	0.0001	0.0138	0.0351
$S_1(4)$	4501.07	-	0.0034	0.0305
$Q_1(4)+S_0(4)$	4542.26	-	-	0.0010
$Q_1(3)+S_0(4)$	4557.45	-	0.0002	0.0044
$Q_1(2)+S_0(4)$	4568.92	-	0.0009	0.0112
$Q_1(1)+S_0(4)$	4576.59	-	0.0021	0.0157
$Q_1(0)+S_0(4)$	4580.44	-	0.0013	0.0081

*The relative intensities given are valid within each of the overlap and quadrupolar groupings.

APPENDIX B

THEORY OF THE INTRACOLLISIONAL INTERFERENCE EFFECT (Ref.: Poll et al. 1976)

The geometry of a colliding pair of HD and Kr molecules is shown in Fig. B-1. The spherical components of the total dipole moment of an HD-Kr pair (in fact, the treatment will be valid for any HD-inert gas atom pair) with respect to the space fixed axes are given by (see Poll and Van Kranendonk 1961, Poll, Hunt, and Mactaggart 1975)

$$\mu_\nu(r\omega R\Omega) = (4\pi/\sqrt{3}) \sum_{L\lambda} \sum_{M} A_{L\lambda}(rR)\ C(\lambda L 1; \nu\text{-}MM)\ Y^*_{\lambda\nu-M}(\omega)\ Y_{LM}(\Omega). \tag{B-1}$$

In this expression ν denotes the spherical component of the dipole moment; r, R, and S are the internuclear distance, the separation of the centers of mass of HD and Kr, and the separation of the mid-point of HD and center of mass of Kr, respectively. The expansion coefficient $A_{L\lambda}(rR)$ gives the r, R dependence of a particular component of the dipole moment whose angular dependence is characterized by the parameters L and λ, and C is a Clebsch-Gordan coefficient. The quantities ω and Ω denote the orientation of vectors $\vec{r}$ and $\vec{R}$ with respect to the space fixed axes and Y's are the spherical harmonics. The parity condition requires that λ+L be odd. For a homonuclear diatomic molecule like

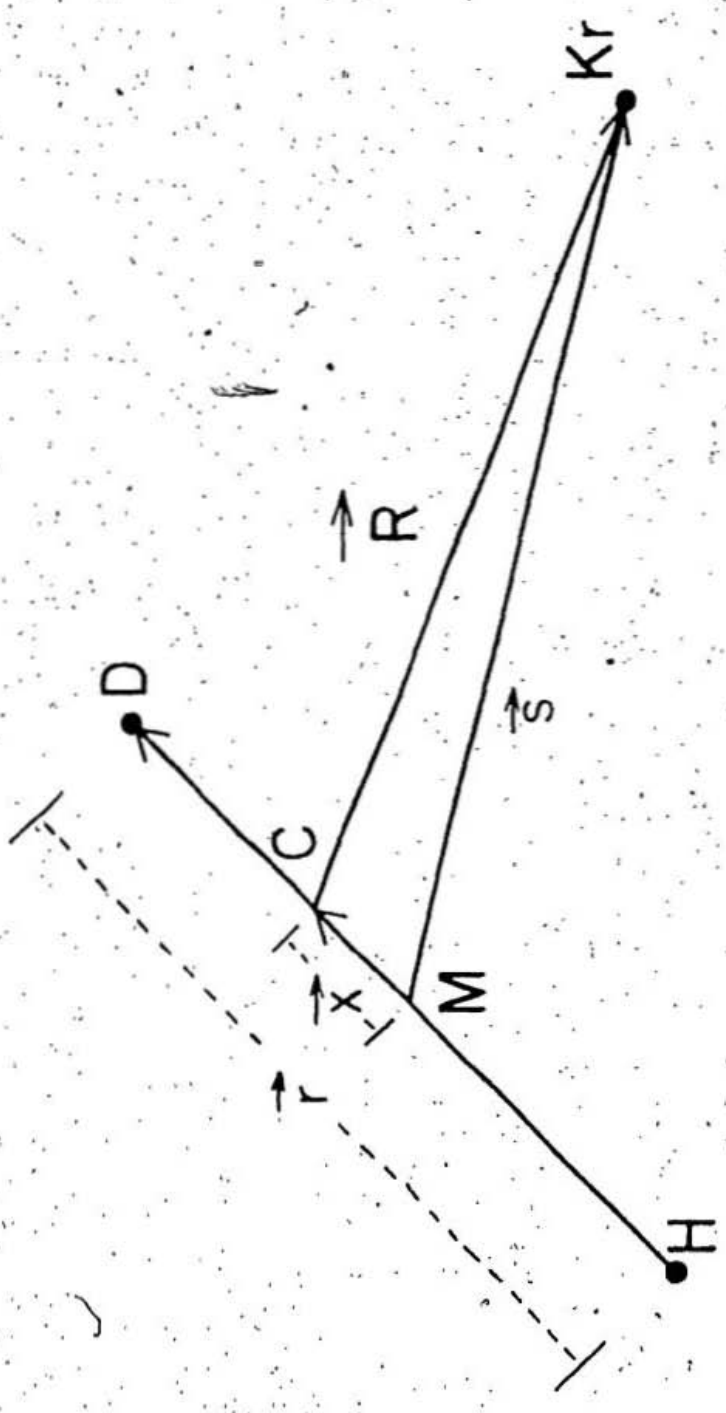

Fig. B-1. The geometry of an HD-Kr collision pair.

H_2, λ can take only even values. However, for a molecule like HD, λ can take both even and odd values.

The spherical component of the total dipole moment (allowed plus induced) of HD will have the expansion coefficient A_{01} (cf. Eq. (B-1)). Therefore we may write

$$A_{01} = P_A(r) + P_I(rR), \tag{B-2}$$

where $P_A(r)$ is the allowed dipole moment of HD along the internuclear axis and is related to P_ν by the relation

$$P_\nu = P_A(r)\ (4\pi/3)^{1/2}\ Y_{1\nu}(\theta\phi), \tag{B-3}$$

and $P_I(rR)$ is the induced dipole moment.

The vibrational-rotational matrix elements of the dipole moment operator, in which we are interested are given by (see, for example, Poll et al. 1975)

$$\langle v = 0Jm|\ \mu_\nu(r\omega R\Omega)\ |v' = 1J'm'\rangle$$
$$= (4\pi/\sqrt{3}) \sum_{L\lambda} \sum_{M} \langle Jm|Y_{\lambda\nu-M}(\theta\phi)|J'm'\rangle B_{L\lambda}(R)\ C(\lambda L1;\nu-MM)Y_{LM}(\Omega), \tag{B-4}$$

where $\langle Jm|Y_{\lambda\nu-M}(\theta\phi)|J'm'\rangle$ is the rotational matrix element and $B_{L\lambda}(R)$ is the matrix element of $A_{L\lambda}(R)$ between the vibrational states 0 and 1. The $B_{01}(R)$ component (corresponding to $L = 0$, $\lambda = 1$) contributes to the intensity of the R lines. Thus

$$B_{01}(R) = P_A(r) + P_I(rR). \tag{B-5}$$

The integrated intensity of a particular branch may be written quite generally as (see Poll et al. 1975)

$$\int \alpha(\nu)\nu^{-1}d\nu = n_a n_b (4\pi^2/3hc) \sum_{JJ'} P_J\, C(J\lambda J';00)^2 \cdot 4\pi \int_0^\infty B_{L\lambda}(R)^2\, g(R) R^2 dR, \qquad \text{(B-6)}$$

where the sum is over all the values of J and J' that contribute to the branch under consideration. The quantities n_a and n_b are the number densities of the absorbing gas (here HD) and the perturbing gas (Kr or Xe), respectively. The total integrated intensity of the $R_1(1)$ line, in particular, may be written as

$$\int \alpha(\nu)\nu^{-1}d\nu = n_a n_b (4\pi^2/hc)\, P_1\, C(112;00)^2 4\pi \int_0^\infty B_{01}(R)^2 g(R) R^2 dR. \qquad \text{(B-7)}$$

On substitution of Eq. (B-5) in Eq. (B-7), we have

$$\int \alpha(\nu)\nu^{-1}d\nu = (4\pi^2/3) n_a\, a_0^2\, \alpha_F\, P_1\, C(112;00)^2 \times \begin{cases} \langle 01|P_A|12\rangle^2 & \text{(B-8a)} \\ + n_b\, a_0^3\, 4\pi \int_0^\infty \langle 01|P_I|12\rangle^2\, g(R)\, R^2\, dR & \text{(B-8b)} \\ + 2 n_b\, a_0^3 \langle 01|P_A|12\rangle \times 4\pi \int_0^\infty \langle 01|P_I|12\rangle\, g(R) R^2 dR, & \text{(B-8c)} \end{cases}$$

where the dipole moment and distances are expressed in the units of ea_0 and a_0, respectively, e being the electronic charge, a_0 is the Bohr radius, and α_F is the fine structure constant. The contributions (B-8a), (B-8b), and (B-8c) are due to the allowed dipole moment, the pure induced dipole

moment, and the intracollisional interference effect, respectively. Clearly, the allowed contribution is proportional to n_a and each of the induced and the intracollisional contributions is proportional to the product $n_a n_b$. The intensity due to the intracollisional interference effect occurs at the position of the allowed line and its width is of the same order of magnitude as that of the allowed line.

In order to estimate the intensity due to the intracollisional interference effect values of the matrix elements $\langle 01|P_A|12\rangle$ and $\langle 01|P_I|12\rangle$ must be known. For HD molecule the value of $\langle 01|P_A|12\rangle$ can be obtained from the intensity of the allowed $R_1(1)$ line (cf. McKellar 1974). The value of $\langle 01|P_I|12\rangle$ is not available, however. Assuming that the charge distributions for HD-Kr and H_2-Kr are identical, $\mu_\nu^{HD-Kr}(\vec{r}\,\vec{R})$ may be expressed in terms of $\mu_\nu^{H_2-Kr}(\vec{r}\,\vec{R})$. Thus

$$\mu_\nu^{HD-Kr}(\vec{r}\,\vec{R}) = (1+\vec{x}\cdot\vec{\nabla}_R)\,\mu_\nu^{H_2-Kr}(\vec{r}\,\vec{R}). \qquad (B-9)$$

For H_2-Kr, both coefficients A_{10} and A_{12} contribute (cf. Eq. (B-1)). The larger contribution comes from the coefficient A_{10}. A model for $A_{10}(rR)$ may be assumed as follows:

$$A_{10}(rR) = m(r)\,\exp[-(R-\sigma)/\rho], \qquad (B-10)$$

where ρ is the range and σ is the Lennard-Jones diameter, and $m(r)$ is the induced moment at $R = \sigma$. Combining (B-9) and (B-10) an expression for the induced dipole moment for

HD-Kr or HD-Xe may be written as

$$P_I = \frac{x}{3}(2/R - 1/\rho)\ m(r)\ \exp[-(R-\sigma)/\rho]. \qquad \text{(B-11)}$$

The quantities $\langle 01|m(r)|12\rangle$ and ρ can in principle be determined. A reasonable fit to the spectra can be obtained by taking $\langle 01|m(r)|12\rangle = 2\times10^{-3}$ a.u. and $\rho/\sigma = 0.12$ for H_2-Kr and $\langle 01|m(r)|12\rangle = 2.2\times10^{-3}$ a.u. and $\rho/\sigma = 0.12$ for H_2-Xe. By making use of the above results for P_I and adopting a value of 2.17×10^{-5} a.u. (Mckellar 1974) for the allowed matrix element $\langle 01|P_A|12\rangle$, the intracollisional interference contributions to the binary absorption coefficient of the $R_1(1)$ line at room temperature can be calculated.

APPENDIX C

TABLE C-1

Relative intensities* of the overlap and quadrupolar transitions of the fundamental band of H_2

Transitions	Wavenumbers (cm^{-1})	Temperature (K)		
		77	196	298
	Overlap Transitions			
$Q_1(4)$	4102.60	-	0.0004	0.0063
$Q_1(3)$	4125.87	-	0.0311	0.1372
$Q_1(2)$	4143.46	0.0022	0.0929	0.1780
$Q_1(1)$	4155.26	1.0000	1.0000	1.0000
$Q_1(0)$	4161.18	0.3311	0.2504	0.1971
	Quadrupolar Transitions			
$O_1(3)$	3568.23	-	0.0279	0.1228
$O_1(2)$	3806.80	-	0.0567	0.1088
$Q_1(3)$	4125.87	-	0.0209	0.0917
$Q_1(3)+Q_0(J)$	4125.87	-	0.0141	0.0632
$Q_1(2)$	4143.46	0.0015	0.0661	0.1268
$Q_1(2)+Q_0(J)$	4143.46	0.0009	0.0416	0.0812
$Q_1(1)$	4155.26	0.9942	0.9942	0.9942
$Q_1(1)+Q_0(J)$	4155.26	0.4232	0.4456	0.4540
$Q_1(0)$	4161.18	0	0	0
$Q_1(0)+Q_0(J)$	4161.18	0.1398	0.1113	0.0894

TABLE C-1 (continued)

Transitions	Wavenumbers (cm^{-1})	Temperature (K)		
		77	196	298
$Q_1(3)+S_0(0)$	4480.26	-	0.0081	0.0255
$Q_1(2)S_0(0)$	4497.85	0.0008	0.0214	0.0328
$S_1(0)$	4497.90	0.6526	0.4935	0.3881
$Q_1(1)+S_0(0)$	4509.65	0.3506	0.2568	0.1834
$Q_1(0)+S_0(0)$	4515.57	0.1158	0.0642	0.0361
$Q_1(3)+S_0(1)$	4712.90	-	0.0196	0.0784
$S_1(1)$	4712.99	1.0000	1.0000	1.0000
$Q_1(2)+S_0(1)$	4730.49	0.0014	0.0579	0.1008
$Q_1(1)+S_0(1)$	4742.29	0.6407	0.6207	0.5633
$Q_1(0)+S_0(1)$	4748.21	0.2116	0.1550	0.1107
$S_1(2)$	4917.00	0.0015	0.0664	0.1274
$Q_1(3)+S_0(2)$	4940.27	-	0.0016	0.0121
$Q_1(2)+S_0(2)$	4957.86	-	0.0047	0.0156
$Q_1(1)+S_0(2)$	4969.66	0.0012	0.0500	0.0871
$Q_1(0)+S_0(2)$	4975.58	0.0004	0.0125	0.1711
$S_1(3)$	5111.32	-	0.0170	0.0749
$Q_1(3)+S_0(3)$	5160.51	-	0.0005	0.0088
$Q_1(2)+S_0(3)$	5178.10	-	0.0015	0.0113
$Q_1(1)+S_0(3)$	5189.90	-	0.0158	0.0632

TABLE C-1 (continued)

Transitions	Wavenumbers	Temperature (K)		
		77	196	298
$Q_1(0)+S_0(3)$	5195.82	-	0.0040	0.0124

*The relative intensities given are valid within each of the overlap and quadrupolar groupings.

REFERENCES

Bejar, J. and Gush, H.P. 1974. Can. J. Phys. 52, 1669.

Birnbaum, A. and Poll, J.D. 1969. J. Atmos. Sci. 26, 943.

Bishop, R.B. 1966. M.Sc. Thesis, Memorial University of Newfoundland, St. John's, Newfoundland.

Blinder, S.M. 1960 a. J. Chem. Phys. 32, 105.

_____. 1960 b. J. Chem. Phys. 32, 582.

_____. 1961. J. Chem. Phys. 35, 974.

Bosomworth, D.R. and Gush, H.P. 1965. Can. J. Phys. 43, 751.

Chang, K.S. 1971. M.Sc. Thesis, Memorial University of Newfoundland, St. John's, Newfoundland.

_____. 1974. Ph.D. Thesis, Memorial University of Newfoundland, St. John's, Newfoundland.

Chapman, S. and Cowling, T.G. 1952. The Mathematical Theory of Non-uniform Gases (University Press, Cambridge, England).

Chisholm, D.A. and Welsh, H.L. 1954. Can. J. Phys. 32, 291.

Crane, A. and Gush, H.P. 1966. Can. J. Phys. 44, 373.

Crawford, M.F., Welsh, H.L., and Locke, J.L. 1949. Phys. Rev. 75, 1607.

Dean, J.W. 1961. National Bureau of Standards Technical Note 120 (U.S. Department of Commerce, Washington, D.C., U.S.A.).

De Remigis, J., Mactaggart, J.W., and Welsh, H.L. 1971. Can. J. Phys. 49, 381.

Durie, R.A. and Herzberg, G. 1960. Can. J. Phys. 38, 806.

Gush, H.P., Nanassy, A., and Welsh, H.L. 1957. Can. J. Phys. 35, 712.

Hare, W.F. and Welsh, H.L. 1958. Can. J. Phys. 36, 88.

Herzberg, G. 1950. Nature 166, 563.

Hołleman, G.W. and Ewing, G.E. 1966. J. Chem. Phys. 44, 3121.

_____. 1967. J. Chem. Phys. 47, 571.

Humphreys, C.J. 1953. J. Opt. Soc. Amer. 43, 1027.

Hunt, J.L. 1959. Ph.D. Thesis, University of Toronto, Toronto, Ontario.

Hunt, J.L. and Welsh, H.L. 1964. Can. J. Phys. 42, 873.

International Union of Pure and Applied Chemistry. 1961. Tables of Wavenumbers for the Calibration of Infrared Spectrometers (Butterworths, London).

Karl, G. and Poll, J.D. 1967. J. Chem. Phys. 46, 2944.

Kiss, Z.J. and Welsh, H.L. 1959. Can. J. Phys. 37, 1249.

Kolos, W. and Wolniewicz, L.J. 1967. J. Chem. Phys. 46, 1426.

Levine, H.B. and Birnbaum, G. 1967. Phys. Rev. 154, 72.

Mactaggart, J.W. 1971. Ph.D. Thesis, University of Toronto, Toronto, Ontario.

Mactaggart, J.W., De Remigis, J., and Welsh, H.L. 1973. Can. J. Phys. 51, 1971.

Mactaggart, J.W. and Hunt, J.L. 1969. Can. J. Phys. 47, 65.

Mactaggart, J.W. and Welsh, H.L. 1973. Can. J. Phys. 51, 158.

Mann, D.B. 1962. National Bureau of Standards Technical Note 154 (U.S. Department of Commerce, Washington, D.C., U.S.A.).

May, A.D., Degen, V., Stryland, J.C., and Welsh, H.L. 1961. Can. J. Phys. 39, 1769.

May, A.D., Varghese, G., Stryland, J.C., and Welsh, H.L. 1964. Can. J. Phys. 42, 1058.

McKellar, A.R.W. 1973. Can. J. Phys. 51, 389.

_____. 1974. Can. J. Phys. 52, 1144.

Michels, A., Boltzen, A., Friedman, A.S., and Sengers, J.V. 1956. Physica 22, 121.

Michels, A., De Graaff, W., Wassenaar, T., Levelt, J.M.H., and Louwerse, P. 1959. Physica 25, 25.

Michels, A. and Goudeket, M. 1941. Physica 8, 347.

Michels, A., Wassenaar, T., and Louwerse, P. 1954. Physica 20, 99.

_____. 1960. Physica 26, 539.

Michels, A. and Wouters, W. 1941. Physica 8, 923.

Pai, S.T., Reddy, S.P., and Cho, C.W. 1966. Can. J. Phys. 44, 2893.

Plyler, E.K., Blaine, L.R., and Tidwell, E.D. 1955. J. Res. Natl. Bur. Standards 55, 279.

Poll, J.D. 1960. Ph.D. Thesis, University of Toronto, Toronto, Ontario.

_____. 1970. Proc. I.A.U. Symposium No. 40 on planetary atmospheres, Marfa, Texas, October 1969 (Reidel Publications, Dordrecht, Holland).

_____. 1975a. Private communication.

_____. 1975b. Private communication.

Poll, J.D., Hunt, J.L., and Mactaggart, J.W. 1975. Can. J. Phys. 53, 954.

Poll, J.D., Tipping, R.H., Prasad, R.D.G., and Reddy, S.P. 1976 (submitted for publication in Phys. Rev. Lett.).

Poll, J.D. and Van Kranendonk, J. 1961. Can. J.Phys. 29, 189.

Prasad, R.D.G. and Reddy, S.P. 1975. J. Chem. Phys. 62, 3582.

Reddy, S.P. 1975. Private communication.

Reddy, S.P. and Chang, K.S. 1973. J. Mol. Spectrosc. 47, 22.

Reddy, S.P. and Cho, C.W. 1965. Can. J. Phys. 43, 793.

Reddy, S.P. and Kuo, C.Z. 1971. J. Mol. Spectrosc. 37, 327.

Reddy, S.P. and Lee, W.F. 1968. Can. J. Phys. 46, 1373.

Russell, W.E., Reddy, S.P., and Cho, C.W. 1974. J. Mol. Spectrosc. 52, 72.

Sears, V.F. 1968. Can. J. Phys. 46, 1163.

_____. 1968. Can. J. Phys. 46, 2315.

Sinha, B.P. 1967. M.Sc. Thesis, Memorial University of Newfoundland, St. John's, Newfoundland.

Stoicheff, B.P. 1957. Can. J. Phys. 35, 730.

Trappeniers, N.J. Wassenaar, T., and Wolkers, G.J. 1966. Physica 32, 1503.

Trefler, M., Cappel, A.M., and Gush, H.P. 1969. Can. J. Phys. 47, 2115.

Trefler, M. and Gush, H.P. 1968. Phys. Rev. Lett. 20, 703.

Van Kranendonk, J. 1957. Physica 23, 825.

_____. 1958. Physica 24, 347.

_____. 1968. Can. J. Phys. 46, 1173.

Van Kranendonk, J. and Kiss Z.J. 1959. Can. J. Phys. 37, 1187.

Varghese, G., Ghosh, S.N., and Reddy, S.P. 1972. J. Mol. Spectrosc. 41, 291.

Varghese, G. and Reddy, S.P. 1969. Can. J. Phys. 47, 2745.

Watanabe, A. 1971. Can. J. Phys. 49, 1320.

Watanabe, A. and Welsh, H.L. 1967. Can. J. Phys. 45, 2859.

Welsh, H.L. 1972. MTP International Review of Science, Physical Chemistry, Vol. 3, Spectroscopy (Butterworths, London).

Welsh, H.L., Crawford, M.F., and Locke, J.L. 1949. Phys. Rev. 76, 580.

Wick, G.C. 1935. Atti. R. Acad. Naz. Lincei (Ser. 6) 21, 708.

Zaidi, H.R. and Van Kranendonk, J. 1971. Can. J. Phys. 49, 385.

PUBLICATIONS

R.D.G. Prasad and S. Paddi Reddy. Infrared absorption spectra of gaseous HD. I. Collision-induced fundamental band of HD in the pure gas and HD-He mixtures at room temperature. J. Chem. Phys. 62, 3582. (1975)*

M. Irfan and R.D.G. Prasad. Photofractions from experimental relative photopeak efficiencies of a 3" × 3" CsI (Tl) crystal. Nucl. Instr. and Meth. 107, 583. (1973).

M. Irfan and R.D.G. Prasad. Relative photopeak efficiencies and photofractions of a 2" × 2" CsI (Tl) crystal. Nucl. Instr. and Meth. 88, 165. (1970)

---

*A copy of this publication is attached.

Reprinted from

THE JOURNAL
OF
CHEMICAL PHYSICS

VOLUME 62 | NUMBER 9

1 MAY 1975

Infrared absorption spectra of gaseous HD. I. Collision-induced fundamental band of HD in the pure gas and HD–He mixtures at room temperature

R. D. G. Prasad and S. Paddi Reddy

Department of Physics, Memorial University of Newfoundland, St. John's, Newfoundland, Canada A1C 5S7

pp. 3582–3589

Published by the

AMERICAN INSTITUTE OF PHYSICS

Infrared absorption spectra of gaseous HD. I. Collision-induced fundamental band of HD in the pure gas and HD–He mixtures at room temperature*

R. D. G. Prasad† and S. Paddi Reddy

Department of Physics, Memorial University of Newfoundland, St. John's, Newfoundland, Canada A1C 5S7
(Received 3 December 1974)

The infrared absorption spectra of the fundamental band of HD in the pure gas for densities up to 50 amagat and in HD–He mixtures for different base densities of HD and a number of total gas densities up to 190 amagat have been studied at room temperature. The collision-induced features of the band in the pure gas and in HD–He mixtures are similar to those previously observed for the spectra of H_2 and D_2 in the pure gases and in their binary mixtures with helium, respectively. In addition, the absorption profiles of the pure gas show the allowed sharp $R_1(1)$ transition due to the individual HD molecules. The binary absorption coefficients of the band derived from the measured integrated intensities are 2.32×10^{-35} and 0.94×10^{-35} cm^6 s^{-1} for pure HD and HD–He, respectively. An analysis of the profiles of the enhancement of absorption of the band in HD–He has been performed by assuming appropriate line shapes, and the three half-width parameters, δ_d and δ_c of the overlap transitions and δ_q of the quadrupolar transitions, are obtained. The half-width δ_c of the intercollisional interference dip of the Q branch increases with density ρ of helium and fits to the equation $\delta_c = a\rho - b\rho^2 (a>b)$. This observation and the conclusions derived from it are similar to those obtained previously for H_2–He.

INTRODUCTION

Although the HD molecule, just as the H_2 and D_2 molecules, has no electric dipole moment in the equilibrium position in its ground electronic state, a weak, oscillating dipole moment results in it because, during a molecular vibration, the displacements of the proton are greater than those of the deuteron and the negative charge center of the electrons lags behind the positive charge center of the nuclei. The occurrence of a rotation–vibration spectrum of HD due to this oscillating electric dipole moment was first predicted by Wick.[1] Weak rotation–vibration absorption bands of HD were first observed by Herzberg[2] near 9650 and 7400 Å and were identified as the 3–0 and 4–0 bands, respectively. Later, a detailed experimental investigation of the 1–0, 2–0, 3–0, and 4–0 bands was made by Durie and Herzberg,[3] who obtained precise vibrational and rotational constants of HD in its ground electronic state. Subsequently, the pure rotational spectrum of HD was observed by Trefler and Gush,[4] who determined the dipole moment of HD by measuring the integrated intensities of four R_0 lines.[5] Recently, McKellar[6,7] made a comprehensive study of the 1–0, 2–0, 3–0, and 4–0 bands of HD and measured the intensity of 13 electric dipole transitions and one electric quadrupole transition. Bojar and Gush[8] also measured independently the intensities of five electric dipole transitions of the 1–0 band of HD. The selection rule for the rotational transitions arising from the electric dipole moment is $\Delta J = \pm 1$ and that for the transitions arising from the electric quadrupole moment is $\Delta J = \pm 2$.

Since the first observation of the collision-induced absorption of the fundamental band of H_2 by Welsh *et al.*,[9] there have been extensive studies of the collision-induced spectra of H_2 and D_2. A comprehensive review of this work has been given by Welsh[10] (see also Reddy and Chang[11] and Russell *et al.*[12] and the references therein). The work on the collision-induced absorption in HD has been very limited, however. The pure rotational collision-induced absorption of HD in gaseous and solid phases has been studied by Trefler *et al*[13]. Recently, McKellar[6] studied the collision-induced fundamental band of HD in the gaseous phase at 77 K. There have been studies of the fundamental band of HD, in solid HD, by Crane and Gush[14] and in HD dissolved in liquid argon by Holleman and Ewing,[15] and of the pure rotational band of HD dissolved in liquid argon by Holleman and Ewing.[16]

According to the theory of the collision-induced absorption of diatomic gases proposed by Van Kranendonk,[17,18] the dipole moment induced in a colliding pair of molecules is represented by the so-called "exponential-4" model. In this model, the induced dipole moment consists of two additive parts. One part is the isotropic short-range overlap moment which varies exponentially with intermolecular separation R and the other part is the anisotropic long-range moment, resulting from the polarization of one molecule by the quadrupole moment of the other molecule, which varies as R^{-4}. The short-range moment contributes mainly to the intensity of the broad Q (i.e., Q_{overlap}) ($\Delta J = 0$) lines and the long-range moment contributes to the intensity of the relatively less broad O ($\Delta J = -2$), ~~and~~ Q (i.e., Q_{quad}) ($\Delta J = 0$), and S ($\Delta J = +2$) lines.

In the present investigation, the collision-induced fundamental absorption band of HD in the pure gas for densities up to 50 amagat[19] and in the mixtures of HD with helium for different base densities of HD and total gas densities up to 190 amagat has been studied at room temperature. Binary and ternary absorption coefficients of the band have been determined from the measured integrated intensities. In addition to the broad collision-induced transitions O, Q, and S, it was possible to observe the allowed $R_1(1)$ ($\Delta J = +1$) transition in the pure HD profiles. Profiles of the enhancement of absorption in HD–He mixtures have been analyzed.

TIGHT BINDING

II. EXPERIMENTAL DETAILS

A transmission-type absorption cell of sample path length 105.2 cm, constructed of a stainless steel tube with an inner diameter 0.75 in. and wall thickness 0.125 in., was used in the present study. It was provided with a stainless steel light guide of rectangular cross section 1.2 × 0.5 cm. Polished synthetic sapphire windows, 1.0 in. in diameter and 0.5 cm thick, of the cell were attached with a thin layer of silicone rubber cement to stainless steel window plates which were sealed to the main body of the cell by means of teflon O rings with pressure applied by appropriate closing nuts.

Hydrogen deuteride supplied by Merke, Sharp, and Dohme Canada Limited and helium supplied by Canadian Liquid Air were used in the experiments. Mass spectrometric analysis of this commercial HD gas showed that it contained 89.9% HD, 6.4% H_2, and 3.8% D_2. On the basis of this analysis, appropriate corrections have been made to the density of HD as well as to the absorption profiles. For example, for the experiments with HD–He, it was necessary to subtract from the "observed" absorption profiles the absorption arising from H_2–He and H_2–HD, which was estimated from the pure H_2 gas and in H_2–He mixtures obtained by us with the same absorption cell. The contribution to the integrated intensity of the HD fundamental band from the intensity of the D_2 fundamental band was found to be insignificant.

The spectra were recorded with a Perkin-Elmer model 112 single-beam, double-pass infrared spectrometer equipped with a lithium fluoride prism and an uncooled lead sulphide detector. A standard General Electric EFJ quartzline projection lamp housed in a water-cooled brass jacket was used as the source of infrared radiation. The slit of the spectrometer, maintained at a width of 50 μ, gave a spectral resolution of ~3.0 cm^{-1} at the origin (3632 cm^{-1}) of the fundamental band of HD and the accuracy of the wavenumber measurement was better than 1.0 cm^{-1}. The spectral region was calibrated with the absorption lines of hydrogen chloride,[20] hydrogen cyanide,[20] atmospheric water vapor,[20] and mercury emission lines.[21]

The atmospheric water vapor has a very strong absorption in the region of the fundamental band of HD. It was rather important to remove all traces of atmospheric water vapor from the path of the infrared radiation from the source to the detector in order to make reliable intensity measurements of this HD absorption band. In our experimental setup, the whole optical system, including the radiation source, the absorption cell, and the monochromator, was enclosed in an air-tight plexiglas box which was provided with a side window, fitted with a neoprene glove to facilitate the necessary adjustments without breaking the air-tight seal. The system was then flushed continuously with dry nitrogen gas produced by evaporating liquid nitrogen by immersing an electrical heater. Initially it took several days of flushing to obtain background recorder traces almost free from atmospheric water vapor absorption.

The method of obtaining absorption profiles with the pure HD gas at various densities is straightforward (see, for example, Reddy and Cho[22]). The procedure to obtain the profiles of enhancement of absorption of the fundamental band of HD in HD–He mixtures was similar to the one described by Reddy and Lee.[23] In a given HD–He mixture experiment, the base density ρ_a of HD was kept constant and the profiles of the enhancement of absorption of the band were obtained for a series of partial densities ρ_b of helium. The densities of HD at 298 K were obtained by interpolation from the isothermal data of hydrogen[24] and deuterium[25] at the same temperature, and those of helium were obtained from its isothermal data.[26] In an experiment with a given base density of HD, the partial density of helium was calculated by the method described by Reddy and Cho.[27]

The absorption coefficient $\alpha(\nu)$ at a given wave number ν (in cm^{-1}) of the HD gas at a density ρ_a in a cell of sample path length l is given by $(1/l)\ln[I_0(\nu)/I(\nu)]$, where $I_0(\nu)$ and $I(\nu)$ are the intensities of radiation transmitted by the evacuated cell and the cell filled with HD, respectively. The corresponding quantity in the mixture experiments is the absorption coefficient $\alpha_{am}(\nu)$ which is given by $(1/l)\ln[I_1(\nu)/I_2(\nu)]$, where $I_1(\nu)$ and $I_2(\nu)$ are the intensities transmitted by the cell filled with HD and with the gas mixture, respectively. Absorption profiles were obtained by plotting $\log_{10}[I_0(\nu)/I(\nu)]$ and $\log_{10}[I_1(\nu)/I_2(\nu)]$ against ν. The integrated absorption coefficients of the band $\int\alpha(\nu)d\nu$ and $\int\alpha_{am}(\nu)d\nu$ (in cm^{-2}) were obtained from the areas under the experimental profiles.

III. EXPERIMENTAL RESULTS

A. Spectra of the HD gas

Figure 1 shows the absorption profiles of the fundamental band of HD in the pure gas at densities 48.8, 38.3, and 27.8 amagat. The positions of the collision-induced single transitions $O_1(2)$, $Q_1(J)$, and $S_1(J)$ for $J = 0$–4, obtained from the constants of the free HD molecule,[28] are marked along the wavenumber axis. In the spectrum of the pure HD gas at 298 K, in addition to the single transitions, a large number of double transitions of the type $Q_1(J)+S_0(J)$ for $J = 0$–4 are expected to occur. In such a double transition, one of the colliding pairs of molecules undergoes the rotation-vibration transition $Q_1(J)$ while the other simultaneously undergoes a pure rotation transition $S_0(J)$. In these profiles a marked dip in the Q branch which occurs at the position of the $Q_1(1)$ line of the free HD molecule is similar to the ones observed in the collision-induced spectra of hydrogen and deuterium. The dip was explained by Van Kranendonk[29] as an interference effect due to negative correlations existing between the overlap dipole moments in successive collisions. In Fig. 1, the separations $\Delta\nu_{pR}^{max}$ between the peaks of the components Q_P and Q_R are 45, 43, and 40 cm^{-1} for the profiles (a), (b), and (c), respectively. One characteristic feature of the profiles in Fig. 1 is the presence of the transition $R_1(1)$ which by virtue of its narrow bandwidth is interpreted as an "allowed" transition. The calculated and observed wavenumbers of the absorption peaks of the fundamental band of HD in the pure gas are listed in Table I. The accuracy of the measured broad peaks of the collision-induced S transitions is believed to be ± 4 cm^{-1} while that of the

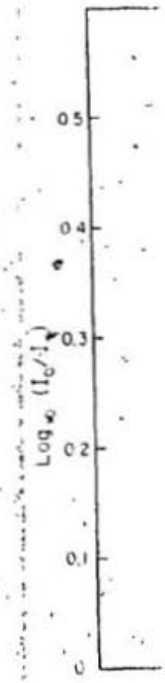

FIG. 1. Abs

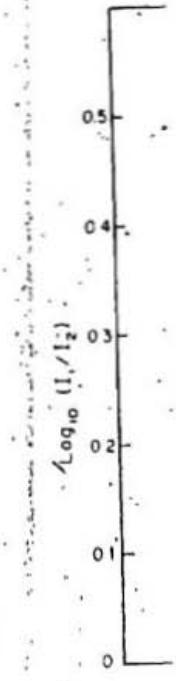

FIG. 2. P
perature.

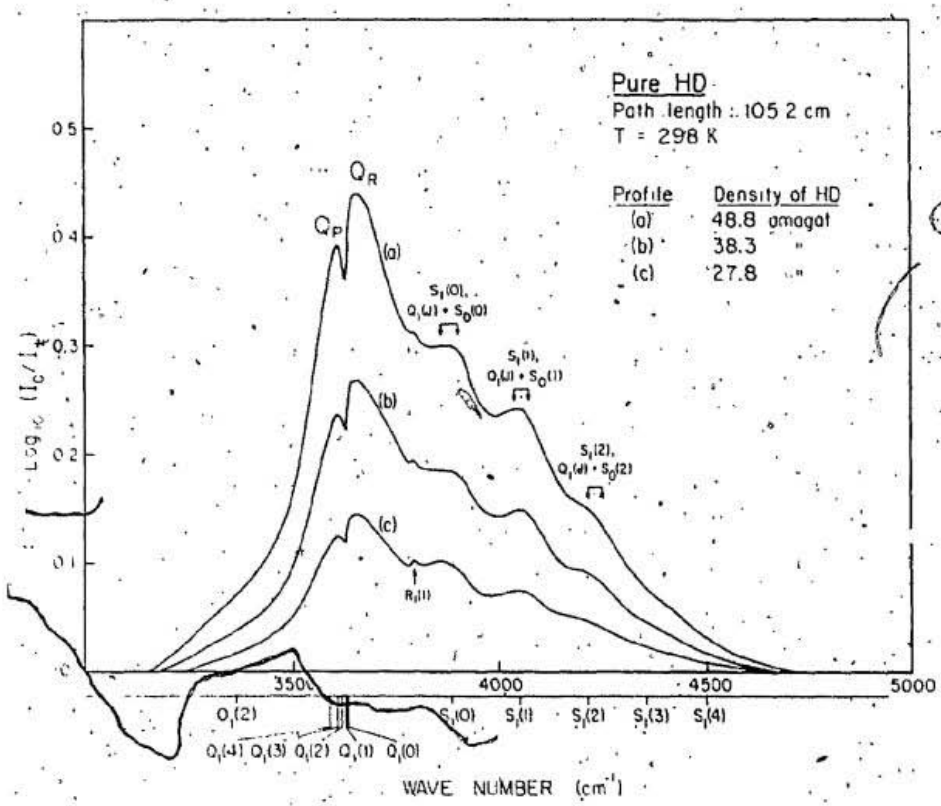

FIG. 1. Absorption profiles of the fundamental band of HD at room temperature for various gas densities.

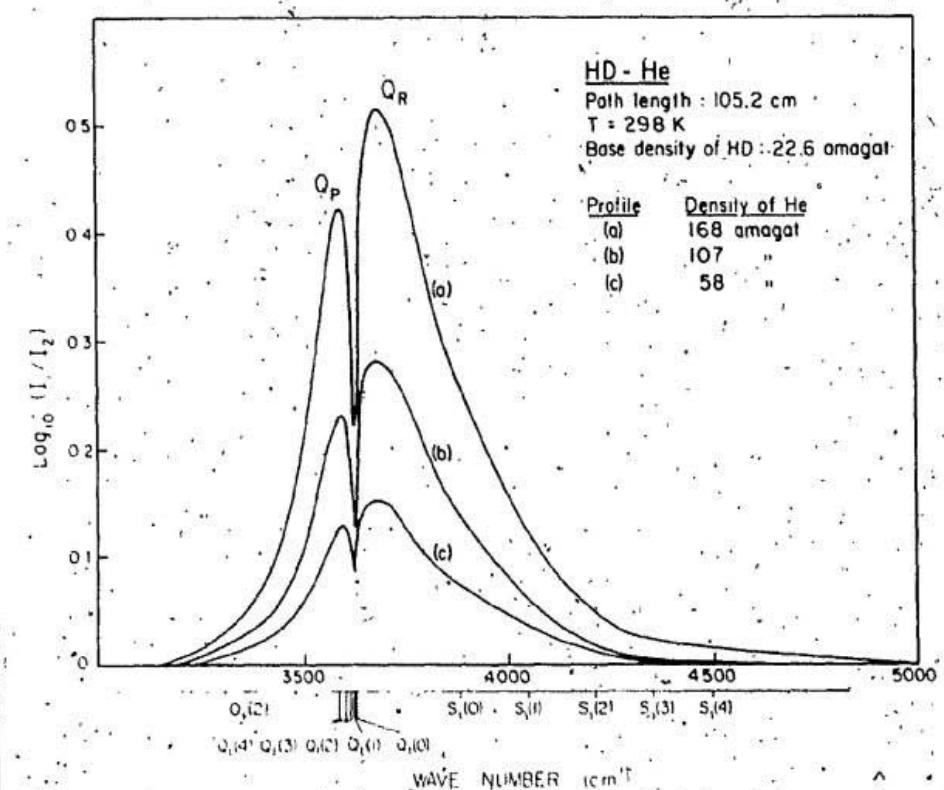

FIG. 2. Profiles of the enhancement of absorption of the collision-induced fundamental band of HD in HD–He mixtures at room temperature.

TIGHT

TABLE I. Assignments and calculated and observed wavenumbers of the absorption peaks in the fundamental band of HD in the pure gas at 298 K.

Mixture	Assignment	Calculated Wavenumber (cm^{-1})[a]	Observed Wavenumber (cm^{-1})
HD–HD	$Q_1(4)$	3593.9	
	$Q_1(3)$	3609.6	
	$Q_1(2)$	3620.5	
	$Q_1(1)$	3628.2	3628[b]
	$Q_1(0)$	3632.1	
	$R_1(1)$[c]	3795.3	3800
	$Q_1(4)+S_0(0)$	3860.6	
	$Q_1(3)+S_0(0)$	3876.1	3880
	$S_1(0)$	3887.6	
	$Q_1(2)+S_0(0)$	3887.6	
	$Q_1(1)+S_0(0)$	3895.3	
	$Q_1(0)+S_0(0)$	3899.1	
	$Q_1(4)+S_0(1)$	4036.6	
	$S_1(1)$	4052.0	
	$Q_1(3)+S_0(1)$	4052.1	4055
	$Q_1(2)+S_0(1)$	4063.6	
	$Q_1(1)+S_0(1)$	4071.3	
	$Q_1(0)+S_0(1)$	4075.1	
	$S_1(2)$	4209.6	
	$Q_1(4)+S_0(2)$	4209.6	4220
	$Q_1(3)+S_0(2)$	4225.1	
	$Q_1(2)+S_0(2)$	4236.6	
	$Q_1(1)+S_0(2)$	4244.3	
	$Q_1(0)+S_0(2)$	4248.1	
	$S_1(3)$	4359.0	
	$Q_1(4)+S_0(3)$	4378.5	
	$Q_1(3)+S_0(3)$	4394.0	4400
	$Q_1(2)+S_0(3)$	4405.5	
	$Q_1(1)+S_0(3)$	4413.2	
	$Q_1(0)+S_0(3)$	4417.8	

[a] Calculated from the constants of the free molecule.[28]
[b] Wavenumber of the Q dip.
[c] See text.

sharper Q dip and the $R_1(1)$ line is considered to be around ± 2 cm^{-1}.

B. Spectra of the HD–He mixtures

The profiles of the enhancement of absorption of the HD fundamental band in three HD–He mixtures for a base density of 22.6 amagat of HD and partial densities 168, 107, and 58 amagat of He are shown in Fig. 2. The broad feature of the Q branch whose observed dip coincides with the wavenumber of the $Q_1(1)$ line of the free HD molecule is similar to those observed in the fundamental bands of H_2 and D_2 in their binary mixtures with He at room temperature.[11,30] For the profiles (a), (b), and (c), the separations $\Delta\nu_{PR}^{max}$ of the Q branch are 85, 83, and 80 cm^{-1}, respectively. The profiles of the enhancement of absorption consist of only single transitions under normal experimental conditions.

C. Absorption coefficients

For the collision-induced band, the integrated absorption coefficients $\int\alpha(\nu)d\nu$ in HD and $\int\alpha_{am}(\nu)d\nu$ in H_2–He mixtures can be represented by the relations

$$\int\alpha(\nu)d\nu = \alpha_{1a}\rho_a^2 + \alpha_{2a}\rho_a^3 + \cdots \quad (1)$$

and

$$\int\alpha_{am}(\nu)d\nu = \alpha_{1b}\rho_a\rho_b + \alpha_{2b}\rho_a\rho_b^2 + \cdots , \quad (2)$$

respectively. Here, α_{1a} and α_{2a} are binary and ternary absorption coefficients of the pure gas, respectively, and α_{1b} and α_{2b} are similar quantities for the mixtures; the quantities ρ_a and ρ_b are the densities of HD and He, respectively. Plots of $(1/\rho_a^2)\int\alpha(\nu)d\nu$ vs ρ_a and of $(1/\rho_a\rho_b)\int\alpha_{am}(\nu)d\nu$ vs ρ_b are shown in Figs. 3 and 4 and are found to be straight lines. The intercepts and slopes of the straight lines, which give the binary absorption coefficient α_{1a} or α_{1b} (cm^{-2} $amagat^{-2}$) and ternary absorption coefficient α_{2a} or α_{2b} (cm^{-2} $amagat^{-3}$), respectively, are calculated by a least-squares fit of the experimental data and their values are listed in Table II. While deriving the absorption coefficients, the contribution to the integrated intensity of the absorption profiles in the pure gas by the allowed $R(J)$ and $P(J)$ transitions at room temperature[8] was considered, but found to be several orders of magnitude smaller than the contribution of the collision-induced transitions.

For both pure HD and HD–He mixtures, the ternary absorption coefficients are very small compared to the binary absorption coefficients. This means, under the experimental conditions used in the present work, most of the absorption intensity arises from the binary collisions. The integrated absorption coefficients can also be represented by the equations

$$c\int\tilde{\alpha}(\nu)d\nu = \tilde{\alpha}_{1a}\rho_a^2 n_0^2 + \tilde{\alpha}_{2a}\rho_a^3 n_0^3 + \cdots \quad (3)$$

and

$$c\int\tilde{\alpha}_{am}(\nu)d\nu = \tilde{\alpha}_{1b}\rho_a\rho_b n_0^2 + \tilde{\alpha}_{2b}\rho_a\rho_b^2 n_0^3 + \cdots , \quad (4)$$

where c is the speed of light and n_0 is the Loschmidt's number. The new coefficients $\tilde{\alpha}_{1a}$ ($cm^6 s^{-1}$) and $\tilde{\alpha}_{2a}$ ($cm^9 s^{-1}$) are related to the earlier ones by the expressions

$$\tilde{\alpha}_{1a} = \frac{(c/n_0^2)\alpha_{1a}}{\bar{\nu}} , \quad \tilde{\alpha}_{2a} = \frac{(c/n_0^3)\alpha_{2a}}{\bar{\nu}} , \quad (5)$$

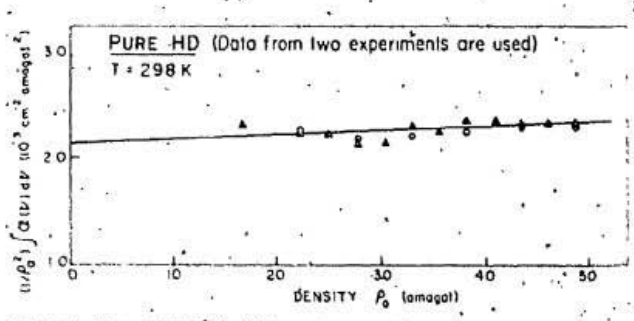

FIG. 3. Plot of $(1/\rho_a^2)\int\alpha(\nu)d\nu$ against ρ_a of HD at 298 K.

FIG. 4. Plot

and similar
effective ban

$$\bar{\nu} = \int\alpha(\nu)$$

and a similar
tures. The
profiles are
ues of $\tilde{\alpha}_{1a}$ an
nary absorp
H_2 and D_2 in
with He at r.
included in t
son.

IV. ANALYS ENHANCEM

In the pre
induced fund.
temperature
gle transitio
the quadrup
number of qu
type $Q_1(J)+S$
enhancement
consist of on
present the
of the absor
gas has been

TABLE II. A
temperature.

Mixture	
HD–HD	
HD–He	
H_2–H_2	
H_2–He	
D_2–D_2	
D_2–He	

[a] Ranges of err

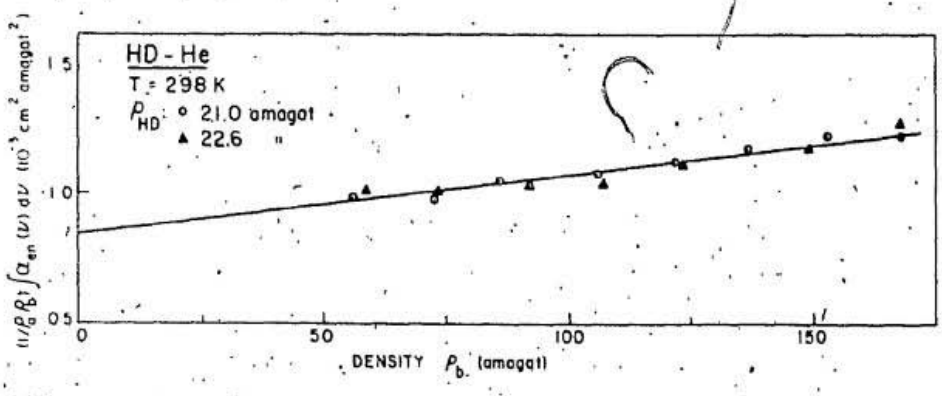

FIG. 4. Plot of $(1/\rho_a\rho_b)\int\alpha_{em}(\nu)d\nu$ against ρ_b for HD–He mixtures at 298 K.

and similar expressions apply for $\bar{\alpha}_{1b}$ and $\bar{\alpha}_{2b}$. Here the effective band center $\bar{\nu}$ is given by

$$\bar{\nu} = \int \alpha(\nu)d\nu \Big/ \int \alpha(\nu)\nu^{-1}d\nu \ , \tag{6}$$

and a similar relation applies to the profiles of the mixtures. The average values of $\bar{\nu}$ for pure HD and HD–He profiles are 3821 and 3736 cm^{-1}, respectively. The values of $\bar{\alpha}_{1a}$ and $\bar{\alpha}_{1b}$ are also included in Table II. The binary absorption coefficients of the fundamental bands of H_2 and D_2 in the pure gases and in their binary mixtures with He at room temperature from the earlier work are included in the same table for the purpose of comparison.

IV. ANALYSIS OF THE HD-He PROFILES OF THE ENHANCEMENT OF ABSORPTION

In the previous section, it is noted that the collision-induced fundamental band of HD in the pure gas at room temperature consists of a superposition of several single transitions, namely, the overlap-induced Q lines, the quadrupole-induced O, Q, and S lines, and a large number of quadrupole-induced double transitions of the type $Q_1(J)+S_0(J)$. On the other hand, the profiles of the enhancement of absorption of HD in HD–He mixtures consist of only single transitions. In this section, we present the analysis of these profiles of the enhancement of the absorption. No analysis of the profiles of the pure gas has been attempted in the present paper.

A. Line shapes

The enhancement absorption coefficient $\bar{\alpha}_{em}(\nu)$ of an overlap-induced transition may be expressed as (see Van Kranedonk,[29] Mactaggart and Welsh[32])

$$\bar{\alpha}_{em}(\nu) = \frac{\bar{\alpha}^0_{em} W_0(\Delta\nu)}{1+\exp(-hc\Delta\nu/kT)} \ , \tag{7}$$

where $\bar{\alpha}^0_{em}$ is the fictitious relative maximum intensity of the overlap-induced transition at $\nu=\nu_m$, ν_m being the molecular frequency of the HD line, $W_0(\Delta\nu)$ with $\Delta\nu = \nu-\nu_m$ represents the symmetrical line shape, and the factor in the denominator, namely, $[1+\exp(-hc\Delta\nu/kT)]$, converts the symmetrized line form into the observed Boltzmann modified line form. According to Van Kranedonk,[29] the quantity $W_0(\Delta\nu)$ can be expressed as

$$W_0(\Delta\nu) = D(\Delta\nu)\, W_0^0(\Delta\nu) \ , \tag{8}$$

where $W_0^0(\Delta\nu)$ is the intracollisional line form arising from the single binary collisions and $D(\Delta\nu)$ is the intercollisional line form which takes into account the correlation existing between the dipole moments in successive collisions. The quantity $D(\Delta\nu)$ has the form[29]

$$D(\Delta\nu) = 1-\gamma[1+(\Delta\nu/\delta_c)^2]^{-1} \ , \tag{9}$$

where γ is a constant (which is assumed to be unity in the present analysis) and δ_c is the intercollisional half-width at half-height. The line shape proposed by Levine and Birbaum[33] was found to represent well the quantity

TABLE II. Absorption coefficients[a] of the fundamental bands of H_2, HD, and D_2 at room temperature.

	Binary absorption coefficient		Ternary absorption coefficient	
Mixture	(10^{-3} cm^{-2} amagat^{-2})	(10^{-35} cm^6 s^{-1})	(10^{-6} cm^{-2} amagat^{-3})	Reference
HD–HD	α_{1a}: 2.14 ± 0.05	$\bar{\alpha}_{1a}$: 2.32 ± 0.05	α_{2a}: 3.7 ± 1.5	This work
HD–He	α_{1b}: 0.84 ± 0.02	$\bar{\alpha}_{1b}$: 0.94 ± 0.02	α_{2b}: 2.3 ± 0.2	This work
H_2–H_2	α_{1a}: 2.4	$\bar{\alpha}_{1a}$: 2.3	α_{2a}: 1.1	31
H_2–He	α_{1b}: 2.08 ± 0.06	$\bar{\alpha}_{1b}$: 1.99 ± 0.06	α_{2b}: −1.40 ± 0.64	11
D_2–D_2	α_{1a}: 1.06 ± 0.02	$\bar{\alpha}_{1a}$: 1.40 ± 0.02	α_{2a}: 0.8 ± 0.2	22
D_2–He	α_{1b}: 0.82 ± 0.01	$\bar{\alpha}_{1b}$: 1.08 ± 0.01	α_{2b}: 0.27 ± 0.03	12

[a] Ranges of error indicated are standard deviations.

$W_0^0(\Delta\nu)$ for the overlap-induced transitions in H_2 (cf. Mactaggart and Welsh [32]) and the same form was used in the present analysis. It may be represented as

$$W_0^0(\Delta\nu) = (2\Delta\nu/\delta_d)^2 K_2(2\Delta\nu/\delta_d) \ , \qquad (10)$$

where K_2 is a modified Bessel function of the second kind and δ_d is the intracollisional half-width (i.e., half-width at half-height of the symmetrized line form).

For the quadrupole-induced components, the Boltzmann-modified dispersion line form (cf. Kiss and Welsh[34]) was used. Here, the enhancement absorption coefficient is represented by the following equations:

$$\tilde{\alpha}_{qn}^{+} = \frac{\tilde{\alpha}_{qm}^{0}}{1+(\Delta\nu/\delta_q)^2} \ , \quad \Delta\nu \geq 0 \qquad (11)$$

and

$$\tilde{\alpha}_{qn}^{-} = \tilde{\alpha}_{qn}^{+} \exp(-hc\Delta\nu/kT) \ , \quad \Delta\nu < 0 \ . \qquad (12)$$

Here, $\tilde{\alpha}_{qn}^{+}$ and $\tilde{\alpha}_{qn}^{-}$ (where $\tilde{\alpha} = \alpha/\nu$ are the absorption coefficients at wave numbers $\nu_m + \Delta\nu$ and $\nu_m - \Delta\nu$ in the high- and low-wavenumber wings, respectively, $\tilde{\alpha}_{qm}^{0}$ is the relative maximum intensity of a quadrupole-induced transition at $\nu = \nu_m$; and δ_q is the half-width at half-height, measured to the high-wavenumber wing.

B. Relative intensities

The relative intensities of the overlap-induced transitions and quadrupole-induced transitions can be calculated from the general theory of Van Kranendonk.[18] For the overlap components $Q_1(J)$, these are given by

$$\tilde{\alpha}_{om}^{0} = P_J \ , \qquad (13)$$

where P_J is the normalized Boltzmann factor for the rotational state J (note $\sum P_J = 1$) and is given by

$$P_J = (1/Z)(2J+1)\exp(-E_J/kT) \ . \qquad (14)$$

Here, Z is the rotational partition function. For the quadrupolar components $O_1(J)$, $Q_1(J)(J \neq 0)$, and $S_1(J)$ of HD–He mixtures, the relative intensities can be calculated in terms of the matrix elements of the HD molecule, $\langle vJ|Q_{HD}|v'J'\rangle$, which were computed by Birnbaum and Poll,[35] and the polarizability α_{He} of helium. Thus, the relative intensities of these components for the transitions in the fundamental band of HD (i.e., $v = 0$, $J \leftarrow v' = 1, J'$) can be expressed as

$$\tilde{\alpha}_{qm}^{0} = P_J C(J2J';00)^2 |\langle 0J|Q_{HD}|1J'\rangle|^2 \alpha_{He}^2 \ , \qquad (15)$$

where $C(J2J';00)$ is a Clebsch–Gordan coefficient.

C. Profile analysis and discussion

Analysis of the profiles of the enhancement of absorption was carried out by a program written for the IBM 370/155 computer. The relative peak intensities of the overlap components were expressed in terms of the peak intensity of the most intense overlap component $Q_{1\,overlap}(1)$ and those of the quadrupolar components in terms of that of the $S_1(1)$. These two peak intensity parameters and the half-widths δ_o, δ_d, and δ_q, defined by Eqs. (9)–(11), respectively, were the adjustable parameters in the program. A series of computations

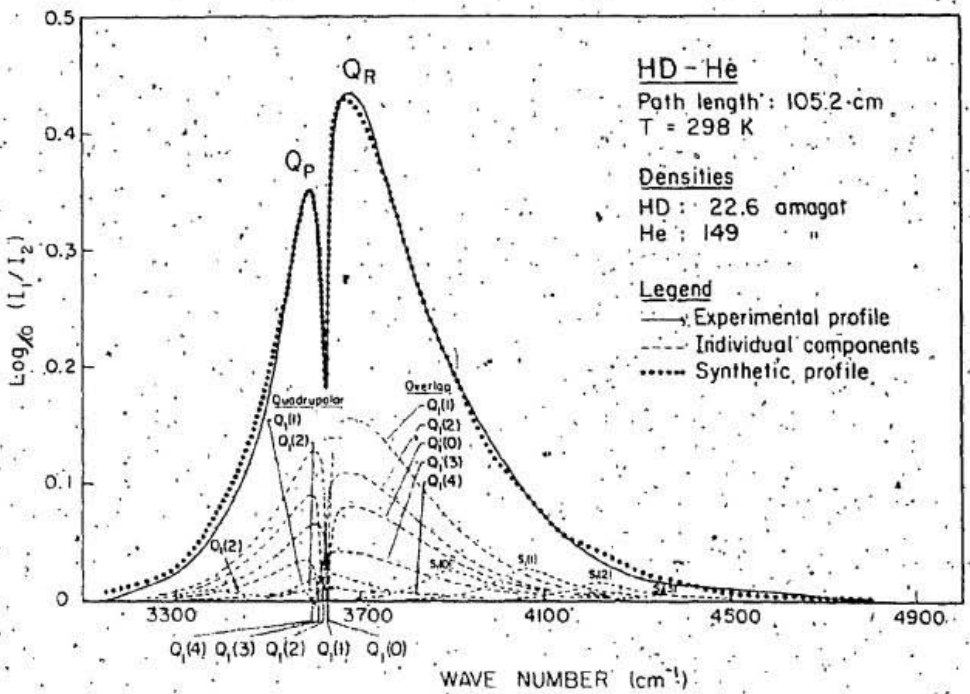

FIG. 5. Analysis of the enhancement absorption profile of the HD fundamental band in a mixture of HD with He at 298 K. The solid curve is the experimental profile. The dashed curve represents the overlap-induced transitions [$Q_1(J)$, for $J = 0$–4] or the quadrupole-induced transitions [$O_2(2)$, $Q_1(J)$ with $J = 1$–4, $S_1(J)$ for $J = 0$–4]. The dots represent the sum of the computed overlap and quadrupolar components. For the sake of clarity, the weaker quadrupolar components $Q_1(3)$, $Q_1(4)$, and $S_1(4)$ are not shown.

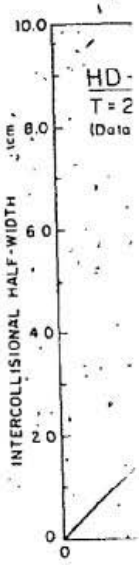

FIG. 6. Plot
298 K against
tal points are
$= a\rho_b - b\rho_b^2$.

were carric
the adjustab
which was
transitions,
the experim
Provision w
adjust the n
account for
tional frequ
served prof
shifted freq

An examp
HD fundame
is shown in
mental and
cept for shi
14 profiles
analyzed.
constant for
obtained for
cm^{-1}. An a
metrized"
lines and th
to the exper
basis of the
sible to est
the quadrup
the band in
and ~ 14%
profile in H
lisional dip
found to var
first linear
range of the

TI
BINDING

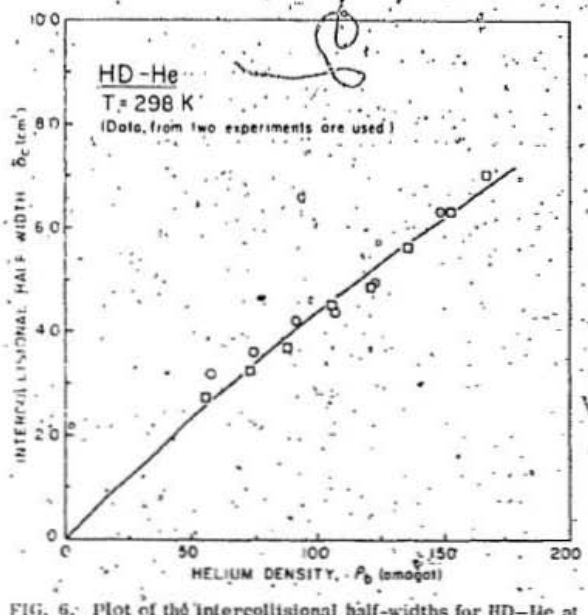

FIG. 6. Plot of the intercollisional half-widths for HD–He at 298 K against the partial density ρ_b of helium. The experimental points are represented by the curve which is given by $\delta_c = a\rho_b - b\rho_b^2$.

were carried out by the computer for different values of the adjustable parameters until the computed profile, which was the sum of the intensities of the individual transitions, gave the best nonlinear least-squares fit to the experimental profile in the entire region of the band. Provision was also made in the computer program to adjust the molecular frequencies ν_m of HD in order to account for any possible perturbations of the HD vibrational frequencies. However, the best fit to the observed profiles in the present work was obtained for unshifted frequencies.

An example of the results of the profile analysis of the HD fundamental band in a particular mixture of HD–He is shown in Fig. 5. The agreement between the experimental and calculated profiles is reasonably good except for slight differences in the wings. On the whole, 14 profiles of the enhancement of absorption have been analyzed. The values of δ_d and δ_q are found to remain constant for the profiles analyzed and the average values obtained for these are $\delta_d = 177 \pm 2$ cm^{-1} and $\delta_q = 95 \pm 10$ cm^{-1}. An analysis was also carried out using a "symmetrized" dispersion line shape[32] for the quadrupolar lines and the resulting best fit of the calculated profile to the experimental profile gave $\delta_q = 77 \pm 3$ cm^{-1}. On the basis of the profile analysis carried out here, it is possible to estimate the contributions of the overlap and the quadrupolar inductions to the integrated intensity of the band in HD–He mixtures; these are ~ 86% overlap and ~ 14% quadrupolar. The best fit obtained for the profile in Fig. 5 gave the half-width δ_c of the intercollisional dip a value of 6.3 cm^{-1}. The quantity δ_c was found to vary with density of helium ρ_b in the mixture at first linearly and then somewhat less rapidly within the range of the present experimental densities. A plot of δ_c against ρ_b is shown in Fig. 6 and was found to be represented adequately by

$$\delta_c = a\rho_b - b\rho_b^2 \quad (a \gg b), \tag{16}$$

where a and b are constants. The values of a and b for HD–He mixtures at 298 K are

$$a = 4.86 \times 10^{-2} \text{ cm}^{-1}\text{amagat}^{-1}, \quad b = 4.96 \times 10^{-5} \text{ cm}^{-1}\text{amagat}^{-2}$$

For the fundamental band, Mactaggart and Welsh[32] have found that the form $\delta_c = a\rho_b + b\rho_b^2$ fits well over a wide range of foreign gas densities extending up to 1200 amagat. However, a close examination of their curve for H_2–He at 300 K shows that, for the densities up to 200 amagat, the curve may be better represented by $\delta_c = a\rho_b - b\rho_b^2$, which is in agreement with our present result on HD–He (maximum $\rho_{He} < 175$ amagat). The collision diameter σ_{12} and the coefficient a of HD–He in Eq. (16) are related by (see Mactaggart and Welsh[32] and Chapman and Cowling[26])

$$a = (1 - \bar{\Delta})\sigma_{12}^3 n_0 / c(\pi m/2kT)^{1/2}, \tag{17}$$

where $\bar{\Delta}$ is the mean persistence of velocity ratio, n_0 is the Loschmidt's number, and m is the reduced mass of HD–He pair. From the expression given by Chapman and Cowling,[26,32] $\bar{\Delta}$ for HD–He was found to be 0.33. When appropriate values of various quantities and the present value of the parameter a are used in Eq. (17), the value obtained for the collision diameter σ_{12} for the overlap induction is 2.92 Å. The Lennard-Jones diameter σ_{12}^{LJ} for HD–He can be obtained by applying the combination rule $\sigma_{12}^{LJ} = \frac{1}{2}[\sigma_1^{LJ} + \sigma_2^{LJ}]$ successively, first from those of H_2 and D_2 to get that of HD, and then from those of HD and He. The value thus obtained for σ_{12}^{LJ} for HD–He is 2.77 Å, which is somewhat less than the value of σ_{12} obtained from the parameter a. This observation is similar to the one made by Mactaggart and Welsh[32] for H_2–He.

ACKNOWLEDGMENTS

The authors are thankful to Professor S. W. Breckon for his continued interest in this work.

*This research was supported in part by a grant (to SPR) from the National Research Council of Canada.

†Holder of a Graduate Fellowship of the Memorial University of Newfoundland, 1972–1975.

[1] G. C. Wick, Atti, R. Acad. Naz. Lincei 21, 708 (1935).
[2] G. Herzberg, Nature 166, 563 (1950).
[3] R. A. Durie and G. Herzberg, Can. J. Phys. 38, 806 (1960).
[4] M. Trefler and H. P. Gush, Phys. Rev. Lett. 20, 703 (1968).
[5] The subscript in R_0, etc., denotes $\Delta v (= v' - v'')$, the change in the vibrational quantum number.
[6] A. R. W. McKellar, Can. J. Phys. 51, 389 (1973).
[7] A. R. W. McKellar, Can. J. Phys. 52, 1144 (1974).
[8] J. Bejar and H. P. Gush, Can. J. Phys. 52, 1669 (1974).
[9] H. L. Welsh, M. F. Crawford, and J. L. Locke, Phys. Rev. 76, 580 (1949).
[10] H. L. Welsh, *MTP International Review of Science, Physical Chemistry, Vol. 3, Spectroscopy* (Butterworths, London, 1972).
[11] S. P. Reddy and K. S. Chang, J. Mol. Spectrosc. 47, 22 (1973).
[12] W. E. Russell, S. P. Reddy, and C. W. Cho, J. Mol. Spectrosc. 52, 72 (1974).

[13]M. Tefler, A. M. Cappel, and H. P. Gush, Can. J. Phys. 47, 2115 (1969).
[14]A. Crane and H. P. Gush, Can. J. Phys. 44, 373 (1966).
[15]G. W. Holleman and G. E. Ewing, J. Chem. Phys. 44, 3121 (1966).
[16]G. W. Holleman and G. E. Ewing, J. Chem. Phys. 47, 571 (1967).
[17]J. Van Kranendonk, Physica 23, 825 (1957).
[18]J. Van Kranendonk, Physica 24, 347 (1958).
[19]Density in amagat unit is the ratio of the gas density in the cell to the gas density at normal temperature and pressure.
[20]*IUPAC Tables of Wave Numbers for Calibration of Infrared Spectrometers* (Butterworths, London, 1961).
[21]C. J. Humphreys, J. Opt. Soc. Am. 43, 1027 (1953).
[22]S. P. Reddy and C. W. Cho, Can. J. Phys. 43, 793 (1965).
[23]S. P. Reddy and W. F. Lee, Can. J. Phys. 46, 1373 (1968).
[24]A. Michels, W. De Graaff, W. Wassenaar, J. M. H. Levelt, and P. Louwerse, Physica 25, 25 (1959).
[25]A. Michels and M. Goudeket, Physica 8, 347 (1941).
[26]A. Michels and W. Wouters, Physica 8, 923 (1941).
[27]S. P. Reddy and C. W. Cho, Can. J. Phys. 43, 2331 (1965).
[28]B. P. Stoicheff, Can. J. Phys. 35, 730 (1957).
[29]J. Van Kranendonk, Can. J. Phys. 46, 1173 (1968).
[30]S. T. Pai, S. P. Reddy, and C. W. Cho, Can. J. Phys. 44, 2893 (1966).
[31]W. F. J. Hare and H. L. Welsh, Can. J. Phys. 36, 88 (1958).
[32]J. W. Mactaggart and H. L. Welsh, Can. J. Phys. 51, 158 (1973).
[33]H. B. Levine and G. Birnbaum, Phys. Rev. 154, 172 (1967).
[34]Z. J. Kiss and H. L. Welsh, Can. J. Phys. 37, 1249 (1959).
[35]A. Birnbaum and J. D. Poll, J. Atmos. Sci. 26, 943 (1969).
[36]S. Chapman and T. G. Cowling, *The Mathematical Theory of Non-uniform Gases* (Cambridge University, Cambridge, England, 1952).